Optimization of the planning and operations of electric distribution grids in the context of high renewable energy penetration

Etta Grover Silva

THÈSE DE DOCTORAT

de l'Université de recherche Paris Sciences et Lettres
PSL Research University

Préparée à MINES ParisTech

Optimisation de la planification et l'opération du réseau de distribution dans le contexte d'une forte pénétration des énergies renouvelables

École doctorale nº432

SCIENCES ET MÉTIERS DE L'INGÉNIEUR

Spécialité ÉNERGÉTIQUE ET PROCÉDÉS

COMPOSITION DU JURY :

Mme Manuela Sechilariu
UTC, Présidente

M Benoît Robyns
HEI Lille, Rapporteur

M Anastasios Bakirtzis
AUTH, Rapporteur

M Raphael Caire
Grenoble INP ENSE3, G2Elab, Rapporteur

M Miguel Heleno
LBNL, Examinateur

M Damien Picault
ENEDIS, Examinateur

M Georges Kariniotakis
MINES ParisTech, Examinateur

M Robin Girard
MINES ParisTech, Examinateur

Soutenue par **Etta Grover-Silva**
le 14 décembre 2017

Dirigée par **Georges Kariniotakis**
and **Robin Girard**

MINES ParisTech | PSL RESEARCH UNIVERSITY PARIS

Contents

List of Tables

List of Figures

Acknowledgements

Writing this dissertation has been a difficult but enlightening task. This experience has forced me to grow in many ways and I am grateful to have had the opportunity to pursue a subject that I am passionate about. Completing my PhD and writing the final document has taught me diligence, determination and endurance. This work was completed with the support of many people. I would first like to thank my family and close friends for encouraging me during the entire period of my PhD. More specifically my office colleagues were a constant source of encouragement for technical and emotional support. I would like to recognize my supervisor Robin Girard for following my work and providing feedback on the technical and scientific choices made during the PhD. I am very grateful for my thesis director George Kariniotakis who was not only there to support me for the technical decisions and guidance but also on a more personal level. He constantly was a support for more logistical and administrative matters as well as a mentor for a multitude of challenges. I would like to thank my aunt Abby to have helped with reading and correcting the final document. I would also like to recognize my significant other, Yoann for helping with the final document corrections but also supporting me throughout my thesis in many ways.

I would like to recognize and thank ADEME for supporting the PhD financially and specifically Patricia Sidat for taking the time to have meaningful discussions about my work. I am grateful to have participated in the SENSIBLE European project which also partially funded the PhD. I would also like to thank the Grid Integration Group at Lawrence Berkeley National Laboratory and more specifically Miguel Heleno for being a close supervisor and teaching me many things about being persistent, precise and rigorous. I would also like to extend my gratitude to the MINES Foundation and the ELECTRA EERA Mobility program that allowed me to complete my collaboration in California with Berkeley Lab.

Nomenclature

Indices

$+$	a variable with a positive domain
$-$	a variable with a negative domain
0	indicating the substation point of common coupling
0	zero sequence impedance
γ	scenario dependent variables
a	phase a
ab	relationship between phase a and phase b
ac	air conditioning (AC) systems
$appx$	indicating an approximation of a previous formulation
b	phase b
c	phase c
cl	cumulative controllable load at a specific node (CL)
d	individual controllable device
ec	price of electricity
edc	price of electricity plus transmission and distribution costs
ef	price of comfort constraint violations in euros per degree
eq	indicating an equivalent formulation
ewh	electric water heater (EWH) systems
ext	external air temperature
H	Hermitian matrix
Hac	over heating in AC systems
ij	branch between nodes i and j

$init$ indicating an initial value

inj the power injection at substation

int internal building air temperature

inv capital investment

j index for node j

Lac under heating in AC systems

$loss$ system losses

n neutral cable

Nac range of acceptable temperature for AC systems

nom indicating the nominal value characteristics of a system

$O\&M$ operations and maintenance (O&M)

p positive sequence impedance

pv PV system

$pvid$ PV maximum possible injection

st storage system

t period of time

ul uncontrollable load (UL)

wtr property of water

Parameters

α_d Heat loss constant of the hot water heater tank thermal insulation

η Efficiency of a device

$\overline{\Theta}$ Maximum temperature allowable

$\overline{P}_{pv,j,t}$ Ideal PV production for node j at time step t

$\overline{S}_{pv,j,t}$ PV maximum apparent power flow at node j

$\overline{V}$ Maximum voltage

$\underline{\Theta}$ Minimum temperature allowable

$\underline{V}$ Minimum voltage

c Cost value

C_d Thermal capacity of an individual device

C_{wtr} Thermal capacity of water

Imb Imbalance of three-phase system

Inv^{max} Total capital cost limit of project

LF Load factor of three-phase system

$P_{ul,j,s,t}$ Active power load at node j scenario s and time step t

$Q_{ul,j,s,t}$ Reactive power load at node j scenario s and time step t

r Electrical resistance

R_d Thermal resistance of an individual device

t Duration of time step

T_{max} Transformer nominal power rating

$v_{t,d}$ Electric hot water use in liters

x Electrical reactance

y Electrical admittance

Z Impedance matrix associated with all phases

z Impedance of a single-phase

Sets

J Set of all nodes within the network $j \in J$

K Set of all nodes within the network for desired analysis

Variables

β difference in phase angles between the currents of two phases

ℓ Square of current magnitude

ϕ current to voltage phase angle

Θ Temperature

θ voltage phase angle

υ Square of voltage magnitude

I Current including magnitude and phase

N The hours of autonomy at nominal rating for a battery system

P Active power

Q Reactive power

S Apparent power

soc Nominal capacity of a battery system

V Voltage including magnitude and phase

Abbreviations

AC Alternating Current

ADN Active Distribution Network

API Application Program Interface

BFM Branch Flow Model

BIM Bus Injection Model

CL Controllable Load

CRE Commission de Régulation de l'Énergie

DER Distributed Energy Resources

DMS Distribution Management System

DR Demand Response

DSM Demand Side Management

DSO Distribution System Operator

EDF Électricité de France

EWH Electric Water Heater

GDP Gross Domestic Product

HVAC Heating Ventilation and Air Conditioning

INSEE Institut National de la Statistique et des Étude Économiques

OLTC On-Load Tap Changer

OPF Optimal Power Flow

PDF Probability Density Function

PV Photovoltaic

QCQP Quadratically Constrained Quadratic Program

QP Quadradtic Programming

RMSE Root Mean Square Error

RTE Réseau de Transport d'Électricité

SDP Semi-Definite Program

SOC State of Charge

SOCP Second-Order Cone Programming

UL Uncontrollable Load

Chapter 1

Introduction

Résumé

L'électricité est devenue critique dans le monde pour améliorer l'économie, la santé et la sécurité d'un pays. Actuellement, la production de cette électricité pour le monde entier est principalement basee sur les ressources fossiles. Les ressources fossiles sont à présent critiquées pour leur durabilité et leur impact sur l'environnement. S'il faut diminuer la consommation des ressources fossiles, il faut développer autres technologies pour fournir une électricité de qualité pour l'avenir. Cette transition des ressources fossiles aux nouvelles technologies non polluantes est souvent appelée la transition énergétique. Cette transition peut apparaître comme une mission colossale mais une transition énergétique à déjà eu lieu en France. Cette transition a impliqué un passage des ressources fossiles aux ressources nucléaires et a été effectué entre les années 1971 et 2001. Les leçons à retenir de cette expérience sont importantes pour réussir la transition vers les énergies renouvelables. La différence principale de ces deux transitions est le passage d'un modèle centralisé à un modèle décentralisé. Cette évolution vers un modèle décentralisé implique une rénovation significative du réseau de distribution. Une possibilité pour cette transformation est de modifier le système actuel passif en un système actif pour optimiser l'infrastructure actuelle. Le Smart Grid est un réseau qui est adapté vers un réseau contrôlable et automatisé. Pour réussir cette transformation, le système actuel sera étudié.

Le système électrique actuel est composé de deux réseaux: le réseau de transport et le réseau de distribution. Ces deux systèmes sont connectés pour créer le système électrique. Ces systèmes utilisent plusieurs niveaux de tension et transformateurs pour amener l'électricité depuis des générateurs centralisés jusqu'aux consommateurs finaux. Ainsi que ce système est efficace, mais il est aussi cher à construire et à maintenir. Ce modèle centralisé est efficace pour fournir une grande quantité de clients en minimisant les coûts d'opération. Le réseau de basse tension est le point de connexion pour une majorité des clients. De ce fait, la qualité de puissance du réseau de basse tension est importante pour satisfaire les consommateurs finaux.

La planification opérationnelle du réseau de distribution est une tâche complexe. Les décisions prises aujourd'hui peuvent avoir des effets sur le long terme et déterminer l'utilisation possible de ces réseaux dans l'avenir. Les investissements, principalement gérés par les opérateurs du réseau de distribution, sont classifiés en deux catégories: la gestion des déffaillances des équipements et les investissements de préventifs. Cette thèse focalise plutôt sur les investissements préventifs notamment les investissements d'adaptation du réseau de distribution actuel pour un fonctionnement plus intelligent. Toutefois, ces investissements sont difficiles à

hiérarchiser du au fait qu'il existe des incertitudes sur l'évolution de la consommation, la pénétration des générateurs décentralisés et l'évolution de la technologie en général. Un besoin existe pour adapter les réseaux passifs existants afin d'être plus actifs. Cette transformation permettra l'augmentation de la pénétration des générateurs décentralisés tout en évitant des renforcements coûteux du réseau électrique.

L'intégration des générateurs décentralisés sur le réseau de distribution peut amener de nouvelles difficultés par exemple le flux de puissance bi-directionels, une déviation du profil de tension et des problèmes de congestion. Ces difficultés peuvent influencer les appareils existants par exemple les régulateurs de tension. De plus, les générateurs décentralisés peuvent être connectés par des acteurs différents qui ont des priorités autre que la qualité de puissance du réseau électrique. Ces installations peuvent contribuer aux problèmes de la qualité de fourniture du réseau électrique et par conséquent augmenter le coût d'opération pour l'opérateur du réseau. Ces difficultés amènent de nouvelles problématiques pour les opérateurs du réseau électrique.

Ces nouvelles difficultés amènent la planification à prendre en compte des solutions intelligentes comme décrites par différents pays. Cette évolution est principalement conduite avec l'objectif d'augmenter la pénétration des énergies renouvelables tout en évitant les investissements coûteux de renforcement du réseau. La stratégie principale implique l'exploitation des flexibilités du réseau de distribution. Plus précisément, cette thèse va explorer trois sources de flexibilité : le stockage, la gestion de la demande et le dispatch down. Pour hiérarchiser ces flexibilités, de nouveaux outils de planification et gestion sont nécessaires.

Les études de flux de puissance optimal sont une possibilité pour l'analyse du réseau intelligent. Ce type d'étude est focalisé sur flux de puissance active et réactive pour minimiser le coût d'opération d'un réseau intelligent. Cet outil est efficace pour la planification et la gestion des réseaux avec des composants actifs et contrôlables. Les charactéristiques du réseau de distribution impliquent l'utilisation des équations de courant alternatif pour réussir des analyses précises. Ces équations ne peuvent pas être directement intégrées dans un algorithme d'optimisation convexe mais, il existe plusieurs stratégies pour les prendre en considération. Cette thèse fait un focus sur les techniques de relaxation convexe pour la résolution optimale de ces problèmes mathématiques. Les algorithmes développés dans cette thèse s'adressent principalement à la problématique de planification et de la gestion du réseau électrique intelligent.

De nouvelles méthodologies de planification et de la gestion sont applicables pour les réseaux électriques avec une forte pénétration des énergies renouvelables et la possibilité de contrôle. Ces méthodologies considèrent les coûts d'investissement, les stratégies d'opération et les incertitudes pour la gestion du réseau afin de hiérarchiser les investissements. L'intégration des générateurs décentralisés grâce aux outils d'optimisation peut diminuer les coûts d'opération et réduire la production de déchets. Avec des incertitudes élevés concernant la production électrique des énergies renouvelables, la gestion optimal de ces ressources est difficile. Toutefois, il existe des techniques pour une gestion robuste qui considère les incertitudes de la consommation et la production. Les détails de l'organisation de l'introduction sont présentés dans la Fig. 1.1.

1.1 Summary

Electricity is a critical element in society to improve health, safety and the economy around the world. Currently, fossil fuels are the primary source of the majority of electricity consumed in the world. This primary source has recently been questioned for its sustainability and longevity. In order to guarantee a future with easy access to high quality electricity, an energy transition

from fossil fuels to new renewable sources is necessary. In the past, specifically in France, a successful energy transition has already come about. This transition was from fossil fuels to nuclear power achieved between 1971 and 2001. Lessons learned from this past energy transition can be helpful for the success of the current energy transition. The primary difference of the current energy transition is the focus on decentralization as opposed to a more centralized model. This shift from centralized to decentralized production will require a significant adaptation of the distribution network. This adaptation implies the transformation of a passive distribution system to an active controllable system. A distribution network that is an active distribution network (ADN) can also be referred to as a smart grid. For this successful adaptation from passive to active electrical networks, it is important to understand the existing infrastructure and architecture.

The current electric power system is composed of a transmission system and a distribution system. These two systems combined create an interconnected system with varying levels of voltage and varying configurations. This sophisticated infrastructure is expensive and time consuming to develop. However, this architecture is a cost-effective model to provide electricity to a substantial number of clients (e.g. all citizens of a country). The low voltage distribution grid is the connecting point for a majority of industrial and residential clients. Therefore, guaranteeing the power quality at the end-user connection point is important for end-user satisfaction.

The planning for investment decisions resulting in the evolution of the distribution grid are multifaceted, long lasting and have a significant impact on the end-user experience. Distribution system operators' (DSO) investment decisions fall into two main categories: failure management and preventative investments. This thesis will focus primarily on preventative investments including the opportunity to adapt the existing architecture allowing new functionality. However, these investments are challenging due to uncertainties in the future evolution of load, generation and technology. The need for an adaptation of the distribution grid from a passive to an active network is primarily driven by the introduction of distributed energy resources (DER).

DER can create bi-directional flow, voltage deviation and congestion problems in the distribution grid. These new challenges can affect existing grid regulation devices which may not be capable of regulating voltage. Furthermore, DER may be connected by various stakeholders that are not responsible for guaranteeing power quality in the distribution grid. This could possibly increase costs for the distribution system operator (DSO) indirectly. Therefore, DSO are faced with a challenging new environment in relation to operations and planning of future distribution grids.

In order for DSO to plan for more intelligent distribution grid systems, smart grid development goals have been defined by various countries. This evolution is primarily driven by the goal of increasing DER integration and deferring infrastructure investments. The key to this new era of smart grid operations and planning is to optimize the available flexibilities of the distribution grid. Specifically, this thesis will explore three sources of flexibility: storage, demand side management (DSM) and curtailment. In order to perform techno-economic analysis of distribution grid flexibility, sophisticated planning and operations tools are necessary.

OPF is a class of optimization problems where active and reactive power of devices connected to the distribution grid can be optimized to minimize a cost function under power flow constraints. It is an appropriate tool to model the operation and planning of distribution systems that contain active elements. Due to the specificity of the distribution network characteristics, alternating current (AC) OPF is the most appropriate method. An AC OPF problem requires sophisticated techniques for its resolution, however these techniques are well documented in the

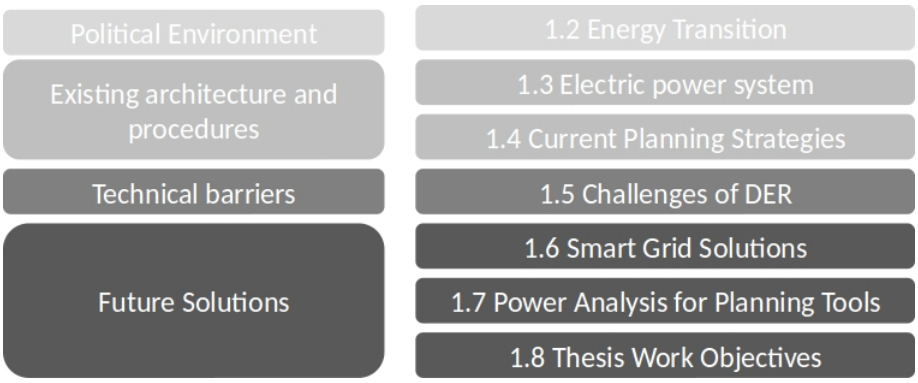

Figure 1.1: Introduction outline

literature. In this thesis, the problem resolution technique of convex relaxations has been chosen to guarantee a low calculation burden and optimal solutions. This thesis will focus on the development of operations and planning methodologies to address new challenges in planning and operations for smart grids.

These new planning methodologies and operational strategies will consider decentralized controllable devices such as storage, DSM and curtailment. They will consider investment costs, operational strategies and uncertainties to prioritize smart grid investments. The integration of DER along with the optimization of grid operations could result in lower maintenance costs and fewer waste products. Due to a high degree of uncertainty in renewable energy generator production, optimal management of decentralized components is difficult. Robust management strategies that consider these uncertainties in load profiles and decentralized production are critical. A figure summarizing the contents in this chapter can be found in Fig. 1.1.

1.2 The energy transition context

The discussion encompassing a future with easy access to high quality electricity is economically and culturally complex, as well as highly technical. A new mix of technologies will be necessary to satisfy an increasing demand and uncertain availability of future resources. With new technologies, new technical, political and cultural challenges arise. This new transformation of the future energy outlook plan is commonly referred to as the energy transition.

Energy and more specifically electricity is an essential part of developed countries daily activity. Once reserved only for the rich, electricity is now accessible by 83 % of the global population as sited by IEA [2]. Since electricity was invented, the GDP and wealth of a country has been closely connected to the availability and quality of the electricity. This has driven countries worldwide to invest in the development of the power transmission and distribution systems. Due to these investments, power systems expanded from small microgrids to interconnected transcontinental networks. The transit of energy from a centralized power plant down to individual customers became the most cost-effective solution.

The high dependency of modern society on electricity sheds light on the importance of guaranteeing the primary sources of electricity production. Over the past decades, the source of electricity production has evolved. As seen in Fig. 1.2, a continual increase in fossil fuels as well as nuclear electricity production is seen between 1971 and 2014. Increasing concerns about the sustainability of fossil fuels is a part of the driving forces of the recent energy transition.

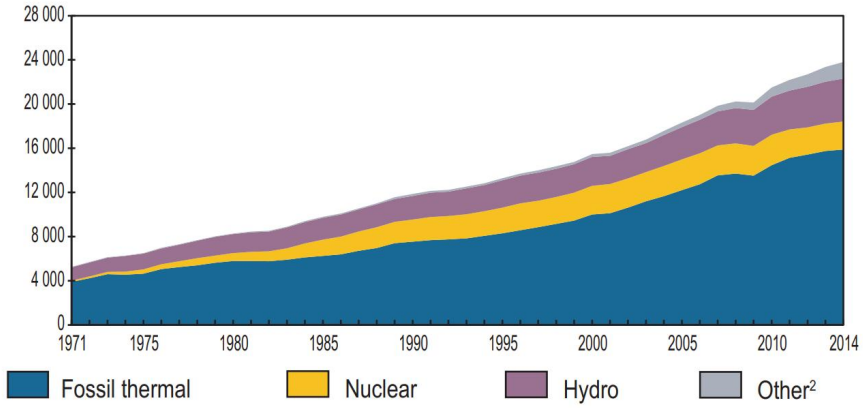

Figure 1.2: World electricity generation by fuel from 1971 to 2014 in TWh published by IEA

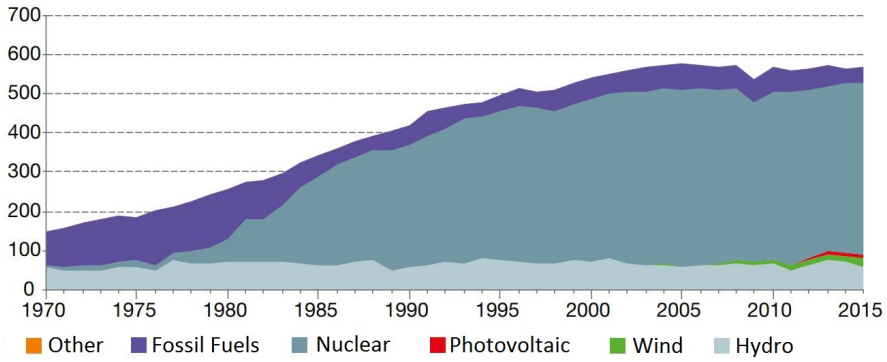

Figure 1.3: Electricity produced in France by source in TWh from 1970 to 2015 [2]

The current concern of stakeholders in electricity markets is to find a strategy of sustainable development that is dependent on renewable primary energy sources while guaranteeing power quality and security of supply in the future.

The energy transition from "traditional" resources to renewable ones is not the first energy transition in the history of the industrialized world. The first major energy transition was initiated by the discovery of fossil fuels in the 1700s. This transition took two centuries and, by the 19th century, fossil fuels became the primary global energy source. In 1973, oil accounted for 70 % of the total primary energy used to produce electricity in France. However, due to various oil embargoes and the growing concern of dependence on Middle Eastern countries' oil production, France invested in a new electricity production technology, nuclear. Between 1971 and 2001, 58 nuclear reactors were built in France. By 2015, a large percentage of the electricity produced in France resulted from nuclear generators as seen in Fig. 1.3. This figure shows the source energy mix of electricity production in France between 1970 and 2015. In the 2009 IEA report, it was reported that the French government had achieved their goal to produce at least 50 % of the electricity used domestically [2] therefore succeeding in their initial goals driving the energy transition started in the 1970s.

This massive development of nuclear power between 1971 and 2001 was primarily driven by EDF as well as substantial subsidies [5]. France had a desire to "create a distinct role for itself in the two decades following World War II". Involved actors started work to enable the trans-

formation into an "all-electric all-nuclear" society and therefore successfully transitioned their electricity production strategy in a period of 30 years. The major energy transition in France to nuclear was reinforced by strong government policy, large subsidies and a strong desire to revitalize France as a powerful world leader. Lessons learned from past major energy transitions included: "a stated ambition for an energy transition is not enough; energy alternatives have to be nurtured through a combination of research and technology development as well as deployment policies over a sustained period; nationalistic sentiments and centralized power appear to be important for marshaling resources in a sustained way; the existence of new types of energy firms and jobs can help governments to stay committed and focused; and the relative costs of new energy technologies also must develop favorably" [6]. These lessons learned can be helpful to ensure the success of the current energy transition.

Similar mechanisms have been put in place for the current energy transition. These mechanisms include subsidies, as well as policy and research funded by the European Union to encourage the development of decentralized generator technologies and their integration into the grid. The current energy transition resembles the previous energy transition in the fact that subsidies are available for the development of new technologies. A notable difference between the two transitions is the focus on decentralized generation as opposed to centralized generation. The integration of new decentralized generators imply a significant development of the distribution grid.

The renovation of the current distribution grid requires a passive system to be evolved into an active system with automation and control. This new active distribution system is often referred to as a smart grid. A smart grid as defined by the CEN-CENELEC-ETSI standards is an electricity network that can integrate, in a cost-efficient manner, the behavior and actions of all users connected to it (generators and/or consumers). This behavioral control ensures an economically efficient, sustainable power system with high levels of quality and security of supply and safety [7]. The next large-scale energy transition is currently emerging often associated in the literature with the term smart grid.

1.3 The electric power system

The development of an electric power system is expensive and time consuming. For example, the full development of the electric power system in France has been an ongoing task for the past hundred years. The three steps of development of an electrical power system include the initial electrification, the expansion of the system to supply a desired quantity of end-users and finally the quality assurance of the delivered electricity. In France this evolution began between 1880-1990 with the first industrial clients. The electric distribution grid was later labeled as a public service in 1906 when the development of distribution grids started to be present in large cities and densely populated areas. At this point, a majority of electricity was generated and used locally with few interconnections between cities. In 1938, the French government pushed to develop interconnections between existing distribution grids. EDF was created in 1946 to unite all the small private power producers into one entity and move towards a more standardized service of electricity in France. In the 1970s, EDF successfully interconnected an electric power system that reached almost all French citizens except individuals in very rural areas [8]. The connection of a majority of French citizens to the electric grid conveniently was completed just before the beginning of the development of centralized nuclear power plants as the primary electric generation source in France.

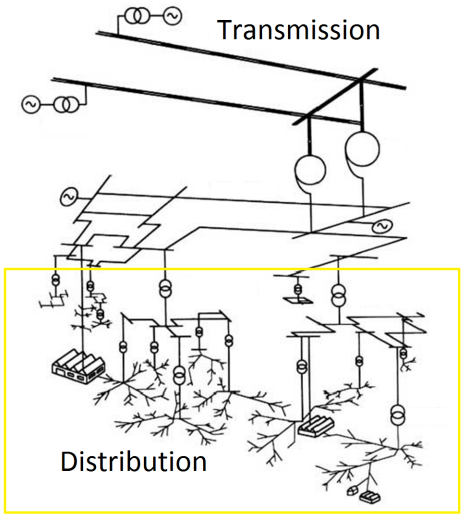

Figure 1.4: Grid components and voltage levels of an example transmission and distribution network [3]

The current architecture of the electric power system contains two primary electric grid structures: the transmission system and the distribution system. These two systems are connected and interact to transit electricity from primarily centralized producers to end-use clients. Therefore, the classical distribution grid is mono-directional which has encouraged a majority of distribution grids to be operated with a radial configuration.

The primary objectives of the transmission and distribution system is to transit electricity from the producer to the end consumer while maintaining power quality, minimizing losses and minimizing operational costs. To achieve this goal multiple levels of voltage are used in the transportation and distribution system to minimize losses and improve end-user power quality. Transformers are used at various stages to step down voltages to a level accessible for industrial, commercial and residential customers. A schematic of the transmission and distribution system and the connection of the two is found in Fig. 1.4. The transmission system is connected to a high voltage partitioning of lines that then are converted to medium voltage through transformers connected to industrial clients. Another transformer is used to lower the voltage to the low voltage distribution level that most commercial and residential customers are connected to [3]. The distribution system is represented by the bottom half of Fig. 1.4 highlighted in yellow. The current distribution grids were designed to distribute energy with a mono-directional flow of power from a substation to end-use customers.

1.3.1 The electric distribution system

The electric distribution system is the lower voltage system that a majority of end-use customers are connected to. Two voltage levels exist in a distribution system: medium voltage and low voltage. Two important technical specifications of a distribution system are the number of phases and voltage levels. In France, the medium voltage distribution grid ranges from 3 to 33 kV. The low voltage distribution system ranges between 110 and 600 V with the standard connection voltage of most customers being 230 V. Unlike the medium voltage distribution grid, the low voltage distribution grid can have single-phase clients. The low voltage distribution grid

is composed of three-phase systems that are connected to one-phase or three-phase end-user clients. The connection of a single-phase client to one phase and a different client to another phase of the three-phase system can create unbalanced loading scenarios. Therefore, low voltage grids often experience imbalances between phases of a three-phase system. Depending on the load profiles of varying clients, imbalances in the system can be more or less elevated.

Residential and commercial customers can use electricity at any time of the day. In France, there are 31.6 million residential customers and 4.9 million commercial customers [9]. Clients subscribe to a maximum power usage and then pay by kWh their total energy use. The end use quality of the power delivered by the DSO is required by legislation in France to be +-5 percent for the medium voltage distribution grid [10] norm C13-200 and +-10 percent for the low voltage distribution grid [10] norm C15-100. This implies that a client has very few limitations, besides the maximum power value, on how much energy and which periods of the day the client is allowed to use energy. The distribution grid operator then is responsible to balance the electric production and consumption that is required to cover the load at the lowest possible cost.

1.4 Planning strategies for distribution systems

The investment strategy of a country in relation to the electric distribution system can significantly affect the experience of end-users and the future development of smart grid functionality. These investment decisions are often expensive and are long-lived. Investments in electrical lines, transformers, or security equipment could last from 2 to more than 40 years. The planning strategy often must find an investment schedule considering for example the current investment price, the life span of the investment, the timing of the proposed investment in relation to the long-term investment strategy, risk assessment of aging material, time of implementation and attempting to prepare for future possible new uses of the distribution grid. The planning strategy must take these considerations into account to find the optimal economic strategy.

The distribution grid investment strategy of the French DSO is managed by Enedis which is funded by a user tariff (Tarif d'Utilisation des Réseaux Publics d'Electricité) proposed by the CRE and approved by the government. The investment choices of Enedis must satisfy power quality and safety regulations while minimizing the environmental impact and the final cost to the society. The main axis pursued for the maintenance and expansion of the current electric grid include: resolution of specific technical problem, long term architecture planning, required annual investments including new customer connections or replacement of broken components and future environmental concerns that require the reduction of CO_2 emissions [4]. These planning goals lead to two main categories of infrastructure investments: failure management and preventative investments that reduce future failures, improve the quality, or reduce the cost of service. This thesis will focus primarily on preventative investment planning that addresses increasing load and grid adaptation to encourage renewable energy integration.

Preventative investments are difficult to calculate due to high uncertainty in future failures or power quality issues, new strategies or technologies that have not been extensively tested, the evolution of load profiles and the future penetration of decentralized generators. For the testing and validation of new innovative solutions, numerous test platforms and demonstration projects have been developed [11, 12, 13]. These projects attempt to analyze and validate the cost benefits of innovative technologies that may facilitate grid operations, improve system efficiency and increase the penetration of renewable energy systems. Pilot projects can be expensive and time consuming. Therefore, mathematical modeling is also used for techno-economic analysis of

network renovations.

1.4.1 Increasing demand - new clients and evolution of existing clients

For new customer connections or the evolution of the maximum power subscribed by a client, studies addressing existing line capacity are necessary. These studies are often power flow calculations for worst-case scenarios, in order to minimize risks. The recent evolution of electric meters allows for a more detailed data collection of client consumption. The new more sophisticated metering devices allow for an increased controllability of appliances and the possibility to connect small decentralized generators with associated tariff schemes. This large push to renovate electric meters has significantly increased the observability and the possibility of controllability in the low voltage distribution grid. However, the exploitation of the controllability is not yet widely implemented. These new smart meters allow for the more precise analysis and optimization of existing architecture to avoid unnecessary costly infrastructure investments [14]. The evolution of the distribution grid is also dependent on the trends of electric demand country wide. For this reason, it is important to address briefly the analysis of RTE which is more specifically related to the transmission grid but has direct effects on the evolution of the distribution grid.

The evolution of the demand for electricity varies for each country based on political strategy, cultural context, climate conditions, etc. Specifically, in France, there are varying scenarios for future electric demand as published by RTE [15]. Fig. 1.5 shows three primary trends of total electric consumption for the three main energy sectors: residential, industrial and commercial. These three scenarios are developed from detailed analysis of historical data and current trends in all three sectors. The primary influence creating three possible demand scenarios is based on three key unknown factors: i) energy efficiency of future appliances, ii) new end-user appliances deployment such as EVs or the switching between energy sources such as replacing an oil boiler with a heat pump, and iii) unknown increase in population therefore increasing housing density and economic activity.

As seen in Fig. 1.5 the dotted line represents RTE's plan for electric generation to have sufficient energy to meet the load requirements. For two out of three scenarios, the projected generation in relation to the projected demand increases in the next 4 years.

1.4.2 Integration of decentralized generation

The current procedure of Enedis to connect decentralized generators includes verification of short circuit security, harmonics produced by generator, perturbations of the communication system with safety components, flicker in voltage profile, maximum line capacity study, and indicating a set maximum possible current injected by the generator. These regulations force the DSO to often reinforce existing lines when installing new generators or creating new separate lines specifically for the generator [14]. The overall goals of France for the energy balance objectives in relation to the transmission grid is important to understand the possible effects on the distribution grid.

The energy production in France as stated by RTE will most likely have an increasing trend to match the increasing trend of load. In RTE's adequacy report [15], the evolution of renewable energy, nuclear power and fossil fired plants is discussed. Fig. 1.6 shows the evolution of supplied energy for each technology to meet an increasing demand in the high-need scenario and a constant demand in the low-need scenario. More specifically, Fig. 1.7 shows the renewable

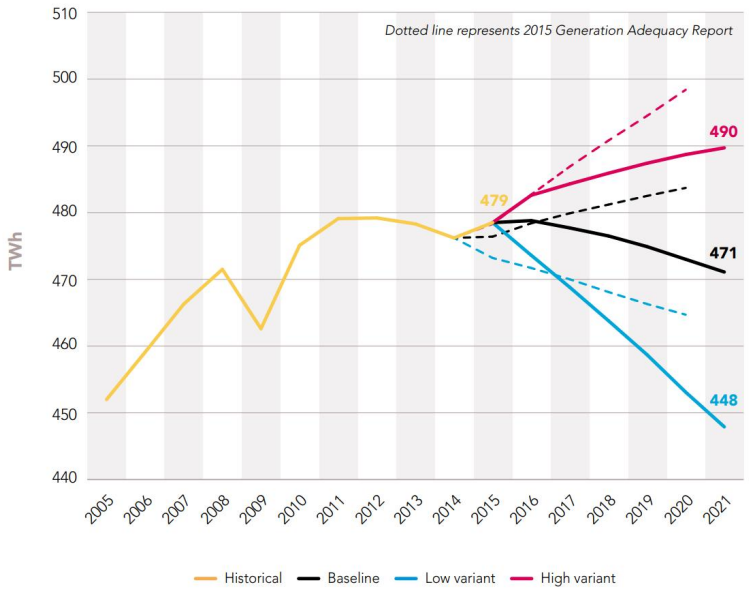

Figure 1.5: Annual domestic electricity demand in mainland France at reference temperatures

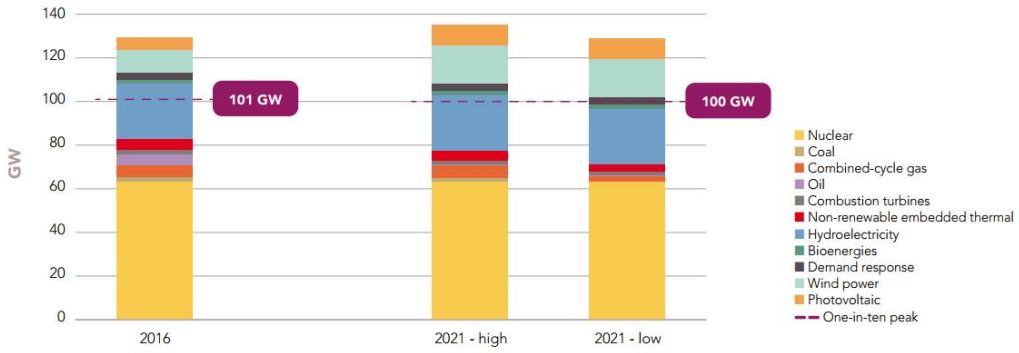

Figure 1.6: Forecast trend in supply in France between 2016-2021

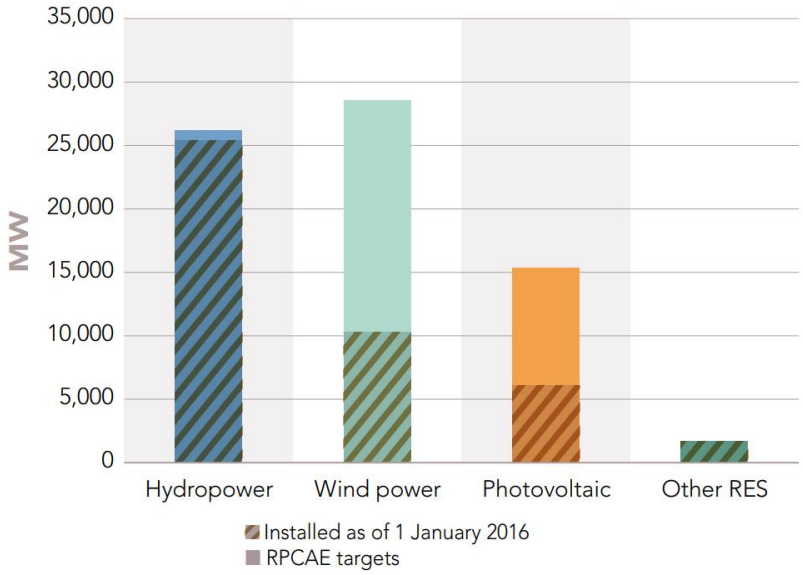

Figure 1.7: Regional plans for the climate, air and energy (RPCAE) renewable energy targets for mainland France

energy development targets in France for the next 5 years (2016 to 2021).

1.4.3 Mathematical tools for distribution grid planning with DER

There are two main groups of mathematical tools that exist for distribution grid planning. These tools include the tools that are actually used by current DSO and the proposed more innovative tools that exist in academic literature. The current tools used by the DSO include different techno-economic indicators to evaluate investment choices. For example, in France, these indicators include return on investment, rate of return or discounted benefit as described in [3]. Mathematical modeling tools such as power flow analysis are also used to give insights into the behavior or expected operation of a distribution grid. The presence of new decentralized generators, can significantly affect the voltage profile of a distribution grid. Therefore, detailed power flow models are necessary to quantify these effects for intelligent planning of these generators. Current assumptions for power flow analysis used by the French DSO can be found in Fig. 1.8. Often these power flow studies use simplifications of grid operations and single time step analysis. Existing power flow algorithms include the forward/backward sweep, Newton Raphson method [16, 17], fast-decoupled load-flow method [18, 19], z-bus matrix construction method [20], and loop impedance method [21, 22]. A power flow calculation is capable of calculating the currents and losses in all the branches (lines, cables, and transformers), the voltage in load buses, the reactive power in generator buses and the active and reactive power in the slack bus (primary substation in a distribution grid). This method gives full detail of the electric system for a given instance.

Power flow analysis is effective for certain grid analysis studies, but in the context of an ADN, power flow analysis is incapable of optimally managing controllable devices. More adapted methodologies that exist for ADN in the literature include OPF analysis. OPF analysis is not very commonly used in distribution grid planning. In contrast to a power flow analysis, an OPF

algorithm is capable of performing multi-period analysis. A multi-period analysis is important when temporally dependent variables such as storage are present. An OPF can also take into account the bounds of each variable including voltage and current limits of a network and generator power limits. Therefore, the OPF is more appropriate for smart grid analysis.

Many OPF algorithms are proposed in the literature for power systems applications as described in [23]. These algorithms are grouped into three main categories: DC approximations, non-linear convex approximations or non-convex problems. In the context of distribution grids, DC approximations are often not accurate enough for planning and operations algorithms. DC approximations can be used to reduce calculation time and eliminate convergence problems. However, a DC approximation makes linear assumptions about the losses in the lines and does not consider the transit of reactive power flows. These two characteristics are critical in the distribution grid. Due to a high ratio between the resistance and the reactance of lower voltage networks, losses are not linear but quadratic as a function of the current. The reactive power transit in a distribution system can also have effects on the voltage profiles and congestion problems. Therefore, full AC power flow models should be used when performing distribution grid analysis.

Full AC power flow models are non-linear and non-convex. Non-convex problems are often solved by decomposition or heuristic techniques which can be costly in terms of calculation burden. Within the non-linear convex category, there exist two main convex relaxations: the SDP relaxation and the SOCP relaxation. Both of these relaxations have been proposed in various papers for distribution power system analysis. These papers often address operations of distribution grids [24] [25] [26] [27] [28] [29] [28] [30]. Few are presented as planning algorithms [31] [32] [33]. An OPF is capable of calculating optimal set points of controllable devices during multi-period analysis. It assumes a centralized control that optimizes the entire network. This implies that one actor is controlling all the controllable devices with one primary objective. The lack of controllability and observability in current distribution grids make the OPF somewhat unrealistic. However, increased decentralized generators could make this control and optimization more important.

1.5 Challenges of decentralized energy resources

Some possible decentralized generators that are often connected to the distribution grid include PV, wind turbines and micro-hydroelectric generators. These decentralized generators bring about new challenges for the distribution grid operators. These challenges include bi-directional or increased power flow within the network, voltage profile deviation and compromised safety of equipment. To exacerbate these challenges, uncertainties in the distribution grid are high due to reduced aggregation effects in comparison to medium and high voltage grids. Unpredictable variation in load and generation can create high fluctuations in network power flow therefore causing unpredictable changes in the voltage profile.

The principal challenges associated with DER are discussed in [34]. The primary difficulty in relation to the quality of power delivered can be related to voltage level, and power conditioning. Localized voltage regulation is important at the distribution level. The voltage level can be significantly affected by high variations of power flow in the electrical lines. Undesirable effects such as flicker or voltage deviations can occur. Power conditioning through voltage regulation devices (e.g. tap changing transformers or static var compensator) is not always compatible with decentralized generators. Decentralized generator inverters can also contribute to harmonics in

	Etude HTA	Etude BT
Modèle des réseaux	- Réseau HTB vu comme une source/récepteur d'énergie de puissance infinie. - **Réseau HTA supposé triphasé équilibré**, représenté par un schéma monophasé équivalent. Conducteurs HTA représentés par des modèles en Pi : résistance et inductance séries + capacitance parallèle. - **Réseau BT agrégé** sous la forme d'un nœud de consommation/production au secondaire des transformateurs HTA/BT.	- Réseau HTA vu comme une source/récepteur d'énergie de puissance infinie. - **Réseau BT supposé triphasé déséquilibré**, représenté par un schéma triphasé équilibré avec neutre et un coefficient statistique de déséquilibre entre phases. Conducteurs BT représentés par des résistance et inductance séries.
Modèle des utilisateurs	- **Puissance ponctuelle aux nœuds de production et de consommation (pas de profils temporels).** - Foisonnement de consommation considéré : puissance consommée en aval du transformateur HTB/HTA répartie aux nœuds de consommation au prorata de leur puissance maximale mesurée le jour le plus chargé de l'année P^*_{max}. - Tangente phi des consommateurs fixée à 0,4 par défaut.	- **Profils temporels individualisés de puissance pour chaque consommateur**, qui indiquent une moyenne et une variance de puissance à chaque pas horaire en jour ouvré et en jour férié. - **Puissance constante des producteurs** : nulle ou maximale selon les études. - Foisonnement de consommation considéré : aléa supposé gaussien autour de la puissance moyenne individuelle. - Tangente phi des consommateurs fixée à 0,5 par défaut.

Figure 1.8: Hypothesis used by the French DSO for medium voltage and low voltage distribution systems planning studies [4]

the grid which reduce power quality, affect negatively regulation and safety devices [34].

Additionally, DSO are not the only entity installing decentralized generators, adding further challenges to guarantee power quality. Individuals, companies and also private power producers have increased their interest in DER in the past years due to increasing environmental concerns and subsidies for renewable energy development. While in France, one primary player exists (EDF), new players are emerging offering alternative energy generation possibilities. These new decentralized generators may be used for alternative uses not aligning with the objectives of EDF or Enedis. However, these generators may still be connected to the distribution grid. This implies a new usage of the existing architecture. This introduction of multiple players forces the DSO to adapt current planning and operational strategies to host such demands.

1.5.1 Increased or bi-directional current

DER generators can act as current sources connected to decentralized nodes throughout the network. The injection of current into a distribution grid at a decentralized node can cause local challenges. If a high capacity of DER is installed in an area that has low load, current can flow from the decentralized node towards the substation. This reverse current flow can have effects on safety devices, voltage regulation devices and maximum current limits of distribution lines. Certain nodes may have so much DER installed in networks with low loading scenarios that reverse current exceeds maximum current values of the electrical line. Therefore, possibly requiring a re-sizing of the current electrical line based on the peak load resulting from peak injection of the generator.

Safety devices in distribution grids can be significantly affected by an increase or reverse

power flow created by decentralized generators. Fuse coordination can be affected by DER due to the fact that DER change downstream current. If DER do not disconnect early in a fault situation, security devices attempting to clear the fault could malfunction. This can cause further damage to conductors, insulators or DER itself. Existing breakers, reclosers and fuses may also be affected if these devices are already operating close to their rated maximum device current. DER can increase the existing currents running through these devices therefore exceeding maximum current limits. Faults on adjacent feeders can have tripping effects on DER, therefore disconnecting the DER for no reason and propagating the fault signal. When generators are connected to a low voltage system with a grounded wye connection, the DER can have a negative effect on the ground fault coordination of utility breakers and reclosers. For a more extensive and more detailed list of other safety concerns see [35].

1.5.2 Voltage regulation devices

Generally, DER will increase the voltage profile locally where it is installed due to the injections of power into the distribution grid. The DER can inject active power but also reactive power. Active power injection when correlated with local loading of the feeder can decrease losses in the distribution system. However, injected active power far away from load can increase losses. Reactive power injection is not allowed in some countries due to undesirable effects of interactions with existing voltage regulation components such as switch capacitor banks or OLTCs. However, reactive power control to assist volt var regulators has been shown to be promising [36] [37].

If DER do not attempt to regulate local voltages, normally switch capacitor banks are unaffected. However, if DER do attempt to control local voltages or change downstream current of the regulating device, line drop compensation calculations may no longer be accurate. Both switch capacitor banks and step type voltage regulators attempt to calculate the downstream voltage based on the current close to the device. Assumptions of downstream voltage are no longer accurate if DER attempt to change local voltage or inject significant power into the grid. Therefore, downstream voltage regulation calculations are no longer accurate [35].

1.6 Innovative smart grid solutions

In the current context of smart grids, the existing electric grid infrastructure should evolve in the following areas as stated by the US Congress: increased digital information and controls, dynamic optimization of grid operations, deployment of distributed resources, incorporation of demand-side resources and demand response, deployment of smart technologies and integration of smart appliances and consumer devices, deployment of storage and peak-shaving technology, provision of timely information and control options to consumers, standard development for communication and interoperability of equipment and identification, and lowering of unreasonable barriers to adopt smart grid technology, practices, and services [38].

Smart grid solutions are often proposed to optimize existing infrastructure therefore delaying power electronic and infrastructure investments. The idea of a smart grid is to optimize certain flexibilities available in the grid as opposed to allowing a passive operational scenario. A review of ADN enabling technologies can be found in [39]. This review covers a general summary of existing solutions to transform a passive traditional distribution system into an ADN. These strategies include the active control of generator dispatch, transformer tap positions, voltage regulators, reactive power and system configuration. The strategies discussed in [39] to be the most common ones found in the literature include demand side management, storage devices,

dynamic line rating, voltage and power control, fault current limiters and advanced distribution protection. This thesis will focus primarily on three of these solutions including storage devices, demand side management and power control in the form of curtailment.

1.6.1 Storage

The advantages of storage devices in ADN are well documented in [40]. Techno-economic analysis is necessary to evaluate if the advantages of battery systems outweigh their costs. The main categories of storage benefits as described by [41] include bulk energy services, ancillary services, transmission infrastructure services, distribution infrastructure services and customer energy management services. The primary benefits analyzed in this thesis include lines loss reduction, electric energy time-shifting, minimization of DER curtailment and mitigation of congestion problems.

With variable prices of electricity, retail electric energy time-shift can become economically advantageous. Economic benefits occur when storage units absorb energy during periods when electric prices are low and resell the electricity during periods when electric prices are high. This mechanism allows storage devices to reduce operational costs for a DSO or reduce electric bills for residential and commercial customers. Naturally a distributed storage device managed by the DSO can also decrease line losses. Distributed storage devices may also significantly reduce necessary curtailment when installed close to decentralized generators. When attempting to optimize a whole feeder, a centralized optimization algorithm is most effective to determine the operational set points of each storage device. These types of algorithms can coordinate the operation of decentralized storage devices so that a conflict of interest does not occur possibly creating more problems for the DSO.

1.6.2 Demand side management

Demand side management can be implemented passively by giving price signals to end-user customers and encouraging behavioral changes. Active control of devices is another technique. Often these devices that are possible to control are devices that are not time sensitive. For example, the washing machine that must be finished by a certain time in the evening but the precise hour when the machine is launched is less important. The second type of controllable load has some inherent storage, for example hot water heaters or space heating equipment. If the thermal inertia of a thermal electrical load is large enough, these devices can be turned off for certain periods without affecting significantly end-user comfort. This type of demand side management is based on a sort of decentralized thermal storage characteristic that when cumulated can have significant effects on operational grid costs.

1.6.3 Curtailment

Curtailment is the active reduction of power of a decentralized generator below the ideal power output operational set point because the grid is incapable of absorbing the produced power. This can be caused when decentralized generation is high and electric consumption is low. The injection of large amount of power into an unloaded feeder can result in backwards power flow, voltage rise and congestion problems. This strategy is implemented usually if there is not another solution to consuming the excess energy. It can be cost-effective in comparison to infrastructure reinforcements but can negatively affect the payback period of the generator.

1.7 OPF analysis for planning tools

OPF algorithms are capable of analyzing multi-period problems and calculating optimal set points of controllable variables. An OPF analysis allows the consideration of flexibilities of smart grids to be considered during the planning phase. An optimization algorithm is capable of minimizing or maximizing multiple parameters while considering the boundaries and requirements of each variable (i.e. power quality constraints). This approach is effective in grid simulation because it is capable of taking into account the system of equations used to describe a power flow in electrical lines while minimizing certain parameters such as losses. Optimum power flow has been used in the management and planning of the transmission grid however the use of optimum power flow in distribution systems is less frequent. An extensive review of optimization algorithms in the context of transmission system planning can be found in [42].

Optimization algorithms are capable of integrating the benefits of smart grid operations and devices into the planning process. These types of algorithms have been proposed in the literature but are rarely used in current planning strategies of the DSO. OPF analysis can include DC or AC power flow equations depending on the system analyzed. The classic power flow problem (AC model) calculates the active and reactive power flow at each node. However, AC power flow calculations are non-linear, non-convex and high-dimensional, which can be computationally intensive. Methods for resolving this non-linear system of equations include the forward/backward sweep, Newton Raphson method [16, 17], fast-decoupled load-flow method [18, 19], z-bus matrix construction method [20], and loop impedance method [21, 22].

The resolution of an OPF requires evolved techniques due to the fact that the problem formulation is high-dimensional and non-linear. Furthermore, these equations are considered non-convex. Convexity is the characterization of a set of values. A set of values is convex if any line drawn between two points in the set is also included in the given set [43]. This implies that, with solving techniques such as the interior-point method, simply following the gradient of the solution set will allow the algorithm to find the absolute minimum or maximum of the function. If a problem is not convex, following the gradient of the set will not result in finding an absolute minimum or maximum. Therefore, other techniques are used to attempt to find the absolute minimum of the solution set. These techniques include heuristics methods that consist of testing the solution space and comparing final values, thereafter selecting the best values. Examples of heuristic methods include particle swarm optimization [44], artificial bee colony [45] [46], differential evolution [47] and a hybrid tabu search particle swarm optimization [48]. However, heuristic algorithms often require a long calculation time as noted in [49] when compared to convex relaxation algorithms. The relaxation of certain equations to create a convex problem has been widely explored in the literature [50, 51]. The convex problem may not represent exactly the initial problem but can still find an optimal solution to the original problem. The advantages of heuristics include a real representation of the initial problem. The disadvantages include a substantial calculation burden and a final solution that is not guaranteed to be optimal. The advantages of convex relaxations are a low calculation burden and if the relaxation is proven to be exact, a guaranteed optimal solution.

The family of convex relaxation algorithms that is most commonly used for distribution grids is called a Quadratically Constrained Quadratic Program (QCQP). In multiple studies, the non-convex power flow equations have been cast as a QCQP as shown in [52, 53]. Within the QCQP family, two convex relaxation algorithms exist including the Second-Order Cone Program (SOCP) or the Semi-Definite Program (SDP). An SDP convex relaxation has been proved to be exact under certain conditions by [54]. While an SOCP relaxation has also proved to be exact

under certain conditions as stated in [55, 50, 56]. However, these relaxations have been proven to be inexact during periods of high renewable energy production feeding into the grid due to elevated line losses [57]. In order to determine the hosting capacity of a distribution grid, it is critical to have a precise and accurate calculation methodology when RE production is high. An example of this difficulty could be high photovoltaic (PV) production during the summer season. In order to overcome the challenge of inaccurate results at periods of high PV injection, [57] presents an AC optimum power flow algorithm that integrates linear cuts, implemented in a iterative fashion, to ensure an exact and feasible relaxation of the power flow equations. This single-phase AC optimum power flow algorithm has then been developed into a multi-temporal algorithm in order to more effectively evaluate the benefits of grid connected storage in [58].

1.8 Thesis work objectives

Through power flow modeling and optimal power flow modeling, strategies of distribution planning and operations will be explored during this PhD. The main contributions of this thesis are the proposed methodologies for the planning and operations of distribution grids through sophisticated OPF tools. The author of the thesis studies the current methodologies and tools available for the distribution system planning and operations. These methodologies are analyzed for their applicability in smart grids with high renewable energy penetration. New methodologies are proposed that improve the current methodologies existing in the literature. Case studies are implemented to demonstrate the concrete results possible of such studies. The contributions of this thesis are summarized as:

- evaluation of the importance of three-phase unbalanced power flow equations in the context of planning and operations of distribution grids
- development of a methodology for the simultaneous optimal sizing and placement of decentralized storage devices
- development of a methodology that considers uncertainties while generating day-ahead storage and controllable load schedules through stochastic optimal power flow analysis

This thesis is divided into three main sections. First, (Ch. 2), low voltage three-phase unbalanced systems are analyzed to identify the specificity of these systems and how these specificities affect the planning and operations of such systems. A more detailed literature review is presented specifically related to three-phase unbalanced systems. An analysis of the effects of these imbalances on the power flow equations is presented. A case study is implemented to quantify these effects. In conclusion, accuracy improvements of the detailed analysis of three-phase systems are deemed to be insignificant in the context of OPF planning and operations analysis. This conclusion motivates further studies in the thesis to consider single-phase estimations for each phase as opposed to fully developed unbalanced three-phase equations.

Second, (Ch. 3), deterministic OPF planning methodologies are presented for decentralized storage analysis. Multi-temporal aspects of an OPF algorithm are presented including a case study calculating the hosting capacity of an example distribution grid. Further adaptation of the OPF algorithm is presented for the use of optimal sizing and placement of distributed storage devices. A case study is presented showing the advantages of optimal distributed storage devices. The chapter concludes by presenting the real world applications of presented methodologies.

Figure 1.9: Thesis document outline and main contributions

Chapter	State of the art	Methodologies	Case studies
Ch 2	• Three-phase unbalanced multi-phase systems and OPF applications		Three-phase power flow calculations comparing fully developed unbalanced three-phase equations with single phase approximations
Ch 3	• OPF algorithms applying to distribution grid for storage analysis	Simultaneous optimal placement and sizing of distributed storage elements	• Multi-temporal OPF used to calculate hosting capacity • Improved performance of distribution grid with optimally sized and placed storage devices
Ch 4	• Uncertainties that affect operations in the distribution grid • Stochastic OPF algorithms used for distribution grid analysis	Stochastic OPF for the robust day ahead planning of grid flexibilities such as storage and DSM	Performance improvements of stochastically managed storage and DSM

Third, (Ch. 4), uncertainties in generation and load profiles are discussed. A methodology for integrating these uncertainties into the operations of distribution grids is presented. A case study showing the added benefits of DSM and storage is analyzed. Conclusions are drawn about the importance of considering uncertainties in the operations and planning process for distribution grids. A schematic outline of the thesis topics is found in 1.9.

Chapter 2

Low voltage unbalanced distribution networks

Résumé

Les réseaux de distribution sont composés de lignes à moyenne et basses tensions qui distribuent l'électricité au client final. Lorsque l'on considère leur planification et gestion, il est essentiel de prendre en considération les freins spécifiques au réseau de distribution basse tension. Ces spécificités incluent un ration R/X plus important, une grande amplitude du à un nombre important de lignes électriques et à l'existence de déséquilibres entre les phases. Garantir une puissance de qualité au niveau de la basse tension pourrait être considéré comme le critère le plus critique du fait de l'impact sur la satisfaction du client final. En revanche, la visualisation et la contrôlabilité manquent cruellement à ce niveau. Les outils existants pour l'analyse du réseau basse tension sont présentés dans la littérature mais ne sont pas spécifiquement adaptés pour les études OPF. Ce chapitre explore les techniques de modélisation existantes pour les systèmes triphasés basse tension ainsi que les modèles OPF existant prenant en compte de multiples phases déséquilibrées. Les calculs sur trois phases déséquilibrées sont comparés avec les estimations monophasées de chaque phases. Les conclusions finales portent sur la précision versus la complexité du couplage entre phases. L'estimation monophasée de chaque phase est définie comme étant suffisante dans les études de planification. Cette méthode est donc celle utilisée pour les chapitres suivant de la thèse.

2.1 Summary

Distribution grids are composed of medium voltage and low voltage lines that deliver electricity to end-users. When considering their planning and operation, it is essential to consider the specific challenges present in the low voltage distribution network. These specificities include a higher R/X ratio, high dimensionality due to a large number of electrical lines and the existence of imbalances between phases. Guaranteeing power quality at the low voltage level could be considered the most critical in relation to end-user satisfaction. However, observability and controllability is significantly lacking at this level. Existing tools for low voltage grid analysis are presented in the literature but are not specifically adapted for OPF studies. This chapter will explore the existing modeling techniques for low voltage three-phase systems as well as existing OPF models considering multiple unbalanced phases. Three-phase unbalanced calculations are

compared to single-phase estimations of each phase. Final conclusions are discussed about the accuracy vs complexity of considering the coupling between phases. The single-phase estimation for each phase is concluded to be sufficient in planning studies and therefore is the method used for the following chapters of the thesis.

2.2 Introduction

In order to accurately analyze low voltage distribution networks, the specificity of these networks must be considered. This specificity includes a higher R/X ratio, a higher quantity of nodes and the possibility of three-phase imbalanced power flow. These challenges will now be addressed individually in relation to their direct consequence on low voltage distribution network analysis.

The primary difference between low voltage distribution grids and medium voltage distribution grids or transmission grids is a high R/X ratio. This implies that the relative value of the line resistance (R) is much higher than the relative value of the line reactance (X). In the case where R is relatively much larger than X, the losses become non-linear. This implies a quadratic relationship between voltage and the apparent power load [59]. A high R/X implies that linear estimations of the losses are no longer accurate. For modeling purposes, to accurately calculate losses and consequently the voltage profile the quadratic current equation is necessary.

The large size of low voltage distribution grids introduces an increased size to the problem. In France, the low voltage distribution grid network is composed of 1.3 million kilometers of electrical lines in comparison to the 100,000 kilometers of the transmission lines [60]. Distribution grids also tend to have a significantly larger number of nodes than a transmission grid. When attempting to optimize a grid with a large number of nodes, the high-dimensional problem results in a high calculation burden. The use of optimization algorithms on these networks require simplification strategies without losing accuracy.

The low voltage distribution network can experience an unbalanced three-phase power flow as opposed to normal operational conditions of medium voltage or high voltage networks that are typically balanced due to equal loading of each phase. These imbalances are a result of low voltage residential and commercial customers being connected to the grid on only one phase. Inherently with the varying electric load profiles of different single-phase customers, power imbalances between the phases can occur [61]. These imbalances can result in increased line losses, protective relay malfunction, system voltage profile deviation, saturation of transformer current or power and decreased end-use power quality [62]. The end quality of three-phase low voltage grids is highly critical for end-use customers and is difficult to control for the DSO.

This chapter therefore addresses these specificities in the context of power flow analysis. Unbalanced multi-phase power flow calculations are compared to single-phase power flow calculations. The three-phase unbalanced power flow equations are developed in the first half of the chapter followed by a case study. The case study is used to complete three comparative studies. The first study compares the unbalanced power flow calculation using presented methods with an existing low voltage distribution grid simulation software, OpenDSS [63]. The second study compares a power flow calculation of the original grid and the simplified grid using simplification techniques presented in section 2.3.3. The third study compares a three-phase unbalanced power flow calculation with a single-phase power flow estimation for each phase. In the second part of this chapter, a literature review is presented for existing OPF multi-phase unbalanced algorithms. Two algorithms found in the literature are implemented. However, these algorithms are found to have convergence problems and difficulty in relation to scalability. In conclusion, single-

phase estimations of three-phase unbalanced systems in the context of optimization algorithms were proven to be sufficient for planning methodologies.

2.3 Single-phase and three-phase unbalanced systems

The power flow equations for a single-phase AC power flow and a three-phase unbalanced power flow are different due to neutral current effects caused by imbalances. These effects can create voltage profiles divergence, increased losses in the neutral line and increased losses within the transformer. The two formulations will be developed and compared in the next two sections.

2.3.1 Single-phase power flow formulation

Two different sets of equations can be used within a power flow model, the bus injection model (BIM) or the branch flow model (BFM). While both models can be effective for various applications, the BFM system of equations will be used due to better convergence characteristics as explained in [50], specifically in relation to a radial network topology.

$$P_{ij} = P_{ul,j} + \sum_{k=1}^{K} P_{jk} + r_{ij} I_{ij}^2 - P_{pv,j} + P_{st,j} \tag{2.1}$$

$$Q_{ij} = Q_{ul,j} + \sum_{k=1}^{K} Q_{jk} + x_{ij} I_{ij}^2 - Q_{pv,j} + Q_{st,j} \tag{2.2}$$

Equation eqs. (2.1) and (2.2) describe the balance of power from the upstream and downstream branches where P_{ul}, P_{pv}, and P_{st} are the instantaneous load, PV production and battery storage charge or discharge at a given time step, respectively. P_{ij}, r_{ij}, Q_{ij}, x_{ij} and I_{ij} are the power, the resistance, the reactive power, the reactance and the current associated with the branch ij, respectively. Q_{ul}, Q_{pv}, and Q_{st} are the instantaneous reactive load, PV reactive production, and battery reactive power values, respectively. The voltage at each node can be calculated by the equation (2.3).

$$|V_j|^2 = |V_i|^2 - 2(r_{ij} P_{ij} + x_{ij} Q_{ij}) + (r_{ij}^2 + x_{ij}^2) I_{ij}^2 \tag{2.3}$$

where $|V_j|$ is the voltage magnitude at node j. The current of each branch is calculated as shown in equation (2.4).

$$I_{ij}^2 = \frac{P_{ij}^2 + Q_{ij}^2}{|V_i|^2} \tag{2.4}$$

2.3.2 Unbalanced power flow formulation

The three-phase unbalanced power flow that takes into account neutral current effects but ignores shunt resistance effects uses the same power balance equations in eq. (2.1) and eq. (2.2) but uses a more complicated equation to calculate the voltage at each node. In order to find the equivalent equation of 2.3 for three-phase unbalanced systems, it must be derived from the basic voltage equation as found in chapter 6 of [64]. The basic voltage equation for a three-phase system is found in eq. (2.5).

$$\begin{bmatrix} V_{an} \\ V_{bn} \\ V_{cn} \end{bmatrix}_i = \begin{bmatrix} V_{an} \\ V_{bn} \\ V_{cn} \end{bmatrix}_j + \begin{bmatrix} z_{aa} & z_{ab} & z_{ac} \\ z_{ba} & z_{bb} & z_{bc} \\ z_{ca} & z_{cb} & z_{cc} \end{bmatrix} \times \begin{bmatrix} I_a \\ I_b \\ I_c \end{bmatrix}_{ij} \tag{2.5}$$

If shunt resistance is considered the three-phase imbalanced voltage equation becomes eq. (2.6).

$$\begin{bmatrix} V_{an} \\ V_{bn} \\ V_{cn} \end{bmatrix}_i = \begin{bmatrix} V_{an} \\ V_{bn} \\ V_{cn} \end{bmatrix}_j + \begin{bmatrix} z_{aa} & z_{ab} & z_{ac} \\ z_{ba} & z_{bb} & z_{bc} \\ z_{ca} & z_{cb} & z_{cc} \end{bmatrix} \times \left(\begin{bmatrix} I_a \\ I_b \\ I_c \end{bmatrix}_{ij} + \frac{1}{2} \times \begin{bmatrix} y_{aa} & y_{ab} & y_{ac} \\ y_{ba} & y_{bb} & y_{bc} \\ y_{ca} & y_{cb} & y_{cc} \end{bmatrix} \times \begin{bmatrix} V_{an} \\ V_{bn} \\ V_{cn} \end{bmatrix}_j \right) \tag{2.6}$$

Due to limited grid characterization data for low voltage grids, shunt resistance values and data for each node is often not available. Therefore, a modified line model is often adopted in order to reduce the calculation complexity and minimize data collection for certain studies. It is also shown in [64] that the shunt admittance is often so small, neglecting shunt admittance effects does not significantly affect the calculated solutions. Therefore, the voltage profile calculation can be simplified to be eq. (2.5) without decreasing the accuracy.

A further simplification is also detailed based on the fact that often full impedance matrices are not well defined for low voltage lines and grids. Therefore, symmetric components are widely used. A different simplified model called the "approximate line segment model" allows the power flow calculation only depending on these two parameters. The impedance matrix is therefore simplified by taking the sequence impedance matrix and assuming equal dependencies between each phase. This assumption can be made for lines that are transposed. The transposition of lines along the length of the line (changing of position of one phase with the others) ensures that the magnetic fields surrounding each line are evenly distributed therefore equalizing the effects of one phase on the other. Therefore, the sequence matrix is then defined in eq. (2.7) assuming transposed lines.

$$\left[\ Z_{eq} \ \right]_i = \begin{bmatrix} z_0 & 0 & 0 \\ 0 & z_p & 0 \\ 0 & 0 & z_p \end{bmatrix} \tag{2.7}$$

The approximate impedance matrix can then be found through a reverse impedance transformation that results in eq. (2.8).

$$\left[\ Z_{appx} \ \right]_i = \frac{1}{3} \times \begin{bmatrix} (2 * z_p + z_0) & (z_0 - z_p) & (z_0 - z_p) \\ (z_0 - z_p) & (2 * z_p + z_0) & (z_0 - z_p) \\ (z_0 - z_p) & (z_0 - z_p) & (2 * z_p + z_0) \end{bmatrix} \tag{2.8}$$

Therefore, the calculation for the voltage of one phase using the approximate line segment model is found in eq. (2.9).

$$V_{an,i} = V_{an,j} + z_p I_a + \frac{z_0 - z_p}{3}(I_a + I_b + I_c) \tag{2.9}$$

where the voltage and current of each phase is composed of a magnitude and an angle as detailed in eqs. (2.10) and (2.11). The impedance is composed of the resistance and the reactance of the lines as shown in eqs. (2.12) and (2.13).

$$V_{an,i} = |V_a| * cos(\theta_{V,a}) + j * |V_a| * sin(\theta_{V,a}) \tag{2.10}$$
$$I_a = |I_a| * cos(\theta_{I,a}) + j * |I_a| * sin(\theta_{I,a}) \tag{2.11}$$
$$z_p = r_p + jx_p \tag{2.12}$$
$$z_0 = r_0 + jx_0 \tag{2.13}$$
$$\tag{2.14}$$

To acquire the equivalent equation of eq. (2.3) for a three-phase unbalanced system, eq. (2.9) is then squared. This results in an equation capable of calculating the square of the voltage magnitude as a function of the voltage between each phase and the neutral line $V_{an,j}$, the positive impedance, the negative impedance and the three currents flowing through each phase I_a, I_b, and I_c. In order to complete this derivation, abbreviations to facilitate the derivation are used as stated in eq. (2.15).

$$\begin{aligned} v_i &= |V_{ag,i}|^2 \\ \phi_a &= \theta_{V,a} - \theta_{I,a} \\ \beta_{ab} &= \theta_{I,a} - \theta_{I,b} \end{aligned} \tag{2.15}$$

The derivation of the eq. (2.9) was performed in the frame of this thesis because this specific formulation was not found in the literature. After developing and deriving this proof, the equation in eq. (2.16) was determined.

$$
\begin{aligned}
&v_j = v_i + 2 * V_i * I_{a,ij} * \left(\frac{r_0 - 2 * r_p}{3} * \cos(\phi_a) + \frac{x_0 - 2 * x_p}{3} * sin(\phi_a) \right) + \\
&2 * V_i * \left[I_b * \left(\frac{r_p - r_0}{3} * \cos(\theta_{V,a} - \theta_{I,b}) + \frac{x_0 - x_p}{3} * \sin(\theta_{I,b} - \theta_{V,a}) \right) + \right. \\
&\left. I_c * \left(\frac{r_p - r_0}{3} * \cos(\theta_{V,a} - \theta_{I,c}) + \frac{x_0 - x_p}{3} * \sin(\theta_{I,c} - \theta_{V,a}) \right) \right] + \\
&2 * I_a * I_b * \left[\left(\frac{2 * r_p - r_0}{3} * \frac{r_0 - r_p}{3} + \frac{2 * x_p - x_0}{3} * \frac{x_0 - x_p}{3} \right) * \cos(\beta_{ab}) + \right. \\
&\left. \left(\frac{r_0 - 2 * r_p}{3} * \frac{x_0 - x_p}{3} + \frac{2 * x_p - x_0}{3} * \frac{r_0 - r_p}{3} \right) * \sin(\beta_{ba}) \right] + \\
&2 * I_a * I_c * \left[\left(\frac{2 * r_p - r_0}{3} * \frac{r_0 - r_p}{3} + \frac{2 * x_p - x_0}{3} * \frac{x_0 - x_p}{3} \right) * \cos(\beta_{ac}) + \right. \\
&\left. \left(\frac{r_0 - 2 * r_p}{3} * \frac{x_0 - x_p}{3} + \frac{2 * x_p - x_0}{3} * \frac{r_0 - r_p}{3} \right) * \sin(\beta_{ca}) \right] + \\
&2 * I_b * I_c * \left[\left(\frac{x_0 - x_p}{3} \right)^2 + \left(\frac{r_0 - r_p}{3} \right)^2 \right] * \cos(\beta_{cb}) + \\
&I_a^2 * \left[\left(\frac{2 * r_p - r_0}{3} \right)^2 + \left(\frac{2 * x_p - x_0}{3} \right)^2 \right] + \left[\left(\frac{r_0 - r_p}{3} \right)^2 + \left(\frac{x_0 - x_p}{3} \right)^2 \right] * (I_b^2 + I_c^2)
\end{aligned}
\tag{2.16}
$$

2.3.3 Simplification of high dimensionality

Often, distribution grids have a very large number of nodes. Certain nodes of a network can be simplified in order to reduce this high number of nodes and therefore reduce the complexity of the power flow calculation. A simplification technique was used in the frame of this thesis in order to reduce the power flow calculation time. The simplification algorithm consists of identifying "active" and "passive" nodes. Once active and passive nodes are identified, all passive nodes can be removed by redefining a new segment that consists of the sum of multiple segments. An active node is defined by a node with more than one downstream element. An element is defined as a downstream node, a load or a generator. Therefore, if there is more than one downstream element, the node must be conserved and it is labeled an "active node". If there is only one downstream element, for example, one downstream node, one consumer or one generator, the node is labeled as a "passive node" and is not critical to conserve for an accurate power flow calculation. These nodes are not necessary because the power balance calculation between these two nodes only concerns the upstream branch, downstream branch and the losses of both. Therefore, calculating the losses across both lines with the combined impedance is equivalent to calculating the losses of each branch individually and then summing them. The node can be removed by redefining a segment that includes the sum of the impedance values of the two original segments. Examples of active and passive nodes can be found in Fig. 2.1.

This node reduction technique consists of testing each node to determine if it is an active or passive node and then removing all passive nodes by redefining new nodes and branches. This simplification is extremely useful for low voltage feeders due to the fact that typically only a third of the nodes are "active nodes" and that the calculation time of a power flow analysis is directly related to the quantity of nodes of a given feeder.

Figure 2.1: Passive node examples indicated by a blue "P" and active node examples indicated by a red "A"

Table 2.1: Feeder characteristics of network 20 [1]

Feeder	Sum of all loads (kW)	Nodes
1	25	76
2	26	609
3	59	833
4	29	69
5	23	63

Table 2.2: Feeder 3 electrical characteristics

Grid element	Characteristic	Value
Nodes	quantity	833
Load Nodes	quantity	59
Resistance	avg value	0.0012
Reactance	avg value	0.0001014
Zero Resistance	avg value	0.00156
Zero Reactance	avg value	0.0001097

2.3.4 Case study

In order to demonstrate the analysis strategies developed in this chapter, a case study consisting of a low voltage grid feeder topology in England is implemented. The chosen grid is network 20 found on the Electricity North West project site [1]. The network 20 consists of five three-phase feeders that are connected to a 800 kVA transformer. The loads reported in the OpenDSS [63] file indicate an initial loading scenario for each feeder as noted in 2.1. Due to the fact that feeder 3 represents 50.5% of the nodes and 36.4 % of the loading scenario, this feeder was considered to be the most important to model. Example feeder characteristics can be found in Table 2.2 and a diagram of the grid topology can be found in Fig. 2.2.

2.3.5 Results

Three power flow calculation comparisons are completed to validate the accuracy of the three-phase unbalanced equations developed in eqs. (2.1), (2.2) and (2.16). The first power flow calculation comparison is between the developed equations eqs. (2.1), (2.2) and (2.16) and an open source low voltage distribution grid software called OpenDSS [63]. The second comparison

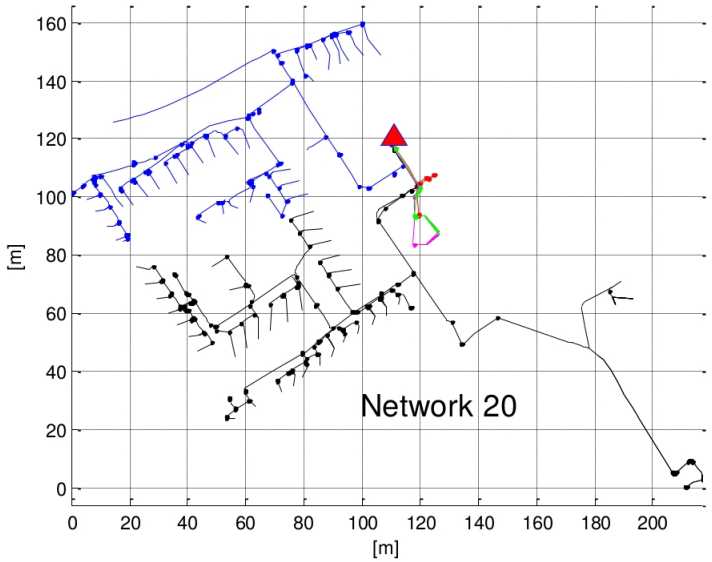

Figure 2.2: Low voltage network used in the case study

is completed between the original grid detailed in Table 2.2 and the simplified grid detailed in Table 2.3 after using the simplification technique detailed in section 2.3.3. The final analysis is a comparison of the fully developed three-phase unbalanced power flow calculation and the single-phase estimation technique for each phase. The evaluation metric used for evaluating the difference between each pair of power flow calculations is the RMSE. Therefore, the RMSE value is the error of one strategy compared to the other.

Comparison of unbalanced power flow calculation and OpenDSS

The full AC three-phase unbalanced power flow calculation was implemented in python using a forward backward sweep method. This calculation was compared to the voltage, active and reactive power values calculated by an open source distribution modeling software developed by Electric Power Research Institute called OpenDSS [63]. This modeling tool has been widely used for the analysis of three-phase unbalanced systems in research and industry. A visualization of the two different load flow calculation strategies is found in Fig. 2.3.

When comparing the voltage profile results of eqs. (2.1), (2.2) and (2.16) and OpenDSS, an RMSE value of between 0.8% and 0.9% of the voltage magnitude was calculated for the three-phases. This small error is a result of the way OpenDSS treats load profiles. Load profiles are voltage dependent in OpenDSS while the load profiles used to calculate voltage profiles by eqs. (2.1), (2.2) and (2.16) are considered to be fixed active and reactive power values. The 0.9% RMSE value for bus voltages was judged to be negligible therefore validating the calculation methods derived in this chapter.

Comparison of original and simplified grid

The grid reduction technique described in section 2.3.3 was applied to the original grid topology of network 20. This node reduction technique successfully reduced the 835 node network to 226 nodes. The new grid characteristics for the network after the reduction technique are found in

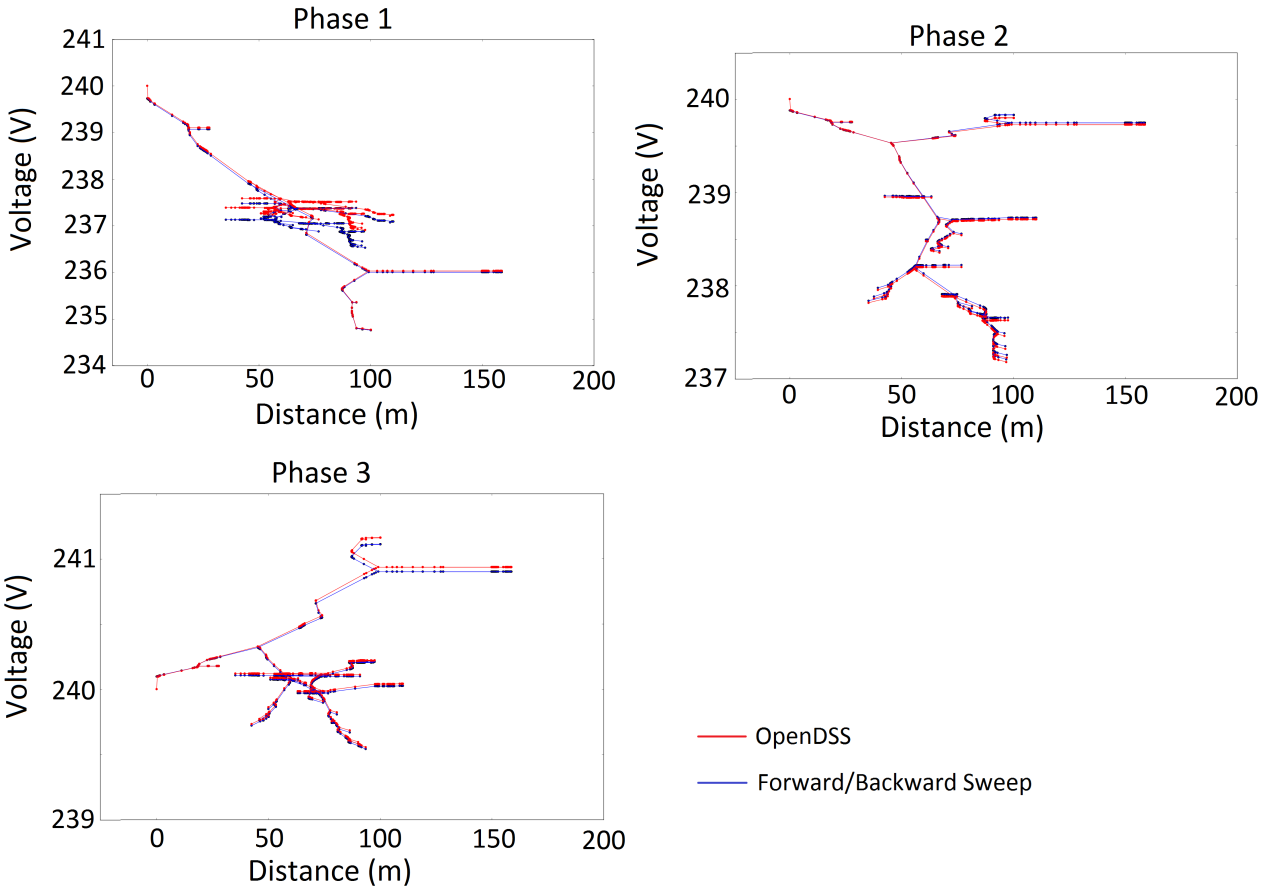

Figure 2.3: Comparison of OpenDSS and load flow calculations using a forward backward sweep and eqs. (2.1), (2.2) and (2.16)

Table 2.3: Simplified feeder 3 electrical characteristics

Grid element	Characteristic	Value
Nodes	quantity	226
Load Nodes	quantity	59
Resistance	avg value	0.00447
Reactance	avg value	0.000377
Zero Resistance	avg value	0.00583
Zero Reactance	avg value	0.000408

Table 2.3.

A comparison of a power flow calculation of the original grid topology and the simplified grid topology was completed to validate the grid reduction technique. The comparison of these calculations can be visualized in Fig. 2.4.

The RMSE value when comparing the original network to the simplified network was zero for voltage, active and reactive power for all phases. This result validates the hypothesis that the reduction strategy has no effect on the final power flow calculation of a network.

Single-phase estimation of unbalanced power flow

Three-phase unbalanced power flow calculations are used to calculate the effects that neutral current can have on voltage profiles. In order to evaluate the importance of these effects, a comparative study was performed between a single-phase representation of each phase as opposed to a fully developed three-phase unbalanced power flow calculation of all three phases. The case study uses the simplified grid as detailed in Table 2.3.

As seen in eq. (2.16), the neutral current effects are relative to the r_p to r_n and x_p to x_n ratio as well as the amount of imbalance within the system. The r_p to r_n and x_p to x_n ratios were calculated based on the grid data specifications. Varying levels of imbalances were therefore simulated in order to quantify the influence of the magnitude of imbalances on the power flow calculations. The parameter that will be used to quantify the imbalance in the system is calculated with eq. (2.17).

$$Imb = \frac{(I_a - I_b) + (I_a - I_c)}{2} \tag{2.17}$$

The load factor may also contribute to the influence of imbalances on the system. For this reason, varying load factors were also simulated and the resulting voltage deviations are observed. The load factor indicator is calculated as detailed in eq. (2.18).

$$LF = \frac{I_a * V_a + I_b * V_b + I_c * V_c}{T^{nom}} \tag{2.18}$$

Unbalanced power flow calculations and single-phase estimations were therefore completed for imbalances between 2% - 70%. Varying loading factors from 10.7% to 52.5% were also

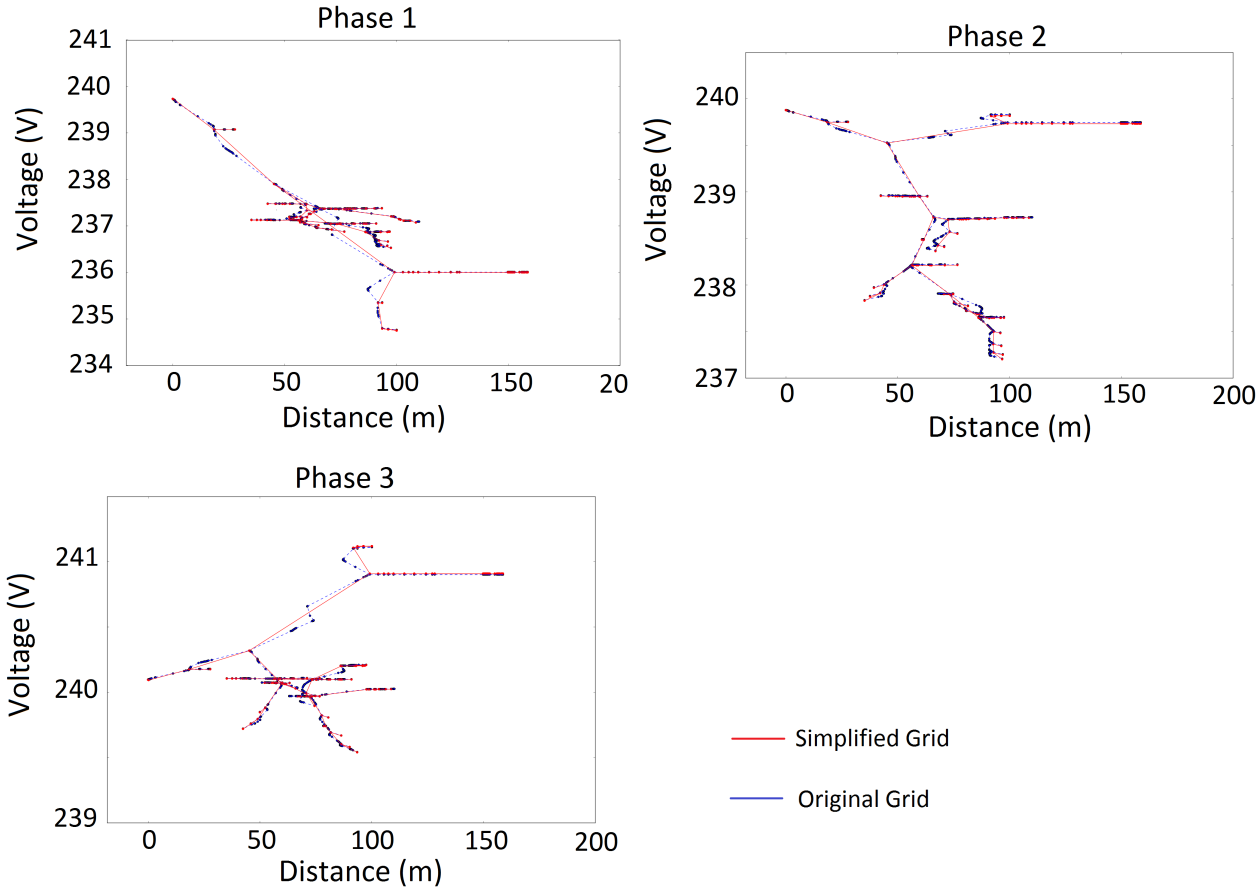

Figure 2.4: Comparison of simplified grid load flow calculation with original one

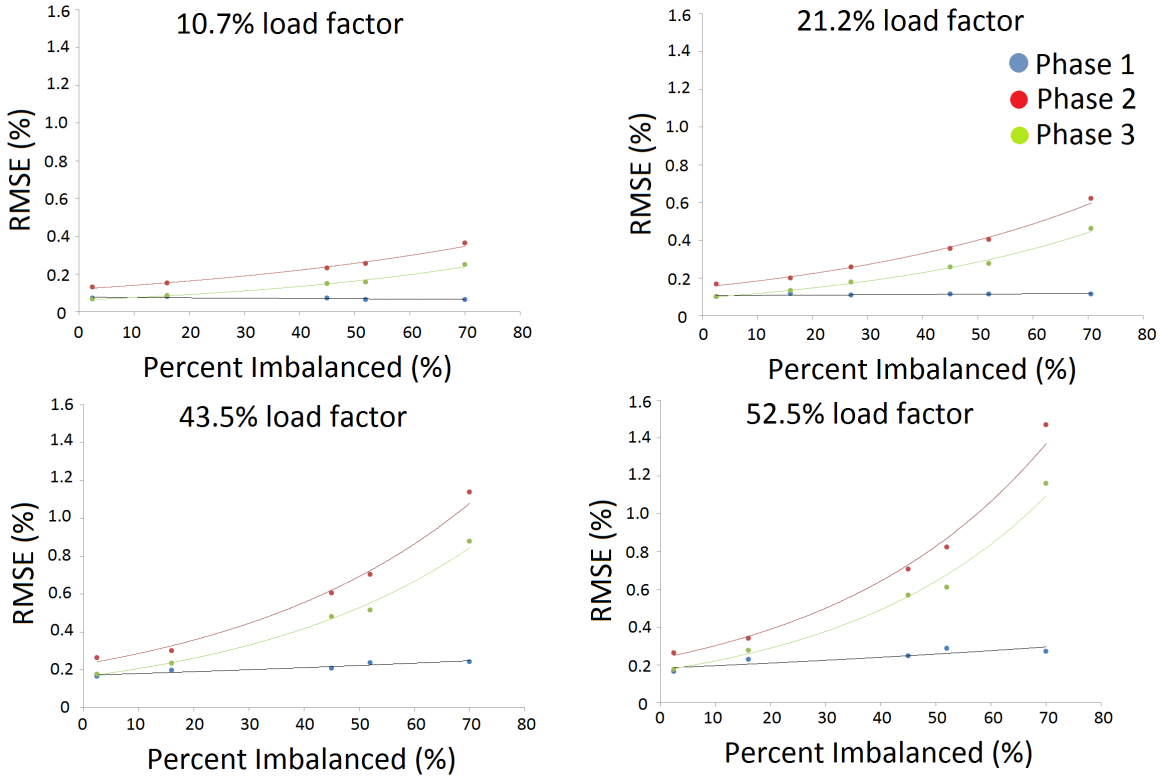

Figure 2.5: Comparison of three-phase unbalanced and single-phase load flow calculation

simulated. The results of the RMSE calculated by comparing the single-phase estimation to the unbalanced power flow calculation is found in Fig. 2.5.

As seen in Fig. 2.5, a 10.7% load factor results in an RMSE value of less than 0.2% for the case with no imbalances and up to 0.4% for the case with 70% imbalances. The highest load factor simulated of 52.5% results in higher errors with an RMSE averaging 0.2% for the case with no imbalances up to an RMSE of 1.6% with 70% imbalances. Even with the highest loading factor and the highest percent of imbalances simulated, the RMSE error values for the single-phase estimation are relatively low.

2.4 OPF multi-phase unbalanced algorithms

2.4.1 Existing algorithms literature review

Few optimization algorithms are capable of analyzing three-phase unbalanced low voltage systems. The advantages of detailed three-phase system models in planning stages have been demonstrated in [65].

The added complexities of low voltage unbalanced systems are important to consider when accurately quantify the problems of renewable energy integration in low-voltage grids. Existing multi-phase optimal power flow algorithms include [66][67][68] [69] [70] [71] [72] [73] [74]. These algorithms include heuristic methods [73], iterative methods [74] [70], non-linear solvers [69], convex relaxations [67] [71] [72] [66] or a recently published new method *Feasible Point Pursuit and Successive Convex Approximation* algorithm [68]. Heuristic and iterative methods can be

time intensive and are not always guaranteed to find a global optimal solution. Non-linear solvers often combine multiple techniques of heuristic and local linearizations of certain equations. Convex relaxations are not always proven to be exact however exactness can be verified. Convex relaxations tend to have very low calculation burden. Therefore, convex relaxations are explored in more detail to identify possible OPF methodologies applicable to low voltage grids.

An algorithm that solves two sub problems with an SDP relaxation consists of an initial decoupled nodal formulation that then solves a global optimization problem that shares the Lagrange function of each node. Exact relaxations were achieved for a 34 bus system but convergence problems arose with a 123 node grid [75]. A multi-phase optimal power flow model proposed by [67] illustrates possible relaxations within the BIM or the BFM implementation. The BIM is a system of equations based on the current balance at each node. The BFM is based on Kirchhoff's current law that the power flowing in the upstream branch is equal to the power flowing in all downstream branches and the losses. A case study is not presented for these two formulations but the BFM formulation is said to be more stable with fewer convergence problems due to the added mathematical difficulty in the BIM of subtracting two small current values. The BFM equations are relaxed using an SDP and implemented in a case study in [72]. A more recent paper elaborating the implementation of the algorithm is published in [71]. The BFM SDP in [67][71][72] was implemented in the context of this thesis in python using the cvxpy package. The cvxpy package was chosen due to the capability of this package to accept and implement Hermitian matrices within the problem formulation. A case study was implemented to assess the effectiveness of multi-phase optimal power flow algorithms that take into account the added complexity of unbalanced three-phase power flow.

2.4.2 Implemented algorithms

The SDP BFM published in [67][71] was implemented at the beginning of this PhD work. At the time of implementation, few details were available describing the algorithm in detail and no case studies has been presented showing the practical application of such an algorithm. Recently, this algorithm has been implemented with multiple case studies as found in [71].

After implementation, the algorithm detailed in [67] had significant convergence problems. An exact relaxation was achieved for a 10 node grid. However, all larger systems that were tested did not converge. This three-phase unbalanced optimal power flow was implemented in order to analyze the performance of this type of algorithm in comparison with a single-phase estimation for each phase. The added benefit of taking into account the coupling between each phase must be weighted against the inconveniences of increased calculation time and complexity.

Due to the fact that few algorithms existed in the literature, the derived equation in eq. (2.16) was explored to possibly propose new relaxations for an OPF multi-phase unbalanced system algorithm. However, no promising formulations were found and due to other priorities of this thesis work, research was not continued in this subject area.

2.5 Conclusion

Three-phase unbalanced power flow analysis was completed to quantify the advantages of unbalanced power flow calculations in the context of OPF analysis. Varying strategies to help with the analysis of low voltage unbalanced distribution grids have been presented. These strategies include derived equations allowing for the calculation of three phase unbalanced systems.

A strategy allowing the simplification of networks with a large number of nodes was also presented. Finally, a proposal to use single-phase estimations of three-phase unbalanced systems was discussed. Conclusive results show that the additional accuracy of taking into account the neutral current effects on the voltage profile is very small.

A state of the art literature review on multi-phase unbalanced OPF algorithms has been presented. The primary formulation presented in the literature has been implemented in the frame of this thesis. This algorithm had a significant calculation burden as well as convergence problems.

In conclusion, optimal power flow algorithms that exist in the literature and take into account the increased complexity of three-phase unbalanced load flow calculations significantly increase the complexity of the problem and sometimes have convergence problems. The added accuracy achieved by taking into account the coupling between phases, i.e. the neutral current effects, is minimal and therefore insignificant during the planning phase. For specific studies, these imbalances can have significant effects on the planning process such as calculating transformer aging or possible re-balancing strategies in the planning phase that are not considered in this thesis. For this reason, all future model developments will consider single-phase estimations of three-phase systems. These single-phase models take into account individual loading and generation profiles connected to the phase of interest but neutral current effects and the coupling of the three-phases is not considered.

Chapter 3

Planning methodologies for smart grids

Résumé

La grande variabilité et les incertitudes introduites dans les systèmes de distribution modernes à cause des générateurs à énergie renouvelable décentralisés nécessitent de nouvelles solutions pour la gestion du réseau et l'assurance d'une qualité de fourniture. Des analyses multi temporelles sont nécessaire pour l'analyse de variables dépendant du temps tel que le stockage. Le développement de ces outils permet l'analyse de la capacité d'accueil d'un réseau existant ou l'optimisation de la taille et du positionnement du stockage décentralisé. Les algorithmes OPF sont capables de prendre en compte les stratégies de gestion des réseaux intelligents tout comme les limites du réseau pour analyser les bénéfices en termes de coûts des solutions de réseaux intelligents. Ce chapitre présente le développement d'un outil d'analyse OPF multi temporel. Une démonstration de cet algorithme est ensuite présentée pour le dimensionnement optimal et le positionnement sur le réseau d'équipements de stockage de manière simultanée. Les modèles présentés utilisent un algorithme OPF multi temporel avec des relaxations convexes des équations de flux de puissance pour garantir des solutions optimales et une grande performance algorithmique. Les coûts de gestion, les coûts d'investissement et les contraintes du réseau sont pris en compte pendant ce procédé d'optimisation. Des conclusions sont tirées sur l'efficacité d'un tel algorithme dans les stratégies de planification et de gestion. Deux études de cas sont analysées, une pour calculer la capacité d'accueil d'un réseau de distribution et l'autre pour determiner le dimensionnement et le positionnement optimal du stockage.

3.1 Summary

The high variability and uncertainty introduced into modern electrical distribution systems due to decentralized renewable energy generators requires new solutions for grid management and power quality assurance. Multi-temporal analysis is necessary for the analysis of temporally dependent variables such as storage. The development of these tools allows for the analysis of the hosting capacity of an existing network or the optimal size and placement of decentralized storage. OPF algorithms are capable of taking into account Smart Grid operational strategies as well as network limits to analyze the cost benefit analysis of Smart Grid solutions. This chapter presents the development of a multi-temporal OPF analysis tool. An elaboration of

this algorithm is then presented for the simultaneous optimal sizing and placement of grid connected storage devices. The models presented use an (AC) multi-temporal OPF algorithm that uses convex relaxations of the power flow equations to guarantee optimal solutions with high algorithmic performance. Operational costs, investment costs and grid constraints are considered during the optimization process. Conclusions are drawn about the effectiveness of such algorithms in planning and operations strategies. Two case studies are analyzed, one to calculate the hosting capacity of a distribution grid and the other for the exercise of optimal sizing and placement.

3.2 Introduction

Increasing environmental concern is one of the main drivers behind the large-scale development of DER in electric distribution grids. This development involves connection of decentralized generators to the electric grid, for example PV, wind turbines and micro-hydroelectric generators. These DER bring about new challenges for the distribution grid operators. Decentralized renewable energy generators can introduce bi-directional flow within the network, while their production is uncertain and variable due to its inherent dependence on weather conditions. Other specific challenges of the distribution grid include higher uncertainty due to reduced aggregation effects of DER generators, voltage profile deviation and increased power flow in electric lines. These challenges are generally localized, therefore creating local voltage perturbations that may not be visible by the distribution operator.

Solutions to these challenges include infrastructure upgrades such as electric line reinforcement or automation and integration of smart grid functionalities, such as OLTC, DER generation curtailment, storage devices and DSM [76]. Infrastructure upgrade investments are easily calculated. However, new control and flexibility functionality is difficult to quantify economically and integrate into the planning phase of distribution grids. The cost benefit analysis of varying smart grid technologies and management strategies will become more important as DER penetration increases in future distribution grid systems.

Grid storage elements are presented in some papers in the literature as a cost-effective solution to deal with the above challenges. A techno-economic analysis of energy storage elements as a possible solution to problems of DER grid integration is presented in [77]. The cost-effectiveness of different grid storage applications is explored including regulation of transmission and distribution power quality, voltage regulation and control, energy management, smoothing of intermittent renewable energy production, energy back-up, peak shaving, etc. For each specific application, taking into account the operational strategy of the storage device is important when sizing and placing the unit.

The importance of multi-temporal analysis is directly related to the evaluation of the role of storage within an active distribution network. Using storage devices to maximize renewable energy production and improve generation and load mismatch requires the multi-period simulation of the storage capacity limits. This multi-temporal coupling is critical in order to evaluate the technical constraints of the storage elements and the possible benefits. Possible applications of this type of algorithm are the hosting capacity of existing grids or the optimal sizing and placement of battery systems to improve grid operations or increase hosting capacity.

The optimal sizing and placement of storage devices in distribution grids has been addressed through various mathematical modeling methods presented in the literature. This problem is high-dimensional and non-convex. The resolution of this high-dimensional non-convex problem

has been successful with multiple mathematical techniques including analytical, classical, artificial intelligence and other miscellaneous techniques [78]. In a review of energy storage allocation, four main categories are defined to solve this high-dimensional non-convex problem: analytical methods, mathematical programming, exhaustive search and heuristics [33]. OPF are classified as mathematical programming methods and can be used to simulate power system functionality with generators and storage devices while taking into account grid constraints. OPF algorithms are capable of taking into account decision variables and therefore capable of analyzing active management of distribution grids. An example of an OPF that analyzes hosting capacity of an active distribution grid is found in [79], where curtailment strategies and dynamic line rating are explored to increase renewable energy penetration.

OPF algorithms are efficient at analyzing active distribution networks for operation and planning. The two primary problem resolution techniques for solving this high-dimensional non-convex problem include heuristic techniques or linear convex relaxations of the power flow equations. Heuristic algorithms have been used to solve the optimal placement and sizing of storage devices. For example, a two-step process with a master and a sub-problem is proposed in [80]. This method first uses a heuristic algorithm to solve optimal placement and sizing of batteries. Secondly, a daily AC OPF multi-objective function takes into account optimal voltage control, minimization of network losses and total energy costs. Another paper presents a comprehensive sizing and siting algorithm using particle swarm optimization [81]. A different type of heuristic method was used to simultaneously size and place storage units using an artificial bee colony algorithm with an objective function that forces each storage node to be as autonomous as possible [82]. Another heuristic method implemented a multi-objective problem addressing both distribution grid and transmission grid [83]. However, heuristic algorithms often require a larger calculation burden and are not guaranteed to converge to a global optimal solution as noted in [49]. A mixed integer linear programming approach for complete DER portfolio sizing and placement is presented in [84]. The mixed integer strategy uses linearized power flow equations and loss estimations. Mixed integer linear approximations are proven to be effective at solving the non-convex placement and sizing problems. However, the calculation time is high and scalability to large network sizes have not been addressed.

Convex relaxations of the power flow equations generally have a lower calculation burden. The relaxation of the power flow equation into a second order cone has already been theoretically explained and detailed mathematically in [50]. Papers addressing optimal sizing and placement of storage devices using convex relaxations can be found in the literature. An impedance model was used to perform optimal placement and sizing in [85]. An optimal placement and sizing of batteries using a linearized DC power flow for transmission planning with a maximum investment cost is presented in [86]. This linearization is not accurate for the high R/X ratio found in the low voltage distribution systems, which implies electrical losses that are non-linear. The use of an AC OPF for optimal placement [87] or optimal sizing [88] is also found in the literature. In [31] the authors explore a two-step process of sizing and placement of storage units through relaxed power flow equations. However, this sizing methodology calculates power and energy imbalances locally at PV nodes and sizes the battery systems to mitigate these imbalances. Therefore, this methodology sizes the battery systems to reduce PV injection when power quality becomes an issue. This sizing methodology does not compare the cost of storage elements to other cost-effective solutions such as curtailment. The algorithm also does not analyze the possible benefits of batteries participating in an electricity market. A SOCP OPF algorithm is then used in the second step to site the sized battery systems.

The SOCP relaxation of the power flow equations has been proven to be inexact during periods of high penetration from decentralized production. An example of this could be high PV production and low loads during the summer season. In order to overcome the challenge of inaccurate convex relaxations, [57] presents an AC OPF algorithm that integrates linear cuts implemented in an iterative manner to ensure an exact and feasible relaxation of the power flow equations. In a follow-up work, this algorithm has then been developed into a multi-temporal one in order to more objectively evaluate the benefits of grid connected storage and other temporally dependent variables in [58]. A possible application of the multi-temporal OPF algorithm as described in [58] is the calculation of the PV hosting capacity of a network. The PV hosting capacity is defined in [58] as the total PV capacity that can be installed before power quality is not affected. If more capacity is installed, active management techniques such as curtailment or battery peak shaving must be implemented to avoid negative power quality effects. The details of this method are discussed in more detail later in this chapter.

This chapter is two-fold. Firstly, the chapter addresses the importance of multi-temporal analysis to analyze networks with time dependent variables. A case study including the calculation of the hosting capacity of a network with high renewable energy penetration and the presence of storage is presented. Secondly, a methodology is detailed to simultaneously perform optimal sizing and placement of storage devices in a distribution grid from a techno-economical view by considering the investment cost of batteries weighted against the operational benefit.

3.3 Multi-temporal OPF for hosting capacity analysis

3.3.1 Power flow model

Four equations are used for AC power flow calculations: the balance of active power, the balance of reactive power, the voltage magnitude and current magnitude. When considering a radial distribution system with decentralized PV generation and decentralized storage elements, the power flow equations used for this analysis are shown in eqs. (2.1) and (2.2). Eq. (2.1) and eq. (2.2) describe the balance of active and reactive power from the upstream and downstream branches. The voltage magnitude at each node is calculated by eq. (2.3). The current magnitude of each branch is calculated as shown in eq. (2.4). Along with the power flow system of equations, constraints are also present in an OPF formulation.

System constraints

The system constraints of an electrical distribution network include maximum and minimum voltage limits, and maximum and minimum apparent power limits. The network voltage and apparent power limits can be described in eqs. (3.1) and (3.2).

$$\underline{V} \leq V_{t,j} \leq \overline{V} \tag{3.1}$$

$$0 \leq |s_{ij,t}| \leq \overline{s}_{ij} \tag{3.2}$$

where $\underline{V}$ and $\overline{V}$ are the lower and upper limits of the voltage on a line, respectively. $\overline{s}_{ij,t}$ is the maximum apparent power limit of each branch. Individual components such as the PV and battery systems were modeled through their inverter behavior as described in the following sections.

PV inverter model

The PV inverter behavior was modeled as an active and reactive power source with upper and lower limits on active and apparent power injection for a given time step.

$$0 \leq P_{pv,t,j} \leq \overline{P}_{pv,j} \tag{3.3}$$
$$0 \leq s_{pv,t,j} \leq \overline{s}_{pv,j} \tag{3.4}$$

where $s_{pv,t,j}$ is the total apparent power of the power injection as defined in 3.5.

$$s_{pv,t,j} = \sqrt{P_{pv,t,j}^2 + Q_{pv,t,j}^2} \tag{3.5}$$

Battery inverter model

The battery inverter was modeled as either an apparent power injection or an apparent power load for a given node at a given time step. The time coupling variable indicating the SOC was calculated based on a total charging and discharging efficiency associated with the inverter.

$$soc_{st,t,j} = soc_{st,t-1,j} + t\eta_{st}P_{st+,t,j} + t\frac{1}{\eta_{st}}P_{st-,t,j} \tag{3.6}$$
$$\underline{soc}_{st,j} \leq soc_{st,t,j} \leq soc_{st,j}^{nom} \tag{3.7}$$
$$P_{st,t,j} = P_{st+,t,j} + P_{st-,t,j} \tag{3.8}$$
$$-P_{st,j}^{nom} \leq P_{st,t,j} \leq P_{st,j}^{nom} \tag{3.9}$$
$$0 \leq |s_{st,t,j}| \leq \overline{s}_{st,j} \tag{3.10}$$

where η_{st}, $P_{st+,t,j}$, $P_{st-,t,j}$, $\overline{s}_{st}$ and $\underline{s}_{st}$ are the charging efficiency, power absorbed during charging, power injected into the grid, upper limit and lower limit of total apparent power exchange with the grid. $s_{st,t,j}$ is the apparent power at node j as defined by eq. (3.11).

$$|s_{st,t,j}| = \sqrt{P_{st,t,j}^2 + Q_{st,t,j}^2} \tag{3.11}$$

The power flow equations are non-linear and non-convex. Therefore, when solving a high-dimensional power flow problem, convex relaxations have been used to ensure high performance algorithms.

3.3.2 SOCP optimum power flow formulation

The same SOCP convex relaxation used in [89] and [55] is implemented in a multi-temporal model in order to analyze the hosting capacity of a distribution grid. This relaxation entails the replacement of certain equality constraints by inequality constraints and the substitution of certain quadratic terms with linear terms. The equality constraints in question, eqs. (2.4), (3.5) and (3.11), are relaxed using conic functions to limit the apparent power of each branch or the apparent power injected into the grid by the PV and battery systems. Two new variables are also introduced to replace quadratic terms as shown in eq. (3.12) in order to successfully formulate an SOCP problem as explained in [55].

$$\begin{aligned} \upsilon_j &= |V_j|^2 \\ \ell &= |I_{ij}|^2 \end{aligned} \tag{3.12}$$

The objective function is composed of two parts. The first part is the minimization of the total losses of the system. The second part minimizes the curtailment of the PV systems in order to maximize renewable energy injection into the grid. Therefore, the objective function is formulated as seen in eq. (3.13):

$$min \sum_{j=0}^{J} \sum_{t=0}^{T} [r_{ij}\ell_{ij,t} + (P_{pvid,t,j} - P_{pv,t,j})] \tag{3.13}$$

subject to eqs. (2.1), (2.2), (3.1)–(3.4) and (3.6)–(3.10)

$$\upsilon_j = \upsilon_i - 2(r_{ij}P_{ij} + x_{ij}Q_{ij}) + (r_{ij}^2 + x_{ij}^2)\ell_{ij} \tag{3.14}$$

$$\ell_{ij} \geq \frac{P_{ij}^2 + Q_{ij}^2}{\upsilon_i} \tag{3.15}$$

$$s_{pv,t,j} \geq \sqrt{P_{pv,t,j}^2 + Q_{pv,t,j}^2} \tag{3.16}$$

$$s_{st,t,j} \geq \sqrt{P_{st,t,j}^2 + Q_{st,t,j}^2} \tag{3.17}$$

The decision variables of this optimization problem include the curtailment of PV systems and the power load or injection of the battery systems for each time step at each node.

3.3.3 Case study

The optimization of storage elements and PV curtailment was analyzed for a time scale of 0.5 to 4 days. An example medium voltage grid published in [90] was studied in order to evaluate the performance of this algorithm. The network studied is a 12.66 kV 69 nodes grid. A map of the grid topology can be found in Fig 3.3.

Consumption load profiles were simulated using an aggregation load simulator as described in [91] for each low voltage substation and medium voltage consumer. This load simulator takes into account a mix of residential and commercial customers. Residential consumption is simulated with statistically accurate representations of surface area, electric heating and the number of individuals that align with the INSEE building inventory database of France. Industrial load profiles are simulated by assuming a typical industrial activity mix in France from a medium voltage substation. The two medium voltage customers were modeled as office building complexes with typical business hours operation. A peak of 5 MW during the winter and 2.9 MW during the summer was simulated for the medium voltage substation transformer with a maximum apparent power limit of 10 MW. Solar radiation data from a site in the south of France was used to calculate expected PV production as a function of system nominal power.

Four different seasonal scenarios were studied in order to understand a typical annual operation. Within each season, three renewable energy solutions were studied: the hosting capacity of a typical grid topology without storage, the hosting capacity with decentralized storage elements installed at the same nodes as the PV systems and the hosting capacity with centralized storage elements close to the high voltage transformer. The hosting capacity of a feeder was defined as

the maximum capacity of PV that does not violate grid constraints without using curtailment. This considers the defined configuration and repartition of PV systems within the grid. Twenty sites were chosen for PV decentralized installations and nominal power of each system was increased until either current or voltage limits were reached. Therefore, the calculated hosting capacity is for the given configuration and repartition as defined by the case study.

3.3.4 Results

A three-day simulation period with an hourly resolution was chosen in order to allow for at least one full cycle of charging and discharging of the storage elements. Three-day typical profiles were chosen for four different seasons in order to understand the annual performance of the system. Considering only PV installations without storage elements, the maximum current limit of the lines was reached during low loading periods and high peak PV injection in summer. Multiple capacities for 20 decentralized PV systems were tested until curtailment was necessary to not exceed voltage or apparent power limits of the network. The maximum installed capacity where curtailment was unnecessary was achieved with a PV penetration of 10 MW nominal power installed. A total of 701 kWh was curtailed of the 156 MWh produced during a three-day simulation to ensure maximum apparent power limits were not exceeded. During typical daily profiles for fall, winter and spring, no curtailment was necessary for any system. In all simulations, the summer period was the most critical to monitor for power quality verification, therefore the rest of the results section will focus on summer production and load profiles.

Added storage capacity was integrated into the grid in order to quantify the additional possible hosting capacity. Initially storage elements were placed at the same nodes as all PV installations to represent a decentralized storage configuration. Therefore, 20 systems of 116 kWh energy storage capacity were modeled through their inverter behavior. For 10 MW of PV capacity installed, no curtailment was needed within all seasons. The improvement in system performance can be seen in Fig. 3.1 and Fig. 3.2. The curtailment necessary and the losses on the lines are compared in Fig. 3.1.

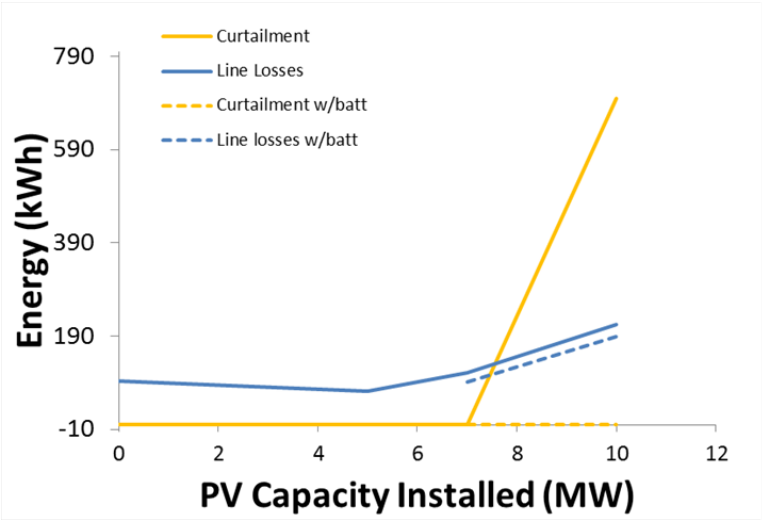

Figure 3.1: Comparison of curtailment and line losses with and without battery systems during a three-day period using typical summer profiles

Table 3.1: For a given amount of coupled time steps, the calculation time in seconds

Time steps coupled	Calculation time (s)
24	8
48	23
96	67

A comparison of the imports and exports at the substation during summer periods can be found in Fig. 3.2.

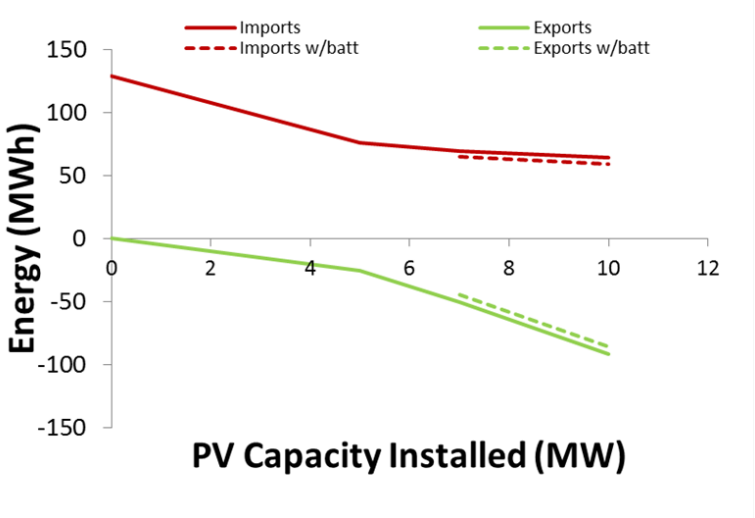

Figure 3.2: Comparison imports and exports with and without batteries during a three-day period using typical summer profiles

The same amount of storage capacity was then used in a centralized configuration. This centralized storage was placed very close to the high voltage transformer offering the same services. The necessary curtailment was also reduced to zero for the 10 MW system. However, the centralized battery system also resulted in higher overall line losses.

Algorithmic performance

The time of execution of the algorithm was recorded for varying time coupling scenarios as shown in Table 3.1.

This multi-temporal coupling allows the optimization of PV curtailment and battery storage utilization for up to a four-day period with a satisfactory calculation burden. It also ensures that the relaxation is exact and applies linear cuts to time steps that are not exact in order to guarantee the exactness of the relaxation.

3.3.5 Discussion

The optimization algorithm proposed uses a convex relaxation algorithm with linear cuts applied to a multi-temporal application for battery storage analysis. This algorithm was shown to be

effective when studying a distribution system for a 3-4 day time span. The multi-temporal algorithm allows for the assessment of battery storage functionality while taking into account the technology limitations such as charging efficiency, discharging efficiency, maximum injection and absorption. The algorithm also calculates an optimal charging and discharging schedule based on the objective function. A French medium voltage distribution feeder was successfully analyzed to determine the hosting capacity, decentralized and centralized battery systems effects on curtailment. This algorithm could be used for comparison studies between different grid stability control strategies such as real-time curtailment, centralized and decentralized battery installations. The use of this algorithm for real-time management could also be effective if real-time predicted PV production profiles and expected load profiles are used as inputs. The optimization of charging and discharging schedules of batteries can effectively increase hosting capacity of a distribution network by reducing the necessity to curtail PV systems.

3.4 Optimal placement and sizing of storage devices

The Optimal placement and sizing of storage devices uses an OPF algorithm that assumes a certain level of smart grid functionality. Operational control of active power of storage and PV inverters are modeled with a multi-temporal OPF. The objective function is formulated in a way to include economic operational benefit and constraints that guarantee power quality. This methodology is capable of taking into account in detail the operational strategy of storage devices in order to make planning decisions about their sizing and placement. Therefore, it is effective for distribution grid planning applications with predefined operational strategies.

3.4.1 Optimal power flow model

The proposed methodology relies on solving the optimization problem with the objective function eq. (3.18) and constraints given by eqs. (2.1), (2.2), (3.1)–(3.4), (3.6), (3.7) and (3.14)–(3.22). The objective function is the sum of the battery investment costs, operation and maintenance costs, the system losses and power imported at the feeder substation. The constraints of this model include the active power limits of PV systems defined by the maximum available power as a function of weather conditions eq. (3.3), apparent power limits of PV systems eqs. (3.4) and (3.16), power flow equations eqs. (2.1), (2.2) and (3.14), relaxation of the current equation eq. (3.15) to represent the power flow equations as a convex SOCP, voltage limits of each branch eq. (3.1), battery SOC constraints eqs. (3.6) and (3.8) and daily nominal power and capacity value constraints eqs. (3.19)–(3.21). Constraint eq. (3.22) limits the ratio of nominal power and nominal capacity to be appropriate for distribution grid storage elements managed on a daily basis. This constraint also allows for fast convergence of the algorithm.

$$\min \quad F_{inv} + F_{O\&M} + F_p + F_{st,p} \tag{3.18}$$

subject to eqs. (2.1), (2.2), (3.1)–(3.4), (3.6), (3.8) and (3.14)–(3.17)

$$P^{nom}_{st,j,d} \geq |P_{st,j,t}| \tag{3.19}$$
$$soc^{nom}_{st,j,d} \geq soc_{st,j,t} \tag{3.20}$$
$$soc^{nom}_{st,j,d} = N^{nom}_{st,j,d} P^{nom}_{st,j,d} \tag{3.21}$$
$$0.1 \leq N^{nom}_{st,j,d} \leq 8 \tag{3.22}$$

The optimal sizing and placement of storage requires the resolution of a temporal and spatial problem. The temporal problem implies a coupling of multiple time steps to ensure coherence of the battery SOC between each consecutive time step. The spatial problem implies the consideration of all nodes as possible placement locations for storage devices. The multi-temporal OPF is already high dimensional. For a grid with 137 nodes, feasibility testing showed that up to 130 coupled time steps resulted in a successful calculation by the solver. While using the Mosek solver, attempts at simulations with more than 130 coupled time steps returned a maximum size exceeded error. Therefore, a certain decoupling is necessary in order to complete an annual analysis. In this algorithm, a daily decoupling was implemented. Therefore, the number t of coupled time-steps is 24. The decoupling was chosen to be done on a daily basis due to the fact that battery systems are often managed on a daily basis. The coupled time steps of a one-day period were then simulated for each day of the year in order to successfully complete an annual analysis. An additional constraint is added to avoid daily accumulation effects by forcing the SOC of the first and last time step of a day to be equal as stated in eq. (3.23).

$$soc_{st,j,0} = soc_{st,j,T} \tag{3.23}$$

Constraint eq. (3.21) is the product of two variables and is non-convex rendering the problem NP-hard. The variable N represents the number of hours of autonomy of the battery system, limited by feasible battery sizes of 0.1 to 8. This relationship between the nominal power and capacity of a battery system is an essential relationship for accurately representing the cost of battery systems. In order to keep this constraint, a linearization is performed through an iterative process. The linearization is shown in equation eq. (3.24).

$$N^{nom}_{st,j,d} P^{nom}_{st,j,d} = \frac{1}{2}\left[N^{nom}_{init,j,d} * P^{nom}_{st,j,d} + N^{nom}_{st,j,d} * P^{nom}_{init,j,d}\right] \tag{3.24}$$

Where $N^{nom}_{0,j,d}$ and $P^{nom}_{0,j,d}$ are the initial values. With these initial values $P^{nom}_{st,j,d}$ and $N^{nom}_{st,j,d}$ are calculated with the algorithm. If the difference between the initial estimation and the final calculated values is larger than a 0.001 for either $P^{nom}_{st,j,d}$ or $N^{nom}_{st,j,d}$, a new iteration is performed assigning $N^{nom}_{0,j,d}$ and $P^{nom}_{0,j,d}$ to the values of $P^{nom}_{st,j,d}$ or $N^{nom}_{st,j,d}$.

The algorithm effectively calculates the optimal size and placement of storage devices for each node for each day. This sizing and placement exercise therefore results in 365 optimal nominal capacity and power values. The final optimal size must then be chosen from analyzing these 365 values. This is done by taking the 75th quantile of the set of optimal values to calculate a final annual optimal size.

3.4.2 Variations of the objective function

The objective function of the general form given by eq. (3.18) can be altered in order to size the battery systems for different purposes. Two objectives are considered in this section. The first

objective function is to size the battery systems to minimize losses in the system. The second possible objective function considers the minimization of losses and the absolute value of the active power injection from the high voltage grid to the medium voltage grid at the substation.

Loss minimization

The first sizing exercise entails using the battery system only for loss cost minimization and allows a comparison between the cost of line losses eq. (3.28), charging/discharging losses of the battery systems eq. (3.29), the sum of battery investment costs eq. (3.26) and battery operations costs eq. (3.27). The objective function is therefore eq. (3.25). The optimal nominal power and capacity is then calculated based only on the economic viability of using batteries for loss reduction.

$$\min \quad F_{inv} + F_{O\&M} + F_p + F_{st,p} \tag{3.25}$$

where:

$$F_{inv} = \sum_{j=0}^{J} m_{st}^{inv} soc_{st,j,d}^{nom} \tag{3.26}$$

$$F_{O\&M} = \sum_{j=0}^{J} m_{st}^{om} t P_{st,j,d}^{nom} \tag{3.27}$$

$$F_p = \sum_{t=0}^{T} \sum_{j=0}^{J} \left(m_{ec,t} r_{ij} \ell_{ij,t} t + m_{ec,t} t \left[\overline{P}_{pv,j,t} - P_{pv,j,t} \right] \right) \tag{3.28}$$

$$F_{st,p} = \sum_{t=0}^{T} \sum_{j=0}^{J} m_{ec,t} \eta_{st} t |P_{st,j,t}| \tag{3.29}$$

subject to eqs. (2.1), (2.2), (3.1)–(3.4), (3.6), (3.8), (3.14)–(3.17) and (3.19)–(3.22)

The losses considered are the line losses, PV curtailment and the losses of the battery system due to the battery charging efficiency. If the sum of the operational costs and the investment costs of the battery systems is higher than the economic gain from loss reduction, the algorithm will calculate zero nominal capacity and power for each node.

Minimization of absolute active power flow at substation

Battery systems can also be used to participate in variable pricing electricity markets. This implies using battery systems to buy and sell electricity from the grid based on the hourly price of electricity. This objective function as detailed in eq. (3.30) allows the calculation of economic gains through battery participation in variable pricing markets and encourages autonomy of the feeder by minimization of the total absolute active power flow imported at the substation $|P_{0,t}|$.

This formulation does not include explicitly the losses associated with the battery charging efficiency because this energy is already counted in the variable $|P_{0,t}|$.

$$\min_{j \in J} \quad F_{inv} + F_{O\&M} + F_p + F_{inj} \tag{3.30}$$

where:

$$F_{inj} = \sum_{t=0}^{T} m_{ec,t} t |P_{0,t}| \tag{3.31}$$

subject to eqs. (2.1), (2.2), (3.1)–(3.4), (3.6), (3.8), (3.14)–(3.17) and (3.19)–(3.22)

These two objective function variations can be used to determine the size and placement of battery storage devices coupled with installed PV systems for specific end-use scenarios. This algorithm does not consider constraints to exclude very small battery systems. Therefore, it is incapable of minimizing the number of nodes that battery systems are installed at. As a result, the algorithm often sizes battery systems for every node. In some cases, it can be desirable by the DSO to consider a limited number of battery systems or a battery system size minimum. If a minimum battery size was introduced into the problem, it would introduce a binary constraint making the problem NP-Hard. Therefore, to remove these small infeasible systems sizes, an iterative approach can be used. At a first stage, nodes with the larger battery sizes are identified with the initial sizing and placement algorithm. Then, final sizing can be performed with added constraints eqs. (3.32) and (3.33) as a second iteration.

$$soc^{nom}_{st,j,d} = 0 \quad for \quad J - K_{st} \tag{3.32}$$

$$P^{nom}_{st,j,d} = 0 \quad for \quad J - K_{st} \tag{3.33}$$

The criteria for choosing final node placement can be determined by choosing a maximum number of battery systems or an acceptable maximum and minimum size of battery systems. For sizing based on a maximum number of systems, K_{st} in eq. (3.33) represents the number of nodes n with the n largest values for the nominal capacity and power. For sizing based on an acceptable maximum and minimum size, K_{st} represents the nodes with nominal power and capacity values within these bounds.

3.4.3 Results

Case Study

The example grid used for this study is a medium voltage distribution grid published in [90]. This grid is composed of 69 nodes with a nominal voltage of 12.66 kV and is assumed to be located in Nice, France. A map of the grid topology can be found in Fig. 3.3.

Generation and Load Profiles

Electric load profiles were simulated using a load simulator as described in [91] for each low voltage substation load profile. Residential and commercial load profiles are simulated with

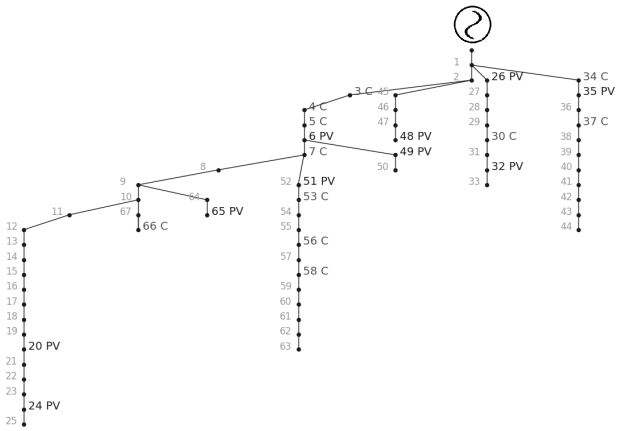

Figure 3.3: Grid topology including low voltage substation (C) and PV system placement (PV)

statistically accurate representations of surface area, electric heating and number of individuals that align with the INSEE household inventory database of France. The location of each load node was chosen randomly due to the fact that no grid load data was available. The medium voltage feeder is assumed to be a 10 MVA transformer serving 21 low voltage substations. Load profiles aligning with meteorological data in Nice, France indicated a peak load of 4.7 MW during the summer and 5.9 MW during the winter with an average load of respectively 2.1 MW and 2.6 MW. Solar radiation data was simulated for Nice, France for the year 2012 by analyzing the global irradiation collected by HelioClim 3 [92]. The PV system production was calculated based on a statistical distribution of direct and diffuse irradiation [93]. This data is then integrated into a projection model to calculate the percentage of direct and diffuse irradiation exposed to the panels [94]. A system performance coefficient is then calculated based on the atmospheric conditions extrapolated from a performance data base of PV systems in the south of France.

An amount of 10 PV systems were randomly assigned to 10 nodes. The size of these systems was also chosen randomly to be between 125 - 1250 kW. Characteristics of the electric load profile nodes can be found in Fig. 3.4 and PV size information can be found in Fig. 3.5.

Economic analysis

In order to analyze the economic viability of battery systems, market price variation and battery system costs were taken into account. Historical variable hourly pricing market data from France was used for 2012.

The capital cost of batteries for nominal capacity and power is determined by analyzing the study [41]. The nine case studies on high performance lead acid battery for transmission and distribution applications were analyzed to calculate the battery investment cost per MWh. Battery costs ranged from 500 k€/MWh to 2.5 M€/MWh. To integrate these costs into the daily analysis, the investment costs per MWh are divided by the lifetime of the system. For all economic analysis, the battery life is assumed to be 10 years as assumed also in [40]. Therefore, the "daily" investment costs ranged from 137.6 €/MWh-day to 678.6 €/MWh-day. Due to the large range of battery investment costs, a sensitivity analysis was completed to determine the price of batteries that is economically viable. In [40], operations and maintenance prices of the battery systems are given to be between 2-6 cents per kWh. For this study this cost is selected

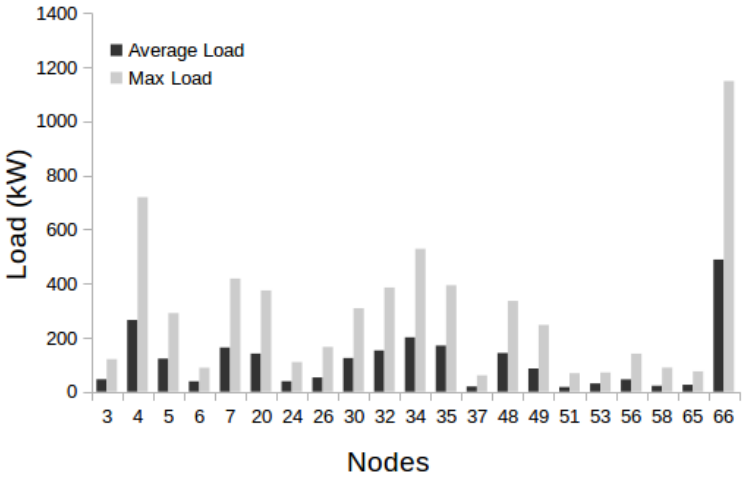

Figure 3.4: Load characteristics for all loaded nodes

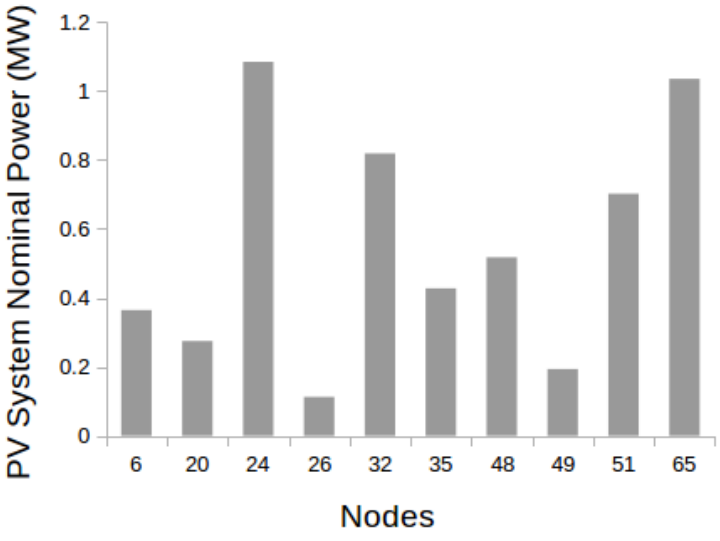

Figure 3.5: PV nominal power ratings for each PV node

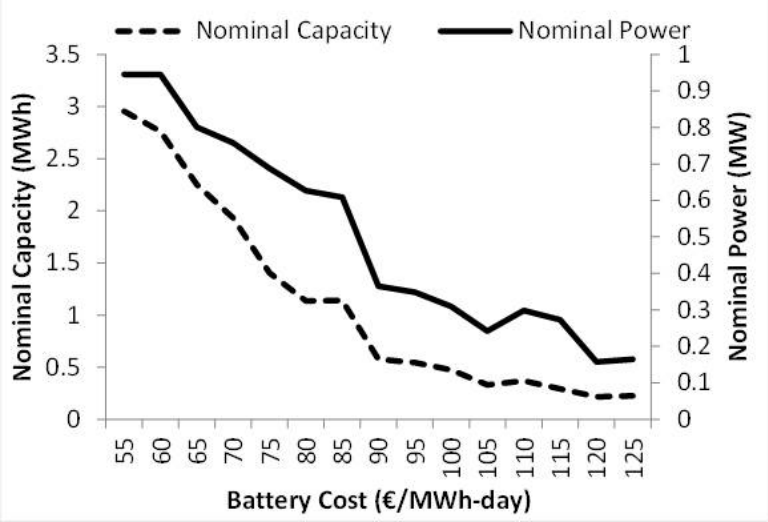

Figure 3.6: Total aggregated nominal capacity and power optimal system size as a function of battery costs

to be 2 cents/kWh.

Results

The two objective functions presented in eqs. (3.25) and (3.30) were analyzed to determine economically viable battery placement and sizing. In all considered scenarios, eq. (3.25) showed that battery investments were not economically viable for only loss minimization with the considered PV penetration and load profiles. A sensitivity analysis of the battery costs was performed with objective function eq. (3.30) to analyze the economic viability of storage systems used for loss minimization in addition to market participation. Results of the nominal power and capacity specifications calculated for each node using objective function eq. (3.30) can be found in Fig. 3.6.

This sensitivity analysis compares the sum of total nominal power and capacity for a feeder in relation to different investment costs. These total nominal capacity and power values are a sum of the individual nominal capacity and power values for each node. The price of batteries calculated by this study to be economically viable are lower than the battery costs found in [41]. For example, a battery with a capacity of 2 MWh and a nominal power rating of 1 MW cost on average 2.238 M€ according to the study [41]. In the sensitivity analysis, if the investment costs of the battery are 85 €/MWh-day, the total ideal nominal capacity and power for the feeder is 1 MWh and 0.6 MW. This per day investment cost can be translated into an initial investment cost by taking into account a life time of 10 years. The calculated initial investment cost of this system is therefore 310.25 k€. This implies that, for this battery to be economically viable, capital costs must be 7.2 times cheaper than the battery costs published in [41].

For the specific example of a battery investment price of 85 €/MWh-day, a sensitivity analysis was performed comparing the PV penetration and associated battery size. This comparison is found in Fig. 3.7

This sensitivity analysis shows a high correlation between optimally sized battery systems and PV system size. Therefore, grid connected battery systems become exponentially more

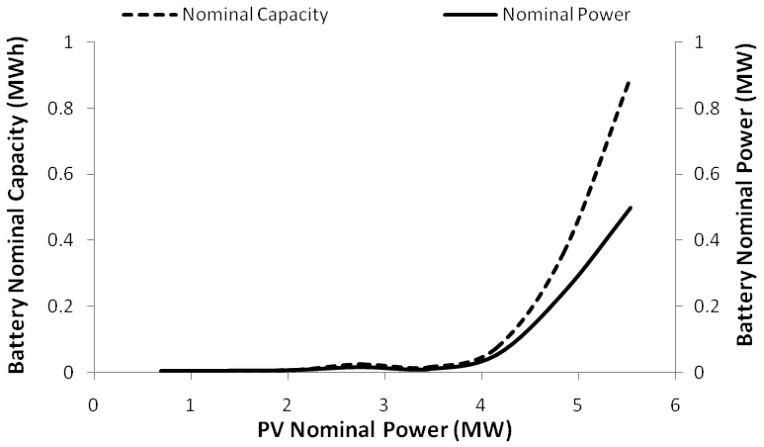

Figure 3.7: Sensitivity analysis of PV penetration in relation to optimal aggregated nominal power and capacity battery size for an investment cost of 85 €/MWh-day

economical with high penetration of DER.

A comparison of centralized and decentralized optimally placed capacity is shown in Fig. 3.8. The centralized storage nodes are considered to be any node on the main branch of the grid topology tree. The list of centralized nodes for this network are therefore 0, 1, 2, 3, 4, 5 and 6. All other nodes are considered to be decentralized placement nodes for storage devices.

As seen from this analysis, decentralized battery systems are prioritized for lower battery investment costs while centralized system sizes are mostly stable over all investment costs. Decentralized battery systems are prioritized when battery costs are low and overall total capacity and power installed is higher. When total capacity and power installed is smaller, the ratio of decentralized to centralized systems is also much smaller.

The partitioning of total nominal battery capacity and power as a function of battery investment cost is found in Fig. 3.9 and Fig. 3.10 to demonstrate the repartitioning of battery capacity and power.

As seen in Fig. 3.9 and Fig. 3.10, certain decentralized nodes including, for example, node 25, 34, 65 and 66, are prioritized for storage placement. These four nodes give three different examples of when storage is advantageous. Node 25 is a priority due to the high nominal PV power installed at node 24 and also due to the fact that this system is at the end of the electric feeder. For the case of node 34, high nominal PV power at node 35 combined with high loading at node 34 makes this node a priority. Nodes 65 and 66 are two nodes relatively close to each other. Node 66 has a high load and node 65 has a large PV system. The algorithm assigned capacity to both nodes, however in all cases a larger capacity is assigned to node 65 than 66 prioritizing a placement closer to the PV system installation rather than the node with a high load.

A closer look is taken into the case study with a battery cost of 85 €/MWh-day. The individual calculated sizes of battery systems for each node can be found in Fig. 3.11.

In Fig. 3.11 a nominal power and capacity value of storage devices is assigned to every node. This is due to the fact that many small systems allow to reduce losses. The size of the battery systems exponentially decreases when the nodes are ranked by size. This shows that certain nodes are high priority but having a storage at all nodes is ideal.

The objective function does not penalize small battery systems, therefore the infeasible small

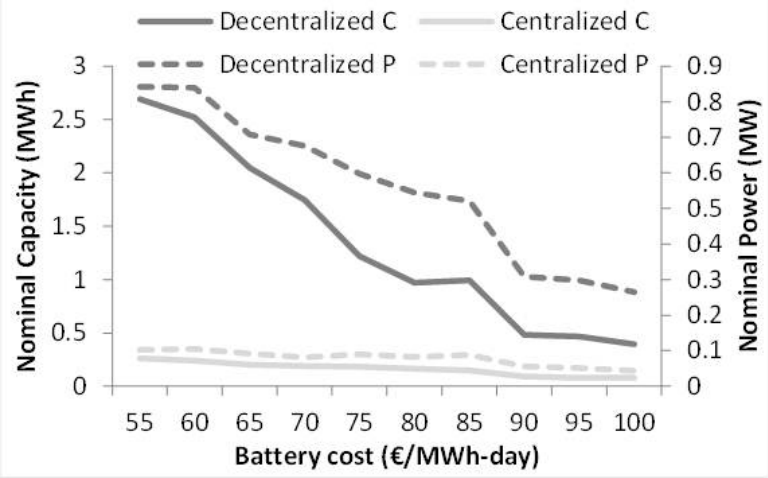

Figure 3.8: Comparison of centralized and decentralized nominal power (P) and capacity (C) optimal system size as a function of battery costs

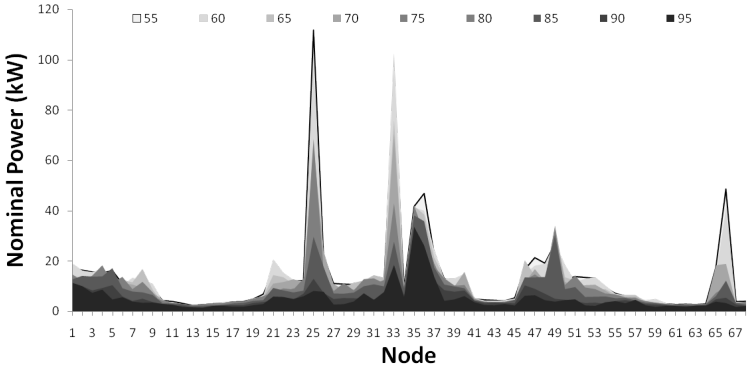

Figure 3.9: Calculated nominal power of battery systems for each node with battery prices varying from 55 €/MWh-day to 95 €/MWh-day

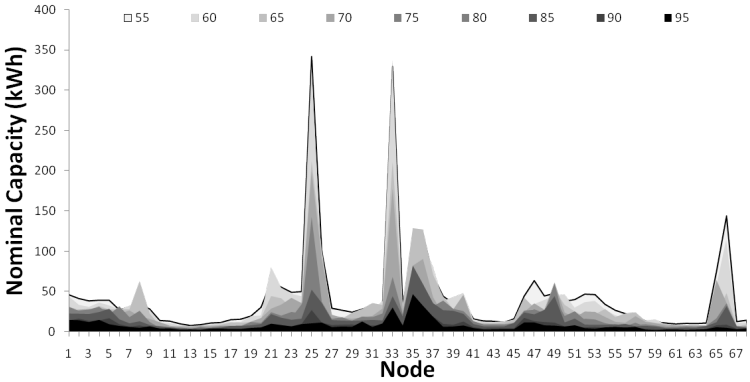

Figure 3.10: Calculated nominal capacity of battery systems for each node with battery prices varying from 55 €/MWh-day to 95 €/MWh-day

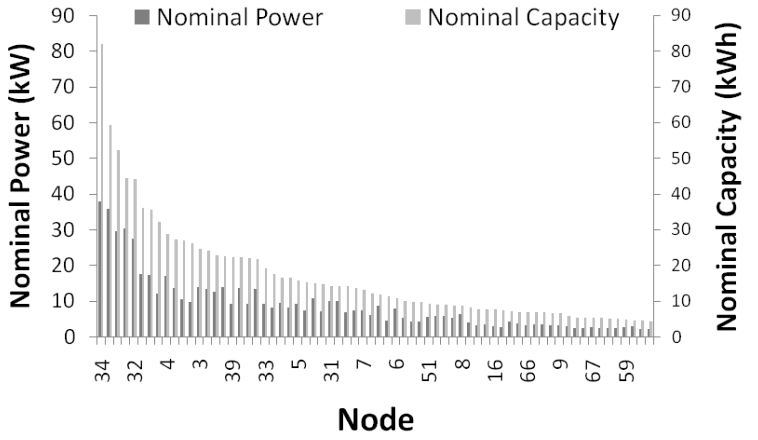

Figure 3.11: Calculated size of battery sizes for battery prices of 85 €/MWh-day

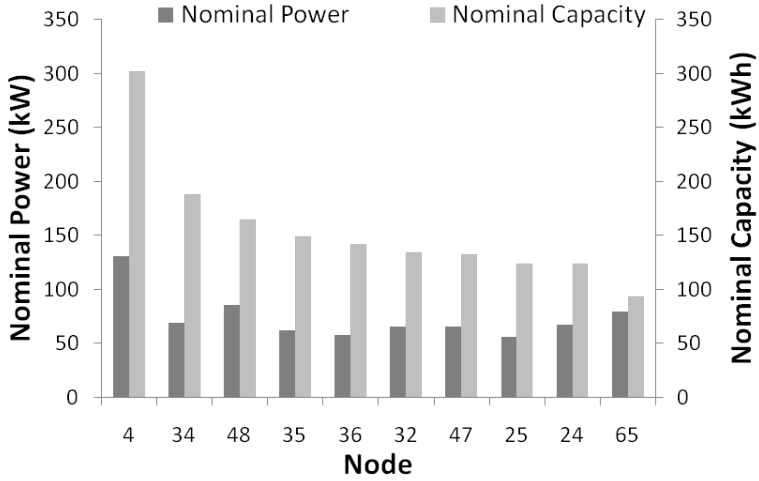

Figure 3.12: Final size of selected nodes with a battery cost of 85 €/MWh-day

battery systems must be eliminated through an iterative qualitative analysis. The final optimal placement and sizing of battery systems can be calculated by limiting the possible nodes where battery systems can be placed. This selection is performed based on the initial sizing and placement analysis. For the case defined by 85 €/MWh-day, the total number of systems installed was fixed to be 10. Therefore, a final analysis is performed by using eq. (3.33) and setting the set K_{st} as seen in eq. (3.34). The final resulting ideal sizing is found in Fig. 3.12.

$$K_{st} = 4, 34, 48, 35, 36, 32, 47, 25, 24, 65 \tag{3.34}$$

After fixing the maximum number of battery systems to be 10, a similar total nominal power and capacity is sized by the algorithm. Due to limited number of nodes for the repartition, the size of each system is therefore significantly larger than when all nodes are considered. Annual analysis results are then calculated by fixing the upper bounds of the nominal power and capacity of each battery system based on the values graphed in Fig. 3.12. The annual statistics of feeder

Table 3.2: Operation of electrical feeder with and without battery integration. Annual analysis for the case of 85 €/MWh-day

Characteristic	With battery	Without battery
Total Cost of Energy Imports (thousand €)	467	489
Total Benefit from Energy Exports (thousand €)	1.64	2.13
PV Benefits (thousand €)	334	314
PV Curtailement (MWh)	1.05	1.39
Nominal PV Power Installed (MW)	5.53	5.53
Nominal Batt Power Installed (MW)	0.74	0.0
Nominal Batt Capacity Installed (MWh)	1.55	0.0

Table 3.3: Calculation time for daily and annual analysis

Algorithm	Simulated time steps	Calculation time (s)
multi-temporal SOCP OPF	24	2.7
multi-temporal SOCP OPF	24x365	2700

operation with and without battery systems, is shown in Table 3.2.

The operation of the above feeder is affected by the presence of optimally placed and sized battery systems that allow for load shifting through pricing signals. The sum of imports and exports at the substation is therefore decreased. The first line in Table 3.2 shows that the optimized battery systems succeed to decrease the cost of imported energy. The level of exported energy shown in line two remains low due to the objective function that minimizes the absolute energy flow at the substation. Line four shows a reduction in PV curtailment due to added battery systems therefore increasing PV benefits as shown in line three.

Algorithmic Performance

The algorithmic performance of the simulation of a single time step and the full annual analysis is shown in Table 3.3.

The iterative approach to calculate $P^{nom}_{st,j,d}$ and $N^{nom}_{st,j,d}$ increases the daily analysis calculation time linearly depending on the number of iterations needed for convergence. The calculation times showed in 3.3 are therefore averages of all analysis performed.

3.4.4 Discussion

This algorithm is capable of calculating the placement and sizing of storage devices in a distribution grid. The optimal battery size is highly sensitive to the investment cost as shown in Fig. 3.7. In the context of a project, the capital investment of the project may be lower than the ideal size of storage capacity and power. If an investment constraint exists, an investment constraint can be integrated into the optimization problem as seen in eq. (3.35).

$$m_{st}^{inv} \sum_{j=0}^{J} soc_{st,j,d}^{nom} \leq \overline{m}^{inv} \tag{3.35}$$

This algorithm does not consider the planning of active demand as an alternative solution to electrochemical storage. While the algorithmic structure is very similar to modeling electrochemical storage elements, the calculation of the cost of demand side management is difficult. The costs are non-linear, client-dependent and data sets quantifying these costs are rare. Other possible solutions that were not explored include infrastructure upgrades.

A challenge identified was the capability to integrate non-linear cost functions with respect to the nominal power and capacity of batteries. Another interesting improvement to the cost function could include the integration of variable battery technologies and the associated variable cost parameters. Future work can be done to integrate these non-linear characteristics into the SOCP convex relaxation algorithm.

3.5 Conclusion

This chapter has presented two different multi-temporal OPF algorithms used for hosting capacity analysis and optimal placement and sizing of storage systems. A multi-temporal analysis is necessary to analyze the added benefits of storage in a smart grid setting coupled with high DER penetration. These storage devices can reduce annual operational costs and increase the hosting capacity of a network. However, the economic benefits of storage devices must be compared to their investment costs during the planning process.

An algorithm is proposed that simultaneously sizes and places battery systems that can be effectively used to analyze the economic viability of operational case studies in comparison to investment and operational costs. The advantages of this algorithm in relation to the literature include:

· A high performance algorithm for solving an annual sizing and placement problem through decomposition into daily analysis

· A methodology to integrate operational case studies of battery management strategies into the planning phase of active distribution grids

· A qualitative study of battery investment costs and their operational benefits to make investment decisions about grid connected storage

· A demonstration of the increasing benefit of grid connected storage in the presence of high DER penetration

This type of innovative algorithm gives insights into the advantages of grid connected storage devices in distribution systems and the integration of operational strategies into the planning phase.

Another important aspect of the distribution grid is the consideration of uncertainties. While deterministic planning tools can be effective for certain applications, uncertainties in decentralized production and load must be taken into account, especially for operational strategies. OPF algorithms for distribution grids are already non-convex and high-dimensional. Integrating more variables into the problem to account for uncertainties is a complex task and will be addressed in the next chapter.

Chapter 4

OPF analysis considering uncertainties

Résumé

Les incertitudes de la génération et des charges distribuées sont assez élevées dans un réseau de distribution en comparaison avec un réseau de transport. Les incertitudes dans la gestion journalière peuvent avoir un effet significatif sur les coûts de gestion. Il en résulte que la flexibilité de la charge et de la génération pourrait être prise en compte pour mieux optimiser les coûts de gestion et reporter les investissements des infrastructures. Une planification robuste des flexibilités à J-1 peut aider à améliorer la gestion du jour J. Planifier les flexibilités d'une manière robuste signifie de prendre en compte des variables incertaines telles que les conditions météorologiques ou les profils de charge. Les techniques existantes de prévisions peuvent être utilisées pour intégrer ces incertitudes dans un problème OPF et ainsi calculer la planification de la flexibilité optimale sous certaines contraintes, et réaliser des analyses stochastiques OPF. Ce chapitre se divise en deux sections principales. Premièrement, une introduction et présentation des challenges d'une OPF stochastique algorithmique est réalisée. Cette section aborde les difficultés associées avec la génération de scénarios et l'intégration dans une OPF. Différentes possibilité pour la modélisation de la flexibilité sont également présentées. Une présentation plus approfondie des contraintes de confort en lien avec les algorithmes utilisés par la gestion de la demande est également détaillée. Deuxièmement, une méthodologie intégrant avec succès les incertitudes dans un algorithme de planification à J-1 pour les composants de stockage et la gestion de la demande. Cet algorithme utilise deux méthodes pour la génération de scénarios et les compare. Un cas d'étude présente une analyse des bénéfices en terme de coûts de la gestion de la demande et la prise en compte des contraintes de confort. Une étude comparative entre une stratégie stochastique et une déterministe est également présentée. La planification stochastique des flexibilités au travers d'un outil de stochastique OPF amène des coûts annuel de gestion inférieurs dans tous les cas. Les contraintes de confort des clients finaux montrent également un impact économique sur les coûts annuels de gestion. Une comparaison entre les violations des contraintes de confort et les coûts annuels de gestion est réalisée montrant une augmentation des coût pour des violations des contraintes de confort réduites.

4.1 Summary

Uncertainties of distributed generation and load are relatively high in the distribution grid in comparison to transmission grids. Uncertainties in daily operation can have significant effects on the operational costs of distribution grids. Therefore, flexibility of load and generation should be considered to better optimize operational costs and defer infrastructure investments. Day-ahead robust scheduling of these flexibilities can help improve day-of operations. Scheduling flexibilities in a robust manner implies taking into account uncertain variables such as meteorological conditions or load profiles. Existing forecasting techniques can be used to integrate these uncertainties into the OPF problem and therefore calculate optimal flexibility scheduling under uncertain conditions, therefore performing stochastic OPF analysis. This chapter is presented in two main sections. First, an introduction and discussion of stochastic OPF algorithmic challenges is completed. This section discusses the difficulties associated with scenario generation and integration into an OPF. Different possibilities for flexibility modeling are also presented. A more in depth discussion about comfort constraints in the context of algorithms that manage DSM is also detailed. Second, a methodology is presented that successfully integrates uncertainties into a day-ahead scheduling algorithm for storage devices and DSM. This algorithm uses two methods for scenario generation and compares the two. A case study is presented demonstrating the a cost-benefit analysis of DSM and the consideration of comfort constraints. A comparative study between stochastic and deterministic strategies is also presented. The stochastic scheduling of flexibilities through OPF simulation tools results in lower annual operational costs in all cases. Comfort constraints of end users are also shown to have economic impacts on annual operational costs. A comparison of comfort constraint violations and annual operational costs is completed showing increased costs for reduced comfort constraint violations.

4.2 Introduction

At the distribution grid level, uncertainties of load and renewable energy generation represent a challenge for the DSO. On the load side, aggregation effects of higher voltage grids are no longer applicable for distribution grids. These aggregation effects tend to smooth out the variability and uncertainty of the total load on an electrical network. Due to a relatively lower load and voltage, the variation of commercial and residential load profiles can have a more significant impact on voltage profiles and congestion problems. On the decentralized generation side, a majority of DER such as solar panels are connected to the distribution grid. The electric production of DER is variable and uncertain due to their dependence on meteorological conditions. The combination of generation and load uncertainties introduce new challenges for DSO to maintain power quality in distribution grids as discussed in section 1.5. In the context of smart grids, these uncertainties are critical when scheduling DER such as grid connected storage, controllable loads or PV curtailment.

While short term uncertainties have created challenges for daily operations, more long term uncertainties also exist in relation to increasing load and decentralized generation. The uncertain evolution of load in combination with an uncertain evolution of DER is challenging for the planning of future operational strategies. Therefore, it is important to integrate into the planning phase innovative operational strategies that mitigate these challenges. Current planning strategies that propose grid reinforcements primarily based on a worst-case operational scenario are expensive and conservative. In the context of increasing load and DER, the worst-

case scenario becomes very expensive. New planning and operational strategies that take into account uncertainties without oversizing electrical systems are necessary. These planning and operational strategies are primarily based on leveraging the flexibilities of distribution grids.

Flexibilities in distribution grids such as generator curtailment, demand side management or storage can help smooth out the volatility of load and generation profiles. These flexibilities can be harnessed to ensure a stable and reliable operation of the distribution grid and optimize economic exploitation [95] [84]. Possible controllable loads include residential hot water heaters or HVAC systems. In particular, the control of individual loads, e.g. HVAC systems [96], brings new sources of uncertainty to the day-ahead planning but also new added flexibility. These added uncertainties include ambient temperature, building occupation, and variations in the consumption habits. However, these appliances used for DSM can be seen as a type of thermal storage and therefore can be controlled without affecting end-user comfort.

DSM has proven to be a valuable resource to compensate the variability of the renewable sources, especially through the control of thermal loads such as HVAC and EWH. As shown in [28], load control can significantly reduce microgrid operation costs as well as C02 emissions. While DSM can add significant flexibility to a distribution grid, the thermal comfort constraints of end-users must be maintained. The scheduling of these flexibilities should therefore take into account uncertainties to allow for the robust optimization of operational costs while satisfying end-user comfort constraints. Effectively taking into account uncertainties of next day operations requires sophisticated forecasting methods.

Sophisticated forecasting is essential for robust scheduling of controllable devices. The importance of forecasting strategies for power systems applications is extensively discussed in [97]. While multiple forecasting strategies exist in the literature, the appropriate forecasting strategy must be selected for each application. In this thesis, forecasts will be used as inputs into an OPF algorithm. This specific use of forecasts is unique because only certain forecasts that influence the limits of the problem or change the value of the objective function will affect the optimization results. Due to the fact that an OPF problem is already high-dimensional, scenario selection is important to minimize the number of scenarios considered therefore keeping the problem size manageable. Only scenarios that influence the problem should be included.

This chapter will explore the advantages of considering uncertainties in a day-ahead flexibility scheduling algorithm. Two new major topics will be presented in this chapter, the consideration of uncertainties and the added benefit of DSM. The integration of uncertainties into an OPF includes deciding the way uncertainties are represented in the problem and the type of forecasting that is used to calculate the uncertainties. The second topic of DSM implies deciding which types of components are controllable and which constraints will be considered for the flexible loads. These topics will be discussed in further detail in this chapter.

4.3 Stochastic OPF for day-ahead scheduling

Optimization algorithms can be found in the literature to solve the problem of day-ahead scheduling of dispatchable resources. Numerous examples of deterministic [26] [27], stochastic [98] [29] and hybrid [28] [30] approaches to optimal scheduling used in the presence of DER and controllable load are presented in the literature. Optimization methods include quadratic programming QP [58] as well as heuristic and meta-heuristic techniques [26] [99]. In the optimal scheduling of DER in multi-node distribution grids, heuristics have the advantage of enabling exact network constraints [26], while QP requires a convex relaxation of the power flow equations [30]. Due

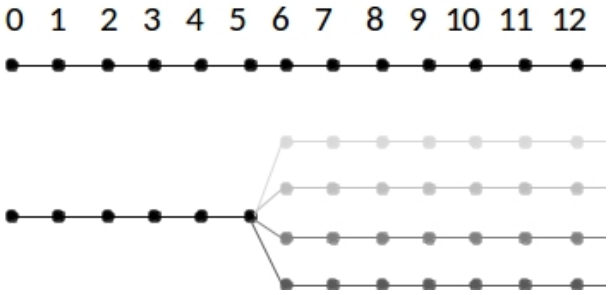

Figure 4.1: Scenario tree with "trunk" period between 0-5 and the branch region between 6-12

to the random aspect of search techniques in heuristic methods, calculation time can be high and the global optimal is not guaranteed. However, QP methods perform significantly better in terms of computational time. Thus, when combined with techniques that guarantee accuracy of the power flow calculations, e.g. linear cuts [57], they become a better solution.

Stochastic approaches have been used in OPF algorithms to represent uncertainties of load and generation profiles. Primarily, these strategies include either scenario trees [100] [29] or statistical parameters of the stochastic variables [101] [102] [103] that are integrated into the optimization problem. The scenario tree approach allows for the representation of a temporal evolution of each stochastic variable. This temporal dependency is important when considering flexibilities that are temporally constrained such as storage devices. The generation of scenarios for optimization algorithm purposes have been explored in [29] [104] [105]. The first method presents probabilistic forecasts that are directly used as scenarios within the optimization problem [29]. The method described in [105] is a more sophisticated technique developed for wind generation scenarios that uses a zero-mean multivariate normal distribution function and a historical covariance matrix to preserve realistic temporal dependencies of each scenario. A more recent paper [104] applied the method developed in [105] to wind generation and load scenarios by generating 500 scenarios for each variable and reducing the scenarios by using probabilistic distance and a fast forward selection algorithm. Besides the probabilistic forecasting technique originally developed for wind scenarios, few other techniques exist specifically applied to PV, load and temperature scenarios.

4.3.1 Scenario representation in an OPF

The integration of scenarios in an OPF algorithm can be completed in different ways. Three different methods were implemented in the frame of this thesis. The difference for each technique implies a different organization of the OPF linear constraint matrix. The technique of integrating a scenario tree into the linear constraint matrix is classified as a probabilistic analytical approach named scenario-based decision making, for taking into account uncertainties in power systems as classified in [106].

The first method includes a scenario tree structure composed of a "trunk" and "branches". This scenario tree implies certain number of time steps where the controllable variable is forced to have the same value across all scenarios for the time steps included in the "trunk". The second period allows the controllable variables to assume multiple values for each "branch". A diagram of an example scenario tree can be found in Fig. 4.1.

A second strategy has only one time step for the "trunk", therefore allowing the controllable

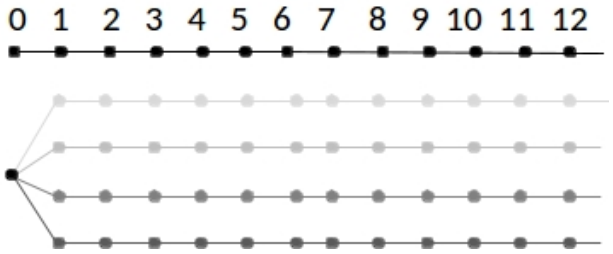

Figure 4.2: Scenario tree with "trunk" period for time step 0 and the branch region between 1-12

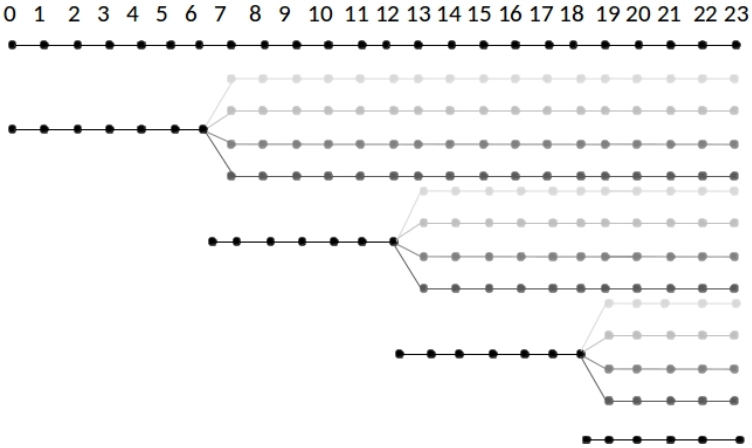

Figure 4.3: Sliding scenario tree formation to solve optimal scheduling problem

variables to vary for almost all the time steps except for the first one. This scenario tree structure is seen in Fig. 4.2.

The third strategy has only a "trunk" for all time steps. This means that all controllable variables for each time step for all scenarios must be equal. This forces the controllable variables for each time step to satisfy all constraints of all scenarios for each time step.

If the first or second strategy is chosen, a sliding optimization is necessary to successfully calculate the optimal schedule for a period longer than the "trunk" period. This sliding technique solves the optimal schedule of the "trunk" based on the varying profiles in each branch. A new tree is then defined for the next period with the set points of the first optimization as an input. A diagram of this sliding optimization technique is shown for the first strategy presented in this section in Fig. 4.3.

The first and second technique allow for controllable variables to have different behavior based on varying scenarios. However, instead of solving one optimization problem, four optimization problems are resolved consecutively as shown in Fig. 4.3. This sliding optimization technique can increase calculation time.

The last strategy forces the control variables to satisfy all of the constraints of each scenario with one single value. This strategy can result in feasibility problems depending on the distance between the scenarios. However, this strategy only requires the resolution of one optimization problem therefore lowering the calculation time.

4.3.2 Scenario generation techniques

The multi-period scenarios described in section 4.3.1 can be generated in various ways. Two scenario generation techniques were implemented in the frame of this thesis to evaluate the effectiveness of the stochastic OPF algorithm. The first technique uses directly probabilistic forecasts for all uncertain variables. Two probabilistic quantiles were chosen for each variable representing a high-end and low-end estimation. These two quantiles were chosen to be 25% and 75%. These two scenarios for each stochastic variable were then considered to be equally probable and were combined in all possible combinations.

The second scenario generation technique implemented a more sophisticated strategy to acquire more realistic scenarios. The scenarios generated for each stochastic variable are calculated with a probabilistic scenario generation technique as described in [105] [104]. The UL, temperature and EWH scenarios were generated directly by using a three-month historical period to calculate the quantiles and the covariance matrix to generate normal Gaussian scenarios.

The PV production profile has a very strong correlation associated with the irradiation. Therefore, the method presented in [105] is less effective. The strong correlation with irradiation may dilute the other causes of variation in PV production such as cloud cover. The PV production profiles were therefore normalized by the clear sky index before applying the scenario generation strategy of [105]. This allows for a more precise analysis of inter temporal variation due to cloud cover that are not correlated with irradiation.

Using this strategy, 50 scenarios were generated for each stochastic variable. Of these 50 scenarios, three scenarios were selected based on the total cumulative values of the day. Therefore, for temperature, EWH, UL and PV, the units of the cumulative values are degree-hour, liters of hot water, MWh and MWh respectively. The three scenarios are chosen by selecting the maximum, minimum and closest to average value of the cumulative values. The scenarios associated with the minimum, maximum and average cumulative values are then used as inputs for the stochastic OPF analysis.

4.3.3 Demand side management of thermal loads

Demand side management is a complicated flexibility to consider due to the fact that end-user comfort may be affected by the DSO management strategy. Whenever considering demand side management in an optimization model, it is important to consider the financial consequences in comparison to client satisfaction. Two primary modeling strategies are presented in the literature for DSM consideration: an aggregated model or individual modeling of devices. Aggregated models make acceptable assumptions about individual devices [100] and they improve aggregated controllability of a distribution grid, but the comfort of individual end-users is not modeled in detail. Thus, individual load models become more appropriate for small scale applications (e.g. buildings) where a detailed comfort representation is required. In [30], individual load models are used in optimization of building operations with DR. A deterministic approach that considers end-user comfort constraints and PV for a three building micro-grid is detailed in [27]. An algorithm proposing an economic penalty for violations in thermal comfort constraints is presented in [29]. It is important when considering DSM, to consider the effects on end-users to properly quantify this flexibility. Therefore, end-user comfort constraints should be explicitly considered in the stochastic OPF problem formulation.

Thermal comfort constraints can be considered as a hard optimization constraint or can be included in the objective function as a cost penalty. Hard optimization constraints can

create more infeasible situations in the optimization simulations. Integrating soft constraints for comfort constraint violations allows for more flexibility in the thermal loads. However, the appropriate price must be associated with these comfort violations. Associating a low cost to comfort violations will result in the preference of under-heating of the houses to reduce total operational costs.

4.4 Proposed stochastic optimal power flow method

This section presents an example algorithm and case study that uses stochastic modeling techniques and considerations as described in section 4.3. The example algorithm and case study demonstrate results that allow for discussion about the above modeling strategy possibilities. The algorithm presented is a method for day-ahead scheduling of DER. The algorithm uses the SOCP convex relaxation of the power flow equations to guarantee an optimal solution and ensure a low calculation burden as mentioned in [57]. During periods of high DER injection, this relaxation can be inexact, therefore, linear cuts are added to the problem to guarantee exactness. The flexibilities considered include electrochemical storage and thermal loads, such as electric heating or cooling loads and EWH. Individual device models are considered in the scheduling task as seen in [30]. The constraints on the DSM devices are therefore thermal comfort constraints of end-users as described in [107]. The integration of comfort constraints into an optimization algorithm has been completed in a paper found in the literature [29]. However, this paper does not consider constraints on the network which is critical in a distribution grid context.

The proposed formulation is based on an interdisciplinary perspective and it merges contributions from three different areas of power systems optimization with primary contributions being:

· a multi-period SOCP adapted to consider uncertainties through scenarios of generation and load

· the optimal day-ahead scheduling of distribution grid flexibilities, considering grid constraints, end-user comfort constraints, and the multi-temporal dispatch of different DER technologies

· the behind-the-meter individual loads devices modeling and scheduling for optimal DR strategies, constrained by the comfort of end-users, and integrated with the distribution grid stochastic dispatch

By combining these contributions in a single stochastic OPF, the methodology aims to provide a valuable discussion on the implications of generation and load uncertainties for distribution grid control and the resulting effects on end-user comfort while considering DSM.

4.4.1 Method overview

The stochastic formulation presented takes into account uncertainties in PV generation, uncontrollable load, temperature and hot water consumption habits of the end-users. High and low scenarios for each variable are selected through a scenario reduction strategy and are considered to be equiprobable. Combinations of these variables' scenarios therefore create scenario constraints that are included in the stochastic optimization problem. The methodology is represented as a flow chart in Fig. 4.4.

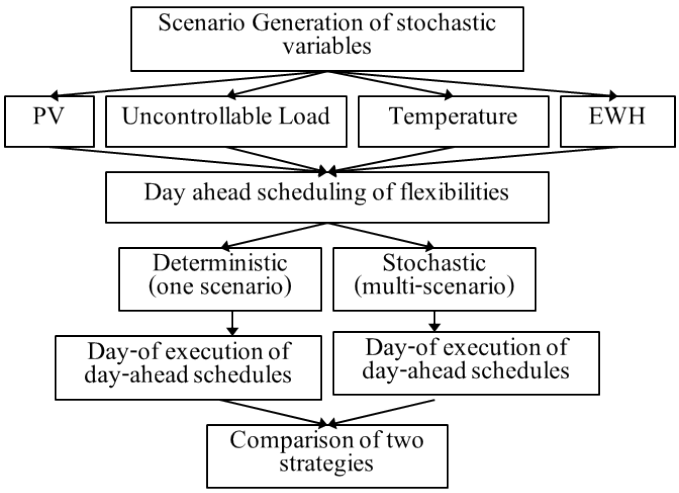

Figure 4.4: Flow chart of proposed methodology to take into account uncertainties in day-ahead operational scheduling of flexibilities

4.4.2 Formulation

The proposed formulation eqs. (4.1) and (4.3)–(4.21) is a multi period (t) multi-scenario (γ) optimal power flow that aims at reducing operational costs through robust scheduling of batteries ($P_{st,j,t}$) and controllable thermal loads, EWH ($P_{ewh,j,t}$) and AC ($P_{ac,j,t}$), located at the nodes (j) of the distribution grid.

Objective function

Two objective functions are presented in this section. One which optimizes the cost of operation of a grid and the second which optimizes the cost of operation plus the cost penalties associated with comfort constraint violations. The operation cost function eq. (4.1) considers different costs for energy imports and exports, following the current regulatory mechanisms adopted by several European countries to promote self-consumption. Hence, the energy exports at the point of common coupling are remunerated at wholesale electricity market price, while the energy consumption costs are charged at the final electricity price. The hourly electricity market price includes fixed rates added to the wholesale electricity price due to transmission distribution cost. The first objective function presented therefore implies strict thermal comfort constraints. This means that eqs. (4.21)–(4.23) $\Theta_{Hac,d,t}$ and $\Theta_{Lac,d,t}$ are forced to be zero. The objective only considering minimization of operational costs is found in eq. (4.1).

$$\min. \sum_{\gamma=0}^{\Gamma} \sum_{t=0}^{T} [m_{edc,t} P_{+,\gamma,t} t + m_{ec,t} P_{-,\gamma,t} t] \tag{4.1}$$

The second possible objective function includes cost penalties for comfort constraint violations. If this objective is used, the temperature constraints described in eqs. (4.21)–(4.23) are relaxed to include a wider range of temperatures but cost penalties are associated with temperatures outside of the desired range.

$$\text{min.} \sum_{\gamma=0}^{\Gamma} \sum_{t=0}^{T} \left[m_{edc,t} P_{+,\gamma,t} t + m_{ec,t} P_{-,\gamma,t} t + \sum_{d=0}^{D} m_{cf} \left(\Delta\Theta_{low,d,\gamma,t} + \Delta\Theta_{high,d,\gamma,t} \right) \right] \tag{4.2}$$

The necessity of introducing cost penalties for comfort constraint violations stems from possible feasibility problems in the thermal models. If infeasibility is a problem, a relaxation of the thermal constraints and introduced cost penalty can resolve these infeasibilities.

Power flow constraints

The constraints of the problem include the nodal power balance considering different DER technologies eqs. (4.3)–(4.6). The eq. (4.7) describes the convex relaxations of the line constraints. The result of each OPF calculation for each time step is compared to a forward backward sweep power flow calculation to verify that the convex relaxation of the line constraint equation eq. (4.7) is exact. If the solution is not exact, linear cuts are added to the problem to guarantee exactness as explained in [57].

$$P_{ij,\gamma,t} = P_{ul,j,\gamma,t} + P_{cl,j,t} + \sum_{k=0}^{K} P_{jk,\gamma,t} + r_{ij} \ell_{ij,\gamma,t} + P_{pv,j,\gamma,t} + P_{st,j,t} \tag{4.3}$$

$$Q_{ij,\gamma,t} = Q_{ul,j,\gamma,t} + \sum_{k=0}^{K} Q_{jk,\gamma,t} + x_{ij} \ell_{ij,\gamma,t} + Q_{pv,j,\gamma,t} \tag{4.4}$$

$$\upsilon_{j,\gamma,t} = \upsilon_{i,\gamma,t} - 2(r_{ij} P_{ij,\gamma,t} + x_{ij} Q_{ij,\gamma,t}) + (r_{ij}^2 + x_{ij}^2) \ell_{ij,\gamma,t} \tag{4.5}$$

$$\underline{V}^2 \leq \upsilon_{j,\gamma,t} \leq \overline{V}^2 \tag{4.6}$$

$$\ell_{ij,t} \geq \frac{P_{ij,\gamma,t}^2 + Q_{ij,\gamma,t}^2}{\upsilon_{i,\gamma,t}} \tag{4.7}$$

Battery system constraints

The eqs. (4.8)–(4.12) represent the battery limits regarding power and state of charge. This includes the definition of power injection limits, charging and discharging variables for the battery systems in eqs. (4.8)–(4.10). The state of charge calculation and limits are also defined in eqs. (4.11) and (4.12). The battery power and state of charge are not scenario dependent as explained in section 4.3.1.

$$P_{st,j} = P_{st+,j,t} + P_{st-,j,t} \tag{4.8}$$

$$0 \leq P_{st+,j,t} \leq \overline{P}_{st,j} \tag{4.9}$$

$$-\overline{P}_{st,j} \leq P_{st-,j,t} \leq 0 \tag{4.10}$$

$$\underline{soc}_{st,j} \leq soc_{st,j,t} \leq \overline{soc}_{st,j} \tag{4.11}$$

$$soc_{st,j,t-1} = soc_{st,j,t} + t\eta_{st} P_{st+,j,t} + t\frac{1}{\eta_{st}} P_{st-,j,t} \tag{4.12}$$

Thermal comfort constraints

The thermal comfort constraints associated with the individual HVAC and EWH controllable devices are shown in eqs. (4.13)–(4.23). These are the first order physically-based load modes – considering the thermal capacity (C), resistance (R), and heat loss constant (α) - to describe the temperature behavior of thermal systems. The full matrix representation of the multi-period power/thermal conversion in a form Ax<>b is presented in [107]. The division of over and under heating is shown in eqs. (4.21)–(4.23) which allows for a piecewise linear penalty function of thermal constraint violations in the objective function. Costs are associated with both under and over heating in the HVAC systems. The penalization was used only for HVAC systems and not for EWH systems due to the fact that HVAC thermal constraint violations are more common than EWH violations.

$$P_{cl,j,t} = \sum_{j=0}^{J} P_{hvac,j,t} + \sum_{j=0}^{J} P_{ewh,j,t} \tag{4.13}$$

$$\sum_{d=0}^{D} P_{ewh,d,t} = P_{ewh,j,t} \tag{4.14}$$

$$0 \leq P_{ewh,d,t} \leq \overline{P}_{ewh,d} \tag{4.15}$$

$$\underline{\Theta}_{wtr} \leq \Theta_{ewh,d,\gamma,t} \leq \overline{\Theta}_{wtr} \tag{4.16}$$

$$\begin{aligned} &\Theta_{ewh,d,\gamma,t} = \Theta_{ewh,d,\gamma,t-1} + \frac{t}{C_d} \times \\ &[-\alpha_d \left(\Theta_{ewh,d,\gamma,t-1} - \Theta_{int,d}\right) - \vartheta_{d,t} C_{wtr} \left(\Theta_d - \Theta_i\right) + P_{ewh,d,t}] \end{aligned} \tag{4.17}$$

$$\sum_{d=0}^{D} P_{hvac,j,t,d} = P_{hvac,j,t} \tag{4.18}$$

$$0 \leq P_{hvac,j,t,d} \leq \overline{P}_{hvac,j,d} \tag{4.19}$$

$$\Theta_{hvac,d,\gamma,t} = \Theta_{hvac,d,\gamma,t-1} - \frac{t}{C_d R_d} \left[\Theta_{hvac,d,\gamma,t-1} - \Theta_{ext,\gamma,t} + \eta_d R_d P_{hvac,d,t}\right] \tag{4.20}$$

$$\underline{\Theta}_{hvac,d} - \overline{\Delta}\Theta_{low} \leq \Theta_{hvac,d,\gamma,t} \leq \overline{\Theta}_{hvac,d} + \overline{\Delta}\Theta_{high} \tag{4.21}$$

$$\underline{\Theta}_{hvac,d} - \Theta_{hvac,d,\gamma,t} = \Delta\Theta_{low,d,\gamma,t} \tag{4.22}$$

$$\Theta_{hvac,d,\gamma,t} - \overline{\Theta}_{hvac,d} = \Delta\Theta_{high,d,\gamma,t} \tag{4.23}$$

$$\tag{4.24}$$

These thermal equations are implemented for each individual device. This allows for a detailed modeling of DSM and the calculation of an optimal schedule for each device.

Stochastic variables

Controllable variables include the active power of EWH for residential clients and HVAC thermal loads for commercial clients ($P_{ewh,j,t,h}$ and $P_{ac,j,t,h}$) and the active power of battery systems ($P_{st,j,t}$). A part of the load is considered to be uncontrollable ($P_{ul,j,t}$). A table summarizing the

Table 4.1: Control variables, scenario dependent variables and stochastic variables

Type	Applicable Variables
Controllable Variables	P_{st} (P_{st+}, P_{st-}), P_{cl} (P_{hvac}, P_{ewh})
Scenario Dependent Variables	P_{ij}, ℓ_{ij}, Q_{ij}, v_i
Stochastic Parameters	P_{pv}, P_{ul}, $v_{d,t}$, Θ_{ext}

controllable variables, stochastic variables and scenario dependent variables is found in Table 4.1.

The scenario structure used in this algorithm is the third scenario structure technique described in section 4.3.1. This scenario structure forces the controllable variables to satisfy all the constraints of each scenario while minimizing the cost of imports and exports at the substation. In the deterministic case, only the constraints of one scenario apply to the controllable variables.

4.4.3 Performance evaluation of deterministic vs stochastic strategy

The effectiveness of the stochastic method is evaluated through two measures as done in [108]. The two measures include the expected value of perfect information (EVPI) and the value of the stochastic solution (VSS). EVPI is the difference between the cost of the stochastic approach and the perfect forecast. VSS is the difference between the deterministic strategy and the stochastic strategy. The stochastic strategy uses high and low scenarios while the deterministic strategy uses average scenarios. The average scenarios rely on one scenario that combines the average conditions of all uncertain variables. The scheduled set points for EWH, HVAC and battery power are implemented with no intra-day adjustments for the real conditions. The thermal equations are used to simulate the evolution of temperatures in the buildings and in the hot water tanks. Energy costs, grid constraint violations and thermal comfort profiles are then analyzed to assess the comfort of end-users in comparison with the economic performance of the optimization strategies.

4.5 Case study

In this section, the proposed methodology presented in section 4.4 is applied to a medium voltage IEEE 37 node network (4.8 kV) assumed to be located in Grenoble, France. A map of the grid topology can be found in Fig. 4.5.

4.5.1 Generation and Load Data

Load profiles including EWH, HVAC and uncontrollable load profiles are simulated using a bottom up load simulator detailed in [91]. The load profile simulator produces a group of individual commercial and residential building load profiles. The group of load profiles are simulated to be statistically accurate representations of residential and commercial customer proportion, electric heating, living surface area and population using the INSEE building inventory database of France. The location of each load profile was determined randomly due to the fact that no grid load data was available. The medium voltage feeder is assumed to have a 5 MVA transformer serving 5 low voltage substations for a total of 312 clients, 300 residential clients and

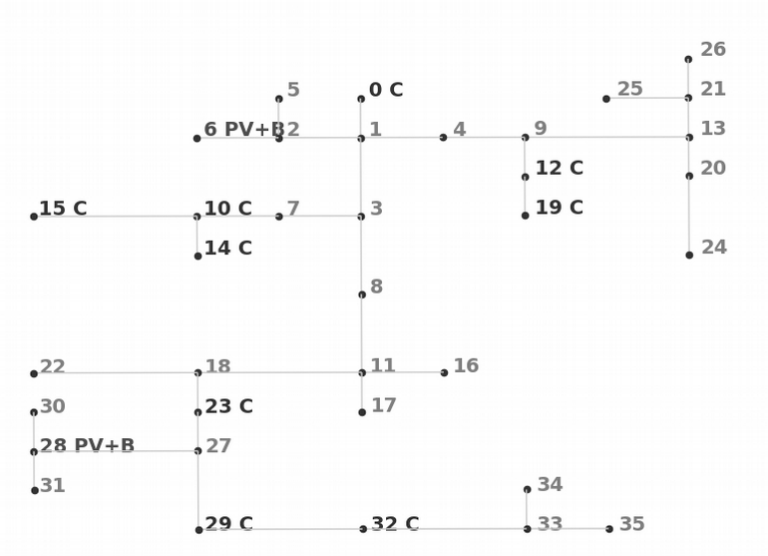

Figure 4.5: Medium voltage IEEE 37 node case study feeder. C indicates a node with load, PV + B indicates nodes with PV and batteries

12 commercial clients. Of the 300 residential clients, 53 residential hot water heaters are controllable. It was assumed that only commercial clients' HVAC systems could be controlled and therefore all of the 12 commercial clients heating and air conditioning devices were assumed to be controllable. A total of 1.2 MW uncontrollable load, 155 kW of controllable EWH and 308 kW of controllable HVAC are therefore considered.

PV production curves were based on the normalized real production of a PV plant in Grenoble, France [109]. The real hourly production was normalized by the nominal power and was used as the coefficient of production for all PV nodes. A total capacity of 2.62 MW of PV is distributed at 5 nodes. Each node with a PV system was assumed to also have a battery system of 250 kW nominal power and 500 kWh nominal capacity, resulting in a total of 1.25 MW and 2.5 MWh of battery systems. The UL, CL and DER characteristics for each node can be found in Table 4.2. The parameters that are used for the HVAC and EWH units are as follows: for EWH, the maximum power per device is between 2.0-6.0 kW, thermal capacities and heat loss coefficient are within 0.0877 – 0.2925 kWh/ ^{o}C and 0.0004-0.0012 kW/ ^{o}C, respectively. Cold water (ϕ_i) and usage temperatures (ϕ_d) are 12 ^{o}C and 65 ^{o}C, while temperature limits are between 60 ^{o}C and 80 ^{o}C. For individual buildings HVAC systems, the maximum power is between 2.44 – 158.67, C and R values are within 0.2244 – 1318.4959 kWh/ ^{o}C and 0.0127-21.0012 ^{o}C/kW, respectively. The comfort temperatures are between 19 ^{o}C and 26 ^{o}C. The case study also uses historical variable market prices for electricity cost in France for 2012.

4.6 Results

The results section will highlight four primary findings: i) the difference in performance by using probabilistic forecasts in comparison to the multivariate covariance matrix approach, ii) cost benefits of combining stochastically managed storage devices with controllable loads, iii) economic advantages of using a stochastic approach instead of a deterministic one and iv) thermal comfort improvements with stochastic techniques. The method described in this chapter has

Table 4.2: UL, CL and DER characteristics per node

Node	0	6	10	12	14	15	19	23	28	29	32
Average UL (kW)	28	-	95	62	95	64	76	66	-	21	8
Maximum UL (kW)	68	-	212	156	212	155	183	159	-	52	20
Nominal PV Power (kW)	-	313	-	819	428	-	518	-	542	-	-
Nominal Battery Power (kW)	-	250	-	250	250	-	250	-	250	-	-
Nominal Battery Capacity (kWh)	-	500	-	500	500	-	500	-	500	-	-
Number of EWH devices	4	-	7	5	4	4	6	6	-	10	3
Number of AC devices	0	-	0	2	1	2	2	1	-	3	0

Table 4.3: Case study labels

Scenario	ST NO CL 2 S	ST NO CL 4 S	ST W T 10€	ST W T 1€	ST 2 S	ST C	ST PV	ST 4 S
1	$p_{pv}^{L} p_{ul}^{H} p_{ewh}^{M} \theta_{ext}^{M}$	$p_{pv}^{L} p_{ul}^{H} p_{ewh}^{M} \theta_{ext}^{M}$	$p_{pv}^{L} p_{ul}^{H} p_{ewh}^{H} \theta_{ext}^{L}$	$p_{pv}^{L} p_{ul}^{H} p_{ewh}^{H} \theta_{ext}^{L}$	$p_{pv}^{L} p_{ul}^{H} p_{ewh}^{M} \theta_{ext}^{M}$	$p_{pv}^{M} p_{ul}^{H} p_{ewh}^{M} \theta_{ext}^{M}$	$p_{pv}^{H} p_{ul}^{M} p_{ewh}^{M} \theta_{ext}^{M}$	$p_{pv}^{L} p_{ul}^{H} p_{ewh}^{M} \theta_{ext}^{M}$
2	$p_{pv}^{H} p_{ul}^{L} p_{ewh}^{M} \theta_{ext}^{M}$	$p_{pv}^{H} p_{ul}^{L} p_{ewh}^{M} \theta_{ext}^{M}$	$p_{pv}^{H} p_{ul}^{L} p_{ewh}^{L} \theta_{ext}^{H}$	$p_{pv}^{H} p_{ul}^{L} p_{ewh}^{L} \theta_{ext}^{H}$	$p_{pv}^{H} p_{ul}^{L} p_{ewh}^{M} \theta_{ext}^{M}$	$p_{pv}^{M} p_{ul}^{L} p_{ewh}^{M} \theta_{ext}^{M}$	$p_{pv}^{L} p_{ul}^{M} p_{ewh}^{M} \theta_{ext}^{M}$	$p_{pv}^{H} p_{ul}^{L} p_{ewh}^{M} \theta_{ext}^{M}$
3	-	$p_{pv}^{H} p_{ul}^{H} p_{ewh}^{M} \theta_{ext}^{M}$	$p_{pv}^{H} p_{ul}^{H} p_{ewh}^{H} \theta_{ext}^{H}$	$p_{pv}^{H} p_{ul}^{H} p_{ewh}^{H} \theta_{ext}^{H}$	-	-	-	$p_{pv}^{H} p_{ul}^{H} p_{ewh}^{M} \theta_{ext}^{M}$
4	-	$p_{pv}^{L} p_{ul}^{L} p_{ewh}^{M} \theta_{ext}^{M}$	$p_{pv}^{L} p_{ul}^{L} p_{ewh}^{L} \theta_{ext}^{L}$	$p_{pv}^{L} p_{ul}^{L} p_{ewh}^{L} \theta_{ext}^{L}$	-	-	-	$p_{pv}^{L} p_{ul}^{L} p_{ewh}^{M} \theta_{ext}^{M}$

been implemented in Python and uses the Mosek optimization API. The computer that is used for the simulation of all calculations is a desktop with a 3.4GHz processor.

Multiple case studies are tested to quantify the effect of each stochastic variable on the total annual operational cost. The test cases consider high (H) and low (L) scenarios for between one and four of the four stochastic variables to analyze the effects of each stochastic variable independently as well as their compounded effects. If the high and low scenario is not used for a stochastic variable the average scenario is used (M). Table 4.3 details the labels for each case study used in the following figures.

4.6.1 Probabilistic forecasts

Probabilistic scenarios are calculated by calculating the quantiles of a historical data set. The studies in this chapter use historical data from the past three months. The quantiles are calculated for each hour individually. This is done for all unknown variables. Examples for PV production, UL and temperature are found in Fig. 4.6, Fig. 4.7 and Fig. 4.8 respectively.

These profiles are acceptable for estimating high and low values of an uncertain variable based on historical data. However, this type of modeling does not produce realistic scenarios that follow the temporal dependencies of the historical values. This is due to the fact that the quantiles are calculated per hour and are therefore independent models of each hour. Another scenario generation technique was implemented based on the methods found in [105]. This method considers the temporal dependencies of each hour to produce more realistic scenarios.

4.6.2 Multivariate covariance forecasts

The method described in [105] is a more sophisticated technique developed for wind generation scenarios that uses a zero-mean multivariate normal distribution function and a historical covariance matrix to preserve realistic temporal dependencies of each scenario. This method was implemented and tested in an OPF problem to evaluate the added value of temporally dependent realistic scenarios as opposed to basic probabilistic scenarios. Example scenarios generated

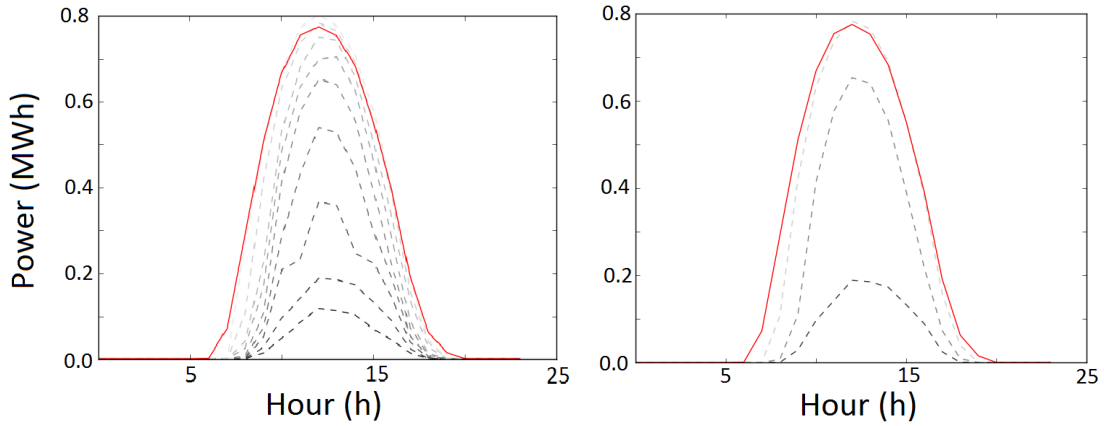

Figure 4.6: PV production quantiles 10 to 90 (left) and the selected high, low and middle quantiles (25th, 75th and 50th) (right) with the real PV realization for the prediction day in red

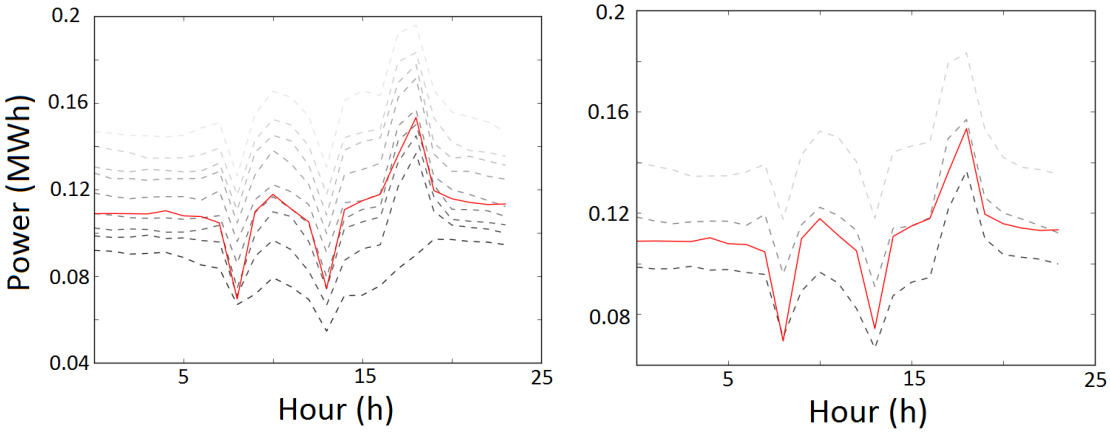

Figure 4.7: Uncontrollable load profile quantiles 10 to 90 (left) and the selected hig, low and middle quantiles (25th, 75th and 50th) (right) with the real load profile realization for the prediction day in red

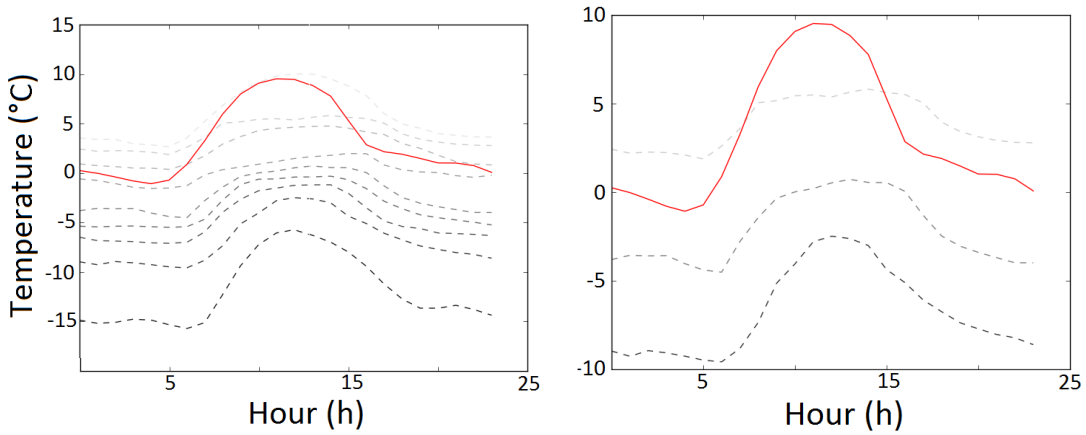

Figure 4.8: Temperature profile quantiles 10 to 90 (left) and the selected high, low and middle quantiles (25th, 75th and 50th) (right) with the real load profile realization for the prediction day in red

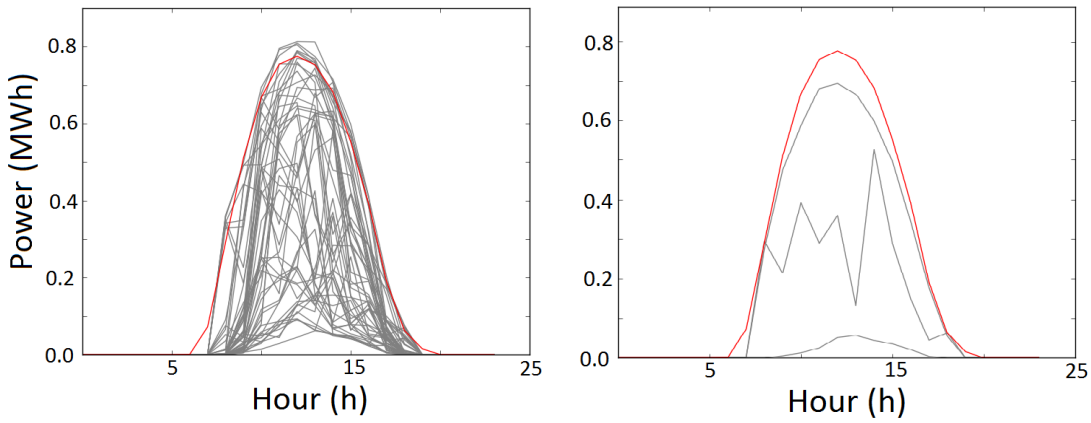

Figure 4.9: PV production scenarios (left) and the selected high, low and middle scenarios (right) with the real PV realization for the prediction day in red

with this technique for PV generation and uncontrollable load are found in Fig. 4.9, Fig. 4.10 and Fig. 4.11 respectively.

From the 50 scenarios generated with this technique, three scenarios were chosen to input into the optimization problem. These three scenarios included one high, one low and one middle scenario. To determine which scenarios were high low and middle, the integral of each scenario was calculated. This results in a cumulative value for each scenario profile. Of these cumulative values, the maximum, minimum and average value were selected. The scenarios generated associated with the minimum maximum and average values were used as inputs to the OPF model.

4.6.3 Annual operational cost benefit

The annual operational costs with grid connected storage devices are calculated using both the stochastic and deterministic day-ahead management strategies. The deterministic case uses the

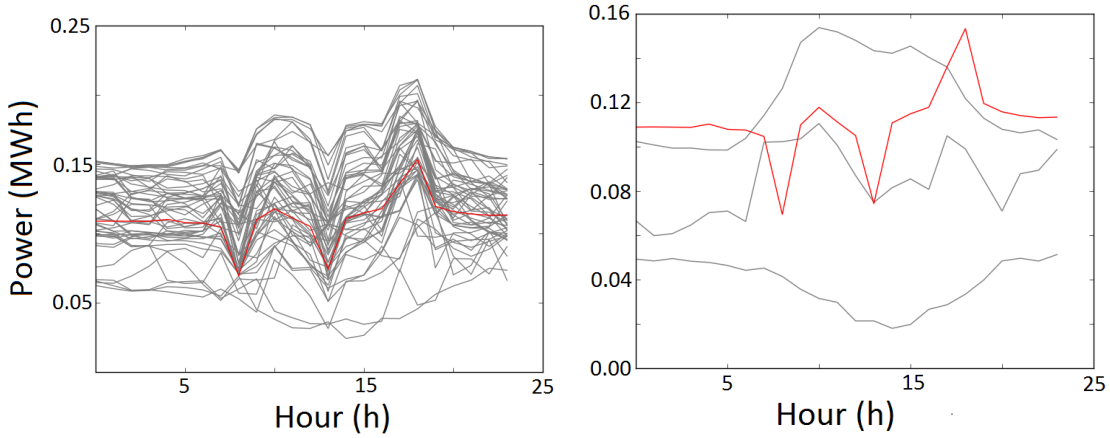

Figure 4.10: Load profile scenarios (left) and the selected high, low and middle scenarios (right) with the real load profile realization for the prediction day in red

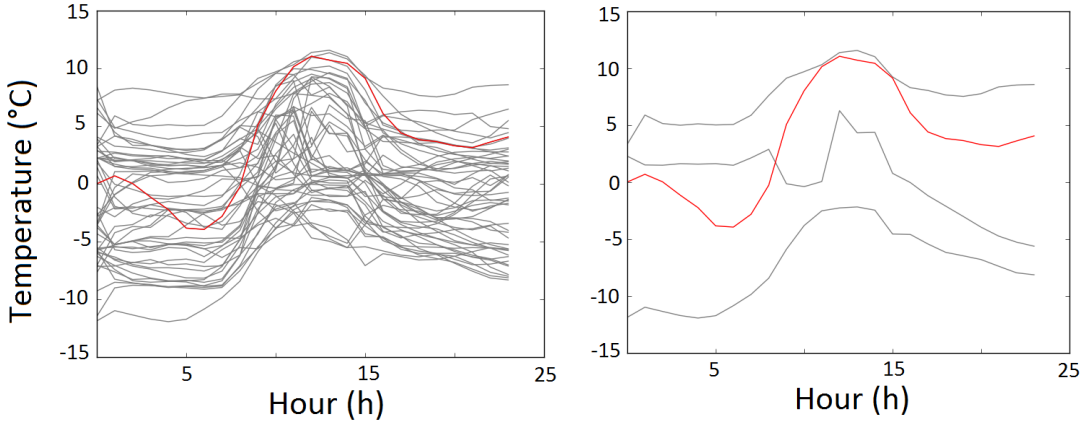

Figure 4.11: Temperature profile scenarios (left) and the selected high, low and middle scenarios (right) with the real temperature profile realization for the prediction day in red

forecast that corresponds to the average of the available forecasts for all stochastic variables. The stochastic case uses combinations of high and low generate forecasts for each stochastic variable. Considering only one variable as stochastic therefore results in two scenarios. Considering two scenarios for two variables will result in four scenarios of equal probability. For example, the simulation cases 'St 2 S' and 'St 4 S' consider two and four scenarios respectively.

Two sets of simulations have been conducted to show the difference in annual operational cost when using probabilistic forecasts or multivariate covariance forecasts. The results are presented by calculating the VSS and EVPI indicators as described in section 4.4.3. Fig. 4.13 and Fig. 4.12 show the stochastic performance evaluated with the two performance analysis measures for annual operational costs. The advantages of the stochastic method in comparison to the deterministic method are discussed in the following topics:

· reduced annual cost due to the integration of controllable load

· impact of considering a higher number of scenarios

· relaxed thermal constraints with cost penalties

A detailed comparison of the stochastic and the deterministic schedules is presented for an example day to better understand why stochastic management strategies are advantageous. Lastly, the thermal comfort constraints violations are quantified for each case.

Reduced costs with controllable load

For both scenario generation techniques, integrating controllable load into the optimal scheduling problem reduces annual costs significantly. The reduction in operational costs is primarily due to variable hourly pricing. If the distribution grid operator is capable of shifting the power demand for HVAC and EWH loads to less expensive periods, annual operational costs are reduced even if the same energy is consumed. This can be seen in the EVPI indicator of Fig. 4.15 and Fig. 4.16. The first two simulations for both scenario generation techniques are performed without controllable load.

Benefit of increasing number of scenarios

In the simulations with no CL, a first comparison of simulating only extreme scenarios or simulating all possible combinations of scenarios can be seen between "St No CL 2 S" and "St No CL 4 S". The simulation of "St No CL 2 S" simulates only the extremes of PV and UL uncertainty. This means the high PV scenario is combined with the low UL scenario and the high UL scenario is combined with the low PV scenario. As seen in Fig. 4.12 and Fig. 4.13 no major economic advantage is seen in using 4 scenarios instead of 2. This could be because the 2 initial scenarios already represent extreme situations that have a dominant impact in the optimization problem.

A similar comparison is completed with the case including CL. The two simulations that represent all possible combinations or just the extremes of PV and UL are "St 4 S" and "St 2 S" respectively. Similar to with no CL, the simulation of "St 4 S" represents all possible combinations of PV and UL while "St 2 S" only represents high PV combined with low load and low PV combined with high load. This comparison shows an increase in cost benefit when considering all 4 scenario combinations.

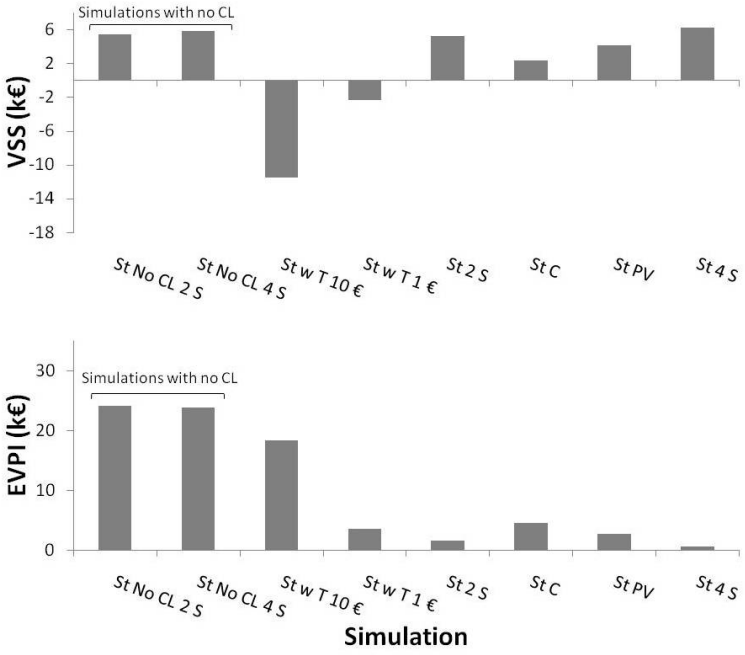

Figure 4.12: Annual costs of operation for the case with only batteries ("St No CL 2 S" and "St No CL 4 S") and with additional flexibility from CL ("St w T 1 €", "St w T 10 €", "St 2 S", "St C", "St PV" and "St 4 S") using probabilistic forecasts

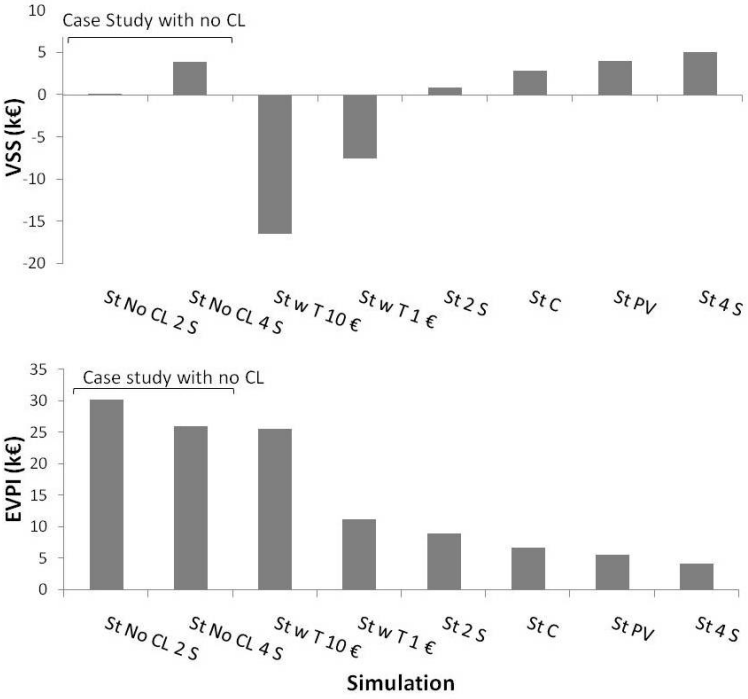

Figure 4.13: Annual costs of operation for the case with only batteries ("St No CL 2 S" and "St No CL 4 S") and with additional flexibility from CL ("St w T 1 €", "St w T 10 €", "St 2 S", "St C", "St PV" and "St 4 S") using multivariate covariance forecasts

Effects of increased costs penalty of comfort constraints

The simulations 'St w T 10 €' and 'St w T 1 €' consider uncertainty in PV and UL as well as considering uncertainty in outside temperature and EWH consumption. The difference between these two simulations is the cost penalty for violating comfort constraints. The value of this cost penalty is either 1 euro or 10 euros. The consideration of uncertainties in temperature and EWH consumption forces the stochastic day-ahead management strategy to satisfy a larger range of outside temperatures or EWH use in the thermal comfort constraints. Therefore, the management strategy is more conservative and increases annual operational costs. This is the reason why these two simulations are the only simulations where the stochastic management strategy is more expensive than the deterministic one shown by the VSS indicator in Fig. 4.12 and Fig. 4.13. In addition, higher annual costs result for the simulation with higher cost penalties for comfort constraint violations, however, comfort constraint violations are reduced.

Example day comparison of stochastic and deterministic scheduling techniques

An example day profile of the different battery and controllable load management schedules for the deterministic and the stochastic strategy is shown in Fig. 4.14. The stochastic day ahead scheduling of loads and batteries on this day proved to reduce costs significantly when simulated with real day-of conditions. This improvement can be explained by the transition periods between the hours 6 to 9 and 14 to 19. In the period between hours 6 to 9 am, the deterministic case is expecting PV injection, therefore it charges the battery. The stochastic case considers the low PV scenario and therefore it performs a more conservative discharge during this period. Instead, it moves the battery discharge to the hours 10-13, where low generation of PV is expected (in low scenario) and the electricity price is high. When the real conditions are simulated for day-of, very low PV production occurs and the deterministic case incurs in high operational cost during the period 10-13. In contrast, the stochastic approach is capable of anticipating low PV generation, discharging the battery when prices are higher and shift the CL to the early morning, avoiding the costs at 16-18 incurred by the deterministic case.

From the analysis performed, a trade-off was observed between annual operational costs and comfort constraint violations in the thermal loads. This trade-off can be considered as a Pareto-optimality state with annual operational costs and end-user comfort defining the Pareto-frontier.

Comfort constraint violations

As shown in Fig. 4.15 and Fig. 4.16, considering uncertainties in external temperature is a Pareto improvement for end-user comfort constraints in HVAC loads while not considering these uncertainties is a Pareto improvement for annual costs. Considering uncertainties in EWH consumption results in very minimal annual operational costs increases, however comfort violations are reduced. Two different values for cost penalties were also tested, 1 €and 10 €. With higher cost penalties for temperature violations, annual costs were higher but fewer comfort violations resulted. In all cases the stochastic algorithm results in lower annual operational costs for the same number of comfort constraint violations when comparing stochastic and deterministic approaches.

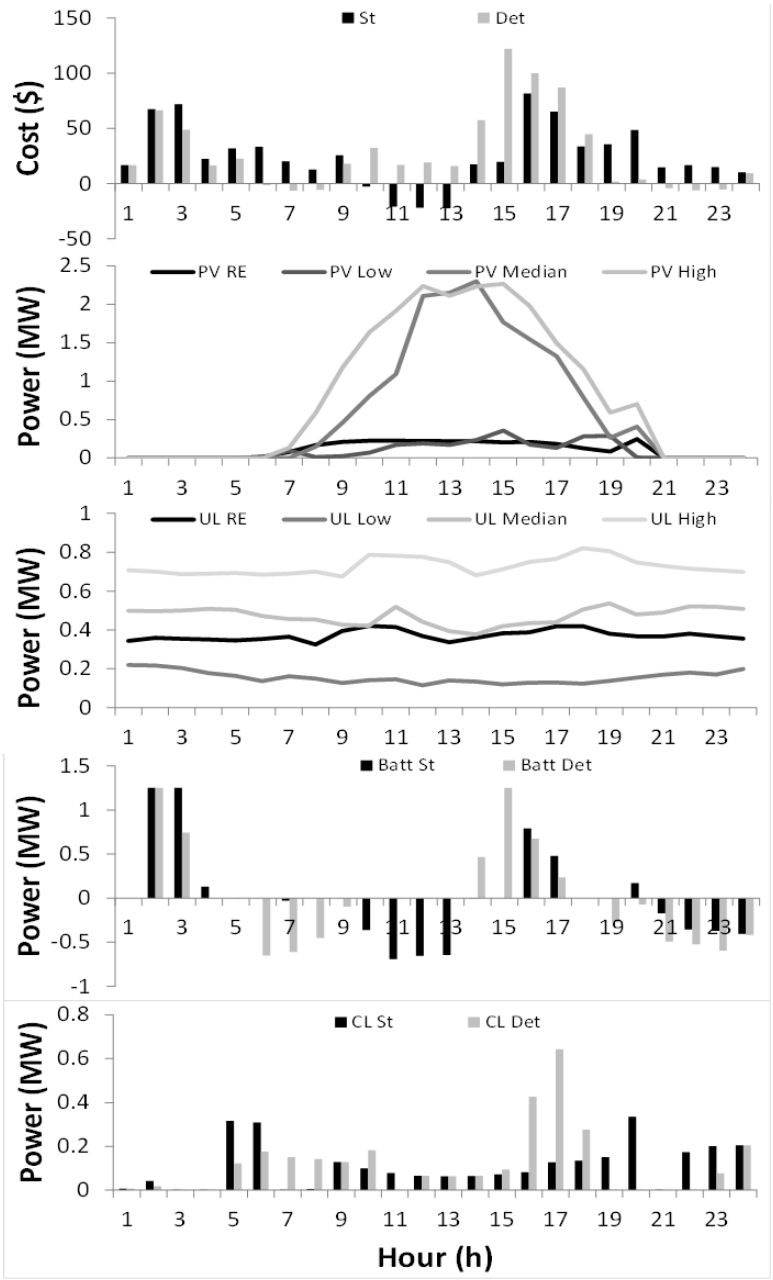

Figure 4.14: Example day where stochastic scheduling results in lower operational costs than the deterministic one. From top to bottom, price of electricity (1), PV scenarios and real PV production (2), UL scenarios and real UL (3), stochastic and deterministic battery schedule (4), stochastic and deterministic controllable load schedule (5).

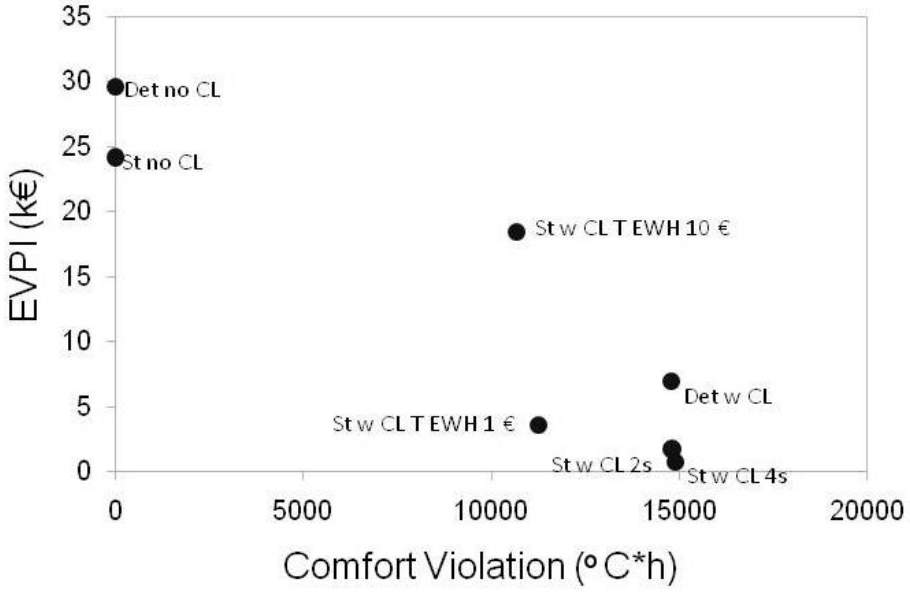

Figure 4.15: Annual operational cost vs annual comfort constraint violations for the total comfort constraint violations of AC and EWH using probabilistic forecasts

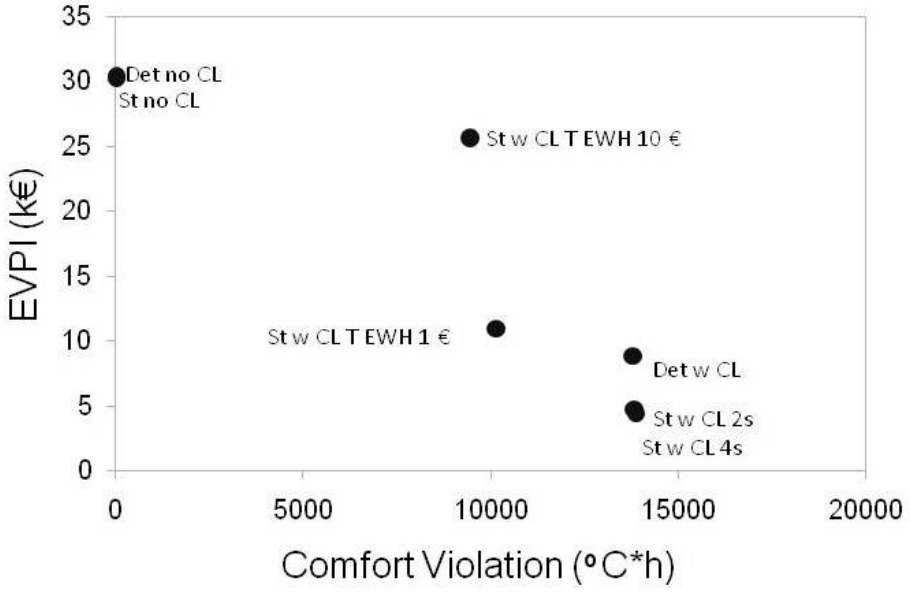

Figure 4.16: Annual operational cost vs annual comfort constraint violations for the total comfort constraint violations of AC and EWH using multivariate covariance forecasts

Table 4.4: Algorithmic performance of deterministic and stochastic methods for 24 coupled time-steps

Method	Number of Scenarios	Forecast Technique	CL present	Time (s)
Deterministic	1	Probabilistic	No	3
Stochastic	2	Probabilistic	No	8
Stochastic	4	Probabilistic	No	14
Deterministic	1	Probabilistic	Yes	6
Stochastic	2	Probabilistic	Yes	15
Stochastic	4	Probabilistic	Yes	44
Deterministic	1	Multivariate covariance	Yes	7
Stochastic	2	Multivariate covariance	Yes	16
Stochastic	4	Multivariate covariance	Yes	47

Algorithmic performance

It is important to consider the calculation time of the day-ahead scheduling strategies presented above. Due to the fact that the stochastic algorithm takes into account multiple scenarios, the calculation time of this algorithm is higher. A performance analysis was completed to compare the time of calculation for the deterministic algorithm and varying number of scenarios in the stochastic algorithm. The average calculation time of each 24 coupled time-steps is shown in Table IV. Therefore, the stochastic algorithm is about 3 times slower with the consideration of 2 scenarios and 6 times slower with the consideration of 4 scenarios.

4.7 Conclusion

This chapter discusses techniques used for stochastic OPF algorithms. Varying techniques used in stochastic OPF are presented including scenario generation, flexibility modeling and thermal comfort constraints representation. A methodology to integrate these techniques into a stochastic OPF is then proposed and two analysis are completed with two different scenario generation techniques. The results in terms of annual operation and comfort constraint violations are presented. Five significant conclusions have been drawn from these simulations:

· there is no significant improvement in operational costs when using a more sophisticated forecasting technique (the multivariate covariance forecasts). However, thermal comfort constraint violations are reduced with this forecasting technique

· annual operational costs are significantly reduced when controllable load such as HVAC and EWH are considered

· the increased number of scenarios reduced annual operational costs for the simulations with CL but increased costs in the simulations without CL

· there is a compromise between annual operational costs and comfort constraint violations when CL is integrated into the problem. The cost of these comfort constraint violations must be

comparable to the energy cost of satisfying these constraints, therefore avoiding significant discomfort for end-users.

The use of the stochastic algorithm resulted in a reduction in the operational costs for the case study presented in comparison with the deterministic strategy. However, given that the stochastic approach permits hedging over a higher number of scenarios for the input variables to anticipate risks, the cost reduction is moderate. Significant savings can be achieved by harnessing DSM. However individual devices and end-user comfort constraints must be considered.

Chapter 5

Conclusions

5.1 Conclusions

The current energy transition is characterized by the desire to transition from traditional fossil fuels to more sustainable sources of electricity production. This transition implies the integration of new technologies such as renewable energy generators. New electric production technologies have presented new design and implementation challenges due to the specificity of each resource. Traditional planning and operational strategies have solved these types of problems in the past by infrastructure reinforcements of the transmission or distribution grid. When considering a high DER penetration, these infrastructure upgrades can become expensive and, consequently, are an economic barrier for renewable energy development.

A majority of these generators are connected to the electric distribution grid due to their relatively small size and the current development strategies for these technologies. Therefore, a new problem emerges requiring optimization of new decentralized components. This decentralized optimization requires a new type of infrastructure including automation and control of a much larger quantity of devices. The automation and control of distribution grids can push back expensive infrastructure upgrades.

A literature review has been detailed, presenting possible alternative solutions to infrastructure upgrades. However, these innovative solutions are often not integrated in the current planning or operations of distribution grids. The author of this thesis therefore has explored the existing methodologies and presented new methodologies to improve on the current methods found in the literature. This literature review included a definition of the existing electric power system followed by a more detailed explanation of the distribution system. Specific challenges of decentralized generators in the distribution grid in relation to voltage profile deviation and safety devices were detailed. The literature review was continued by presenting existing planning strategies with and without massive integration of DER. Innovative smart grid solution such as storage, demand side management and curtailment were proposed as possible alternatives for infrastructure investments. These solutions require sophisticated power flow analysis tools. Existing power analysis tools were presented including power flow analysis and OPF analysis. OPF analysis was described in more detail to justify the choice of this tool as opposed to power flow analysis. These sophisticated algorithms present new mathematical challenges as well which were discussed along with proposed solutions to overcome these challenges.

This thesis has presented work contributing to the advancement of power system analysis for smart grids in the presence of high renewable energy penetration. New sophisticated planning

and operational tools are necessary to analyze the effects of high DER penetration on existing architecture. The optimization of existing networks through automation and control has been discussed, i.e. smart grids. The case studies presented in this thesis assume a controllability of the grid with the possibility of automation through intelligent algorithms. In order to thoroughly explore the application of these types of algorithms, three primary subjects were addressed: three-phase unbalanced systems, distribution planning methodologies, and uncertainties in distribution grid operation. The thesis was presented in three parts. The first section presented the challenges of a three-phase unbalanced systems. The second section presented the difficulties of planning tools for distribution networks and proposed an innovative algorithm for the simultaneous sizing and placement of storage systems. The last section discussed the elevated uncertainties that are experienced by the distribution grid and how these uncertainties can pose challenges for distribution grid operations. A methodology to integrate these uncertainties into a day-ahead planning algorithm was then presented.

Three-phase unbalanced systems found in low voltage distribution grids can exacerbate distribution grid power quality issues. Few OPF analysis tools exist in the literature that are capable of taking into account neutral current effects. These effects can increase voltage profile divergence. Detailed analysis of the three-phase unbalanced power flow equations in comparison with single-phase estimations were presented. The single-phase estimations of three-phase unbalanced systems in the context of OPF analysis for planning were concluded to be sufficient. Therefore, further chapters continue with single-phase estimations of individual phases of distribution grids.

Planning methodologies that are capable of considering smart grid operational strategies were presented in Ch. 3. Existing algorithms using OPF analysis of distribution grids were presented specifically in relations to multi-period OPF analysis. Flexibilities that are temporally constrained such as storage elements were used to increase the hosting capacity of an example grid. A methodology was presented that successfully integrates an operational strategy for storage systems into the sizing and placement exercise through a techno-economic analysis. This methodology successfully integrated operational strategies into the planning phase and quantified the benefits of smart grid operation.

The innovation and specific contributions of this planning methodology in relation to the state of the art is the development of a high performance algorithm for solving an annual sizing and placement problem through decomposition into daily analysis. The methodology presented is innovative because it integrates operational case studies of battery management strategies into the planning phase of active distribution grids. This contribution allows for the qualitative study of battery investment costs and their operational benefits to make investment decisions about grid connected storage.

Uncertainties in distribution grids are relatively high due to lack of aggregation effects for load profiles and generation profiles. The section has presented a state of the art on uncertainty modeling in the context of power system analysis. The algorithmic challenges of integrating these uncertainties were then discussed along with varying modeling methods. DSM was presented as a promising solution to reduce annual operational costs significantly and therefore was integrated in parallel with storage units and curtailment strategies. Finally, a methodology for the integration of these uncertainties in an OPF day-ahead scheduling algorithm of grid flexibilities including DSM, storage and curtailment was presented through a comparison of stochastic and deterministic techniques.

The innovation in relation to the state of the art of this day-ahead scheduling algorithm

is the development of a multi-period SOCP OPF that is capable of considering uncertainties through scenarios of generation and load. This algorithm does not exist in current literature and allows for the optimal day-ahead scheduling of distribution grid flexibilities. To the author's knowledge, there is no paper published that implements an SOCP OPF with integrated individual appliance models for their optimal scheduling and associated thermal constraints while considering uncertainties. This behind-the-meter individual load device modeling and scheduling for optimal DSM integrated with the distribution grid enables a very precise quantification of the benefits of DSM. It is combined with stochastic dispatch of decentralized generators and storage to quantify this benefit in a smart grid context.

The work completed in the frame of this thesis contributes to the need for further smart grid planning and operational methodologies for the future. The success of the energy transition is highly dependent on the intelligent evolution of the current distribution grid. This evolution is critical to guarantee a future with easy access to high quality electricity. Work in this area is a high priority due to the high dependence of the safety, health and economy on electricity worldwide.

5.2 Future work

In relation to planning algorithms that consider sizing and placement of storage devices, this methodology could be enlarged to include a choice of different battery technologies or other types of flexibilities for the DSO. A challenge identified during Ch. 3 was the capability to integrate non-linear cost functions with respect to the nominal power and capacity of batteries. These non-linear costs add mathematical complexity to the problem. Another interesting improvement to the cost function could include the integration of variable battery technologies and the associated variable cost parameters. This would allow the algorithm to not only size and place battery systems but also give suggestions about the best battery technology to install based on the operational use case. Future work can be done to integrate these non-linear characteristics into the SOCP convex relaxation algorithm.

Another possible flexibility to consider in contrast to battery systems is DSM. These studies could be very interesting to analyze the techno-economic advantages of DSM in comparison to electrochemical storage. The algorithmic structure for the consideration of DSM is not complicated however, the calculation of the cost of demand side management is difficult. The costs may be non-linear, client-dependent and data sets quantifying these costs are rare. Other possible solutions that were not explored include the comparison of the cost of infrastructure upgrades with smart grid functionality integration. The cost-benefit analysis of these two alternatives should be further researched.

On the subject of uncertainty scheduling with stochastic OPF algorithms, future work should be completed in more sophisticated scenario reduction techniques. Detailed analysis of which scenarios are most important to include in an OPF analysis could be performed to better understand the effect of extreme scenarios or more realistic scenarios on the optimization problem. The effects of taking into account more scenarios should also be studied to understand the added benefit of a larger number of scenarios in comparison with increased calculation burden. Identifying which scenarios do not affect the optimization problem should be further pursued as well to remove scenarios when they are unnecessary.

Little work was completed to understand the correlations between unknown variables and their effects on the optimization problem. These correlations between unknown variables should

first be quantified and then be integrated into the scenario combination strategy. The added benefit of correlated scenario generation for stochastic OPF analysis can then be quantified. These correlated uncertainties may improve the proposed methodology.

Appendices

Appendix A

Publications

A.1 Articles in peer reviewed journals

- *Optimal sizing and placement of distribution grid connected battery systems through an SOCP optimal power flow algorithm*. Etta Grover-Silva, Robin Girard, Georges Kariniotakis. Accepted to Applied Energy, Elsevier, 2017, DOI : 10.1016/j.aspenergy.2017.09.008
- *A stochastic optimal power flow for scheduling flexible resources in microgrids operation*. Etta Grover-Silva, Miguel Heleno, Salman Mashayekh, Gonçalo Cardoso, Robin Girard, Georges Kariniotakis. Submitted to IEEE Transactions on Sustainable Energy , Under review, 2017

A.2 Conference papers

- *A stochastic multi-temporal optimal power flow approach for the management of grid connected storage*. Etta Grover-Silva, Xwégnon Ghislain Agoua, Robin Girard, Georges Kariniotakis. CIRED 2017 (Congres International des Réseaux Electriques de Distribution), Jun 2017, Glasgow, United Kingdom. pp. 12-15 <hal-01500379>
- *Multi-temporal optimal power flow for assessing the renewable generation hosting capacity of an active distribution system*. Etta Grover-Silva, Robin Girard, Georges Kariniotakis. IEEE/PES Transmission and Distribution Conference and Exposition (T&D), May 2016, Dallas, TX, United States. DOI : 10.1109/TDC.2016.7520043

Optimal sizing and placement of distribution grid connected battery systems through an SOCP optimal power flow algorithm

Etta Grover-Silva[1,2], Robin Girard[1], George Kariniotakis[1]

Abstract

The high variability and uncertainty introduced into modern electrical distribution systems due to decentralized renewable energy generators requires new solutions for grid management and power quality assurance. One of these possible solutions includes grid integrated energy storage. The appropriate size and placement of decentralized storage is highly dependent on purpose of the battery system and expected operational strategy. However, battery operational strategies are difficult to simulate simultaneously during a sizing and placement planning calculation. The motivation of this paper is to propose an algorithm that is capable of integrating sizing, placement and operational strategies of batteries into an Optimal Power Flow (OPF) distribution grid planning tool. The choice of the OPF approach permits to account for grid constraints which is more adapted for grid-connected storage devices compared to other approaches in the state of the art that are based only on an email balance analysis. This paper presents an alternating current (AC) multi-temporal OPF algorithm that uses a convex relaxation of the power flow equations to guarantee exact and optimal solutions with high algorithmic performance. The algorithm is unique and innovative due to the fact that it combines the simultaneous optimization of placement and sizing of storage devices taking into account load curves, photovoltaic (PV) production profiles, and distribution grid power quality constraints. The choice to invest in battery capacity is highly sensitive to the price of battery systems. The investment in battery systems solely for reducing losses an operational costs was proven not to be cost effective, however when battery systems are allowed to buy and sell electricity based on variable market prices they become cost effective. The assumptions used for this study shows that current battery system prices are too high to be cost effective even when allowing battery system market participation.

Keywords: Optimal power flow, storage, smart grids, renewable energy, distribution grid planning

Nomenclature

Parameters

η_{st}	Charging and discharging efficiency of the battery system
$\overline{P}_{pv,j,t}$	Ideal PV production for node j at time step t
$\overline{S}_{pv,j,t}$	PV maximum apparent power flow at node j
$\overline{V}_j$	Voltage maximum at node n
$\underline{V}_j$	Voltage minimum at node n
c_{st}^{inv}	Investment costs of the battery system for the nominal capacity in €/MWh-day
c_{st}^{om}	Operations and maintenance costs of using the battery system for the power use in €/MWh-day
$c_{e,t}$	Price of electricity at time step t
I^{max}	Total capital cost limit of project
$P_{ld,j,t}$	Active power load at node j
$Q_{ld,j,t}$	Reactive power load at node j
r_{jk}	Resistance of branch jk
t	Duration of timestep
x_{jk}	Reactance of branch jk

Sets

J	Set of all nodes $j \in J$
J_{st}	Set of nodes chosen for battery placement $j \in J_{st}$

Variables

$\ell_{jk,t}$	Square of current in branch jk
$\upsilon_{j,t}$	Square of voltage at node j

Email addresses: etta.grover-silva@mines-paristech.fr (Etta Grover-Silva), robin.girard@mines-paristech.fr (Robin Girard), georges.kariniotakis@mines-paristech.fr (George Kariniotakis)

[1]MINES ParisTech, PSL Research University, PERSEE - Center for Processes, Renewable Energies and Energy Systems, France

[2]ADEME - French Environment and Energy Management Agency, France

$C^{nom}_{st,j,d}$ Final nominal capacity of battery systems for each node j for each day d

F_{inj} Function describing the cost of power injected into the feeder at the substation

F_{inv} Function describing the cost of investment of the battery nominal capacity and power

$F_{O\&M}$ Function describing the cost of operation and maintenance of the battery devices

F_p Function describing the cost of losses within the system including PV curtailment

$F_{st,p}$ Function describing the cost of battery losses due to charging/discharging efficiency

$N^{nom}_{st,j,d}$ The number of hours of nominal autonomy of the battery system at node j

$P^{nom}_{st,j,d}$ Final nominal power of battery systems for each node j for each day d

$P_{0,t}$ Active power flow at the substation

$P_{jk,t}$ Active power of branch jk

$P_{pv,j,t}$ Photovoltaic injection at node j at time t after eventual curtailment

$P_{st,j,t}$ Power injected by battery devices connected at node j

$Q_{jk,t}$ Reactive power of branch jk

$Q_{pv,j,t}$ PV reactive power injection at node j after eventual curtailment

$S_{jk,t}$ Apparent power of branch jk

$S_{pv,j,t}$ PV apparent power flow at node j

$soc_{st,j,t}$ State of charge of the storage unit as a cumulation of energy at node j and time step t

$V_{j,t}$ Voltage at node j

1. Introduction

The increasing environmental concerns, is one of the main drivers behind the large scale development of distributed energy resources (DER) in electric distribution grids. This development involves connection of decentralized generators to the electric grid primarily photovoltaic (PV) and wind turbines and also micro-hydroelectric generators bring about new challenges for the distribution grid operators. Decentralized renewable energy generators can introduce bi-directional flow within the network, while their production is uncertain and variable due to its inherent dependence on weather conditions. Other specific challenges of the distribution grid include higher uncertainty due to reduced aggregation effects of DER generators, voltage profile deviation and increased power flow in electric lines. These challenges are generally localized therefore creating local voltage perturbations that may not be visible by the distribution operator.

Solutions to these challenges include infrastructure upgrades such as electric line reinforcement or automation and integration of smart grid functionalities such as on-line tap changers (OLTC), DER generation curtailment, storage devices, demand side management (DSM) [1]. Specific technologies related to flexibilities include privately owned grid connected batteries such as electric vehicles [2] or larger grid operator owned storage used to improve overall economic exploitation of the feeder. Demand side management optimization in smart grids and efficient smart grid technologies have been thouroughly explored for a variety of use cases [3] [4] [5] [6] [7]. Infrastructure upgrades are easily quantified. However, new control and flexibility functionality is difficult to quantify economically and integrate into the planning phase of distribution grids. The cost benefit analysis of varying smart grid technologies and management strategies will become more important as DER penetration increases in future distribution grid systems.

Grid storage elements are presented in the literature as a cost effective solution to deal with the above challenges in distribution grids with high DER penetration. A techno-economic analysis of energy storage elements as a solution to intermittency of DER is presented in [8]. That paper details the cost-effectiveness of different grid storage applications including regulation of transmission and distribution power quality, voltage regulation and control, energy management, smoothing of intermittent renewable energy production, energy back-up, peak shaving, etc. For each specific application, taking into account the operational strategy of the storage device is important when sizing and placing the unit.

The optimal sizing and placement of storage devices in distribution grids has been addressed through various mathematical modeling methods presented in the literature. The problem of calculating the optimal placement and size of storage devices of an electric grid is highly dimensional and non-convex. The resolution of this highly dimensional non-convex problem has been successful with multiple mathematical techniques including analytical techniques, classical techniques, artificial intelligence techniques and other miscellaneous techniques [9]. In a different review of energy storage allocation, four main categories are defined to solve this highly dimensional non-convex problem: analytical methods, mathematical programming, exhaustive search and heuristics [10]. The different existing methods are of different complexity, some being simple, i.e. based on an energy balance of the examined system to size the storage. However, for grid connected systems the placement involves analysis of the impact of storage

devices to the grid. For this reason, techniques based on mathematical programming such as power flow and optimal power flow (OPF) are more appropriate. These methods can be used to simulate distribution system functionality with generators and storage devices while taking into account grid constraints as seen in [11]. OPF algorithms are capable of taking into account decision variables and therefore capable of analyzing active management of distribution grids. An example of an OPF that analyzes hosting capacity of an active distribution grid is found in [12], where curtailment strategies and dynamic line rating are explored to increase renewable energy penetration.

OPF algorithms are efficient at analyzing active distribution networks for operation and planning. The two primary problem resolution techniques for solving this highly dimensional non-convex problem include heuristic techniques or linear convex relaxations of the power flow equations. Heuristic algorithms have been used to solve the optimal placement and sizing of storage devices. For example, a two-step process with a master and a sub-problem is proposed in [13]. This method firstly uses a heuristic algorithm to solve optimal placement and sizing of batteries. Secondly, a daily AC OPF multi-objective function takes into account optimal voltage control, minimization of network losses and total energy costs. Another paper presents a comprehensive sizing and siting algorithm using particle swarm optimization [14]. A different type of heuristic method was used to simultaneously size and place storage units using an artificial bee colony algorithm with an objective function that forces each storage node to be as autonomous as possible [15]. Another heuristic method used to analyze grid connected storage for a multi-objective problem addressing both distribution grid and transmission grid objectives is found in [16]. However, heuristic algorithms often require a larger calculation burden and are not guaranteed to converge to a global optimal solution as noted in [17]. A mixed integer linear programming approach for complete DER portfolio sizing and placement is presented in [18]. The mixed integer strategy uses linearized power flow equations and loss estimations. Mixed integer linear approximations are proven to be effective at solving the non-convex placement and sizing problem however the calculation time is high and scalability to large network sizes have not been addressed.

Convex relaxations of the power flow equations generally have a lower calculation burden. The relaxation of the power flow equation into a second order cone has already been theoretically explained and detailed mathematically in [19]. Papers addressing specifically optimal sizing and placement of storage devices using convex relaxations can be found in the literature. An impedance model was used to perform optimal placement and sizing in [20]. A convex relaxation was used for optimal placement and sizing of batteries with a linearized DC power flow for transmission planning with a maximum investment cost [21]. This linearization is not accurate for the high R/X ratio found in the low voltage distribution systems, which implies electrical losses that are non linear. The use of an AC OPF for optimal placement [22] or optimal sizing [23] are also found in the literature. In [24] the authors explore a two-step process of sizing and placement of storage units through relaxed power flow equations. However, this sizing methodology calculates power and energy imbalances locally at PV nodes and sizes the battery systems to mitigate these imbalances. Therefore, this methodology sizes the battery systems to reduce PV injection when power quality issues become an issue. This sizing methodology does not compare the cost of storage elements to other cost-effective solutions such as curtailment. The algorithm also does not analyze the possible benefits of batteries participating in an electricity market. A second order cone program (SOCP) OPF algorithm is then used in the second step to site the sized battery systems.

While there are multiple sizing and placement algorithms (e.g. [13],[14],[25],[16]), the objective function of each presented methodology varies significantly implying significant variation in the results of the optimization simulations. For example in [13] the objective is composed of minimizing the energy injection, voltage deviation and network losses. In [14] the objective is peak load shaving, improving voltage profile quality and providing active power adjustment capacity. In [25] the investment, replacement and operations costs of PV, diesel generators, and battery banks as well as slack bus power, cost of energy not served, losses and excess energy of HPVDS. In [16] the cost of local generation, the cost of centralized generation, unit cost of storage and the unit cost of power conversion. Due to the fact that the exploitation of a battery system for a specific purpose can have significant effects on the optimal size and placement as stated in [8], the results of the sizing and placement of these studies are very difficult to compare.

The SOCP relaxation of the power flow equations is present in multiple articles in the literature for example [26]. However, it has been proven to be inexact during periods of high penetration from decentralized production. An example of this could be high PV production and low loads during the summer season. In order to overcome the challenge of inaccurate convex relaxations [27] presents an AC OPF algorithm that integrates linear cuts implemented in an iterative manner to ensure an exact and feasible relaxation of the power flow equations. In a follow-up work, this algorithm has then been developed into a multi-temporal one in order to more objectively evaluate the benefits of grid connected storage and other temporally dependent variables in [28].

This paper proposes a novel methodology to simultaneously perform optimal sizing and placement of storage devices to the distribution grid from a techno-economical view by considering the investment cost of batteries weighted against the operational benefit. Operational control of active power of storage and PV inverters are modeled with a multi-temporal OPF. The objective function of the op-

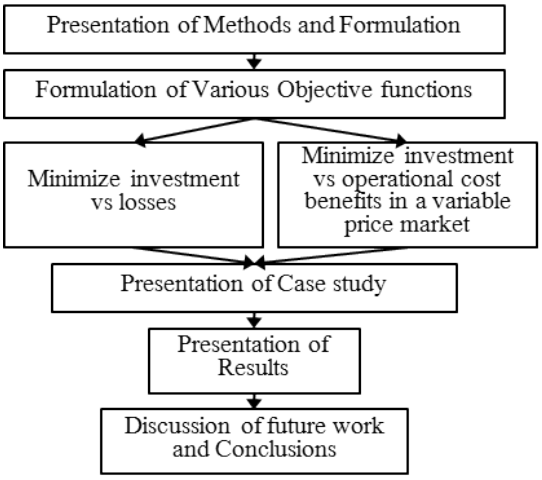

Figure 1: Paper organization

timization problem is formulated in a way to include economic operational benefit and constraints that guarantee power quality.

This methodology is capable of taking into account in detail the operational strategy of storage devices in order to make planning decisions about their sizing and placement. Therefore, it is effective for distribution grid planning applications with predefined operational strategies. The structure of this paper includes section II describing the optimal power flow algorithm, section III illustrating a case study of the proposed methodology and section IV stating significant conclusions. A flow chart of the papers organization is found in 1

2. Optimal power flow model

The proposed methodology relies on solving the optimization problem given by eqs. (1)–(15). The objective function is the sum of the battery investment costs, operation and maintenance costs, the system losses and power imported at the feeder substation. The constraints of this model include the active power limits of PV systems defined by the maximum available power as a function of weather conditions eq. (2), apparent power limits of PV systems eqs. (3) and (4), power flow equations eqs. (5)–(7), relaxation of the current equation eqs. (8) and (9) to represent the power flow equations as a convex SOCP, voltage limits of each branch eq. (10), battery state of charge (SOC) constraint eq. (11) and daily nominal power and capacity value constraints eqs. (12)–(14). Constraint eq. (15) limits the ratio of nominal power and nominal capacity to be appropriate for distribution grid storage elements managed on a daily basis. This constraint also allows for fast convergence of the algorithm.

$$\min \quad F_{inv} + F_{O\&M} + F_p + F_{st,p} \tag{1}$$

subject to:

$$0 \leq P_{pv,j,t} \leq \overline{P}_{pv,j,t} \tag{2}$$

$$S_{pv,j,t} \leq \overline{S}_{pv,j,t} \tag{3}$$

$$S_{pv,j,t} = \sqrt{P_{pv,j,t}^2 + Q_{pv,j,t}^2} \tag{4}$$

$$P_{ij,t} = P_{ld,j,t} + \sum_{j=0}^{J} P_{jk,t} + r_{ij}\ell_{ij,t} + P_{pv,j,t} + P_{st,j,t} \tag{5}$$

$$Q_{ij,t} = Q_{ld,j,t} + \sum_{j=0}^{J} Q_{jk,t} + x_{ij}\ell_{ij,t} + Q_{pv,j,t} \tag{6}$$

$$\upsilon_{j,t} = \upsilon_{i,t} - 2(r_{ij}P_{ij,t} + x_{ij}Q_{ij,t}) + (r_{ij}^2 + x_{ij}^2)\ell_{ij,t} \tag{7}$$

$$S_{ij,t} \geq \sqrt{P_{ij,t}^2 + Q_{ij,t}^2} \tag{8}$$

$$S_{ij,t} \geq \ell_{ij,t}\upsilon_{i,t} \tag{9}$$

$$\underline{V}^2 \leq \upsilon_{j,t} \leq \overline{V}^2 \tag{10}$$

$$soc_{st,j,t} = soc_{st,j,t-1} - t\left(P_{st,j,t} + \eta_{st}|P_{st,j,t}|\right) \tag{11}$$

$$P_{st,j,d}^{nom} \geq |P_{st,j,t}| \tag{12}$$

$$C_{st,j,d}^{nom} \geq soc_{st,j,t} \tag{13}$$

$$C_{st,j,d}^{nom} = N_{st,j,d}^{nom} P_{st,j,d}^{nom} \tag{14}$$

$$0.1 \leq N_{st,j,d}^{nom} \leq 8 \tag{15}$$

The optimal sizing and placement of storage requires the resolution of a temporal and spatial problem. The temporal problem implies a coupling of multiple time steps to ensure coherence of the battery state of charge (SOC) between each consecutive time step. The spatial problem implies the consideration of all nodes as possible placement locations for storage devices. The multi-temporal OPF is already high dimensional. For a grid with 137 nodes, feasibility testing showed that up to 130 coupled time steps was returned results by the solver, any larger coupling returned a maximum size exceeded error. Therefore, a certain decoupling is necessary in order to complete an annual analysis. In this paper, a daily decoupling was implemented. Therefore, the number T of coupled timesteps is 24. A temporal decoupling is applied due to the size limitations of the optimization problem. The decoupling was chosen to be done on a daily basis due to the fact that battery systems are often managed on a daily basis. The coupled time steps of a one day period were then simulated for each day of the year in order to successfully complete an annual analysis. An additional constraint is added to avoid daily accumulation effects by forcing the state of charge (SOC) of the first and last time step of a day to be equal as stated in eq. (16).

$$soc_{st,j,0} = soc_{st,j,T} \tag{16}$$

Constraint 14 is the product of two variables and is non-convex rendering the problem NP-hard. The variable

N represents the number of hours of autonomy of the battery system, limited by feasible battery sizes of 0.1 to 8. This relationship between the nominal power and capacity of a battery system is an essential relationship for accurately representing the cost of battery systems. In order to keep this constraint, a linearization of is performed through an iterative process. The linearization is shown in equation 17.

$$N^{nom}_{st,j,d}P^{nom}_{st,j,d} = \frac{1}{2}\left[N^{nom}_{0,j,d} * P^{nom}_{st,j,d} + N^{nom}_{st,j,d} * P^{nom}_{0,j,d}\right] \quad (17)$$

Where $N^{nom}_{0,j,d}$ and $P^{nom}_{0,j,d}$ are initial values assigned. With these initial values $P^{nom}_{st,j,d}$ and $N^{nom}_{st,j,d}$ are calculated with the algorithm. If the difference between the initial estimation and the final calculated values is larger than a 0.001 for either $P^{nom}_{st,j,d}$ or $N^{nom}_{st,j,d}$ a new iteration is performed assigning $N^{nom}_{0,j,d}$ and $P^{nom}_{0,j,d}$ to the values of $P^{nom}_{st,j,d}$ or $N^{nom}_{st,j,d}$.

The algorithm effectively calculates the optimal size and placement of storage devices for each node for each day. This sizing and placement exercise therefore results in 365 optimal nominal capacity and power. The final optimal size must then be choosen from analyzing these 365 values. This is done by taking the 75th quantile of the set of optimal values to calculate a final annual optimal size.

2.1. Variations of the objective function

The objective function of the general form given by Eq. eq. (1) can be altered in order to size the battery systems for different purposes. Two objectives are considered in this Section. The first objective function is to size the battery systems to minimize losses in the system section. The second possible objective function considers the minimization of losses and the absolute value of the active power injection from the high voltage grid to the medium voltage grid at the substation.

2.1.1. Loss minimization

The first sizing exercise entails using the battery system only for loss minimization and allows a comparison between loss minimization eq. (21), losses associated with charging/discharging of the battery systems eq. (22) and the sum of battery investment costs eq. (19) and battery operations costs eq. (20). The objective function is therefore eq. (18). The optimal nominal power and capacity is then calculated based only on the economic viability of using batteries for loss reduction.

$$\min \quad F_{inv} + F_{O\&M} + F_p + F_{st,p} \quad (18)$$

where:

$$F_{inv} = \sum_{j=0}^{J} c^{inv}_{st} C^{nom}_{st,j,d} \quad (19)$$

$$F_{O\&M} = \sum_{j=0}^{J} c^{om}_{st} t P^{nom}_{st,j,d} \quad (20)$$

$$F_p = \sum_{t=0}^{T}\sum_{j=0}^{J} c_{e,t} r_{ij} \ell_{ij,t} + c_{e,t} t \left[\overline{P}_{pv,j,t} - P_{pv,j,t}\right] \quad (21)$$

$$F_{st,p} = \sum_{t=0}^{T}\sum_{j=0}^{J} c_{e,t} \eta_{st} t |P_{st,j,t}| \quad (22)$$

subject to:eqs. (2)–(15)

The losses considered are the line losses, PV curtailment and the losses of the battery system due to the battery charging efficiency. If the sum of the operational costs and the investment costs of the battery systems is higher than the economic gain from loss reduction, the algorithm eq. (18) will calculate zero nominal capacity and power for each node.

2.1.2. Minimization of absolute active power flow at substation

Battery systems can also be used to participate in variable pricing electricity markets. This implies using battery systems to buy and sell electricity from the grid based on the hourly price of electricity. This objective function as detailed in eq. (23) allows the calculation of economic gains through battery participation in variable pricing markets and encourages autonomy of the feeder by minimization of the total absolute active power flow imported at the substation $|P_{0,t}|$. This formulation does not include explicitly the losses associated with the battery charging efficiency because this energy is already counted in the variable $|P_{0,t}|$.

$$\min_{j \in J} \quad F_{inv} + F_{O\&M} + F_p + F_{inj} \quad (23)$$

where:

$$F_{inj} = \sum_{t=0}^{T} c_{e,t} t |P_{0,t}| \quad (24)$$

subject to:eqs. (2)–(15)

These two objective function variations can be used to determine the size and placement of battery storage devices coupled with installed PV systems for specific end-use scenarios. This algorithm does not consider constraints to exclude very small battery systems. Therefore it is incapable of minimizing the number of nodes that battery systems are installed at. As a result the algorithm often sizes battery systems for every node. However, in some

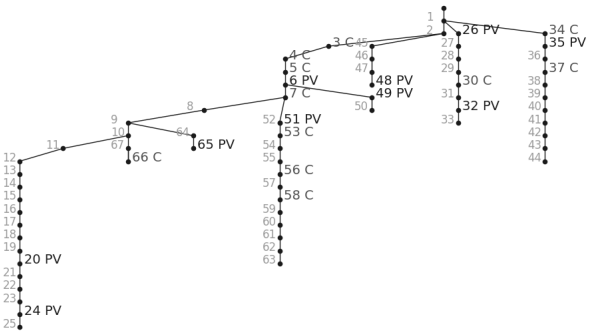

Figure 2: Grid topology including low voltage substation (C) and PV system placement (PV)

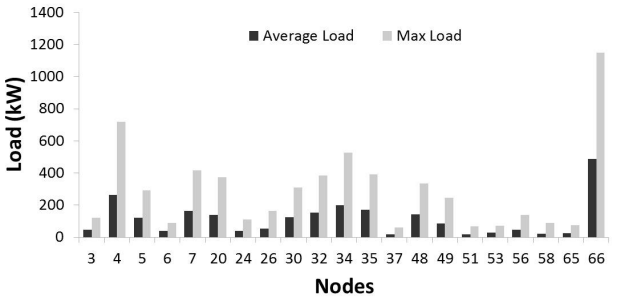

Figure 3: Load characteristics for all loaded nodes

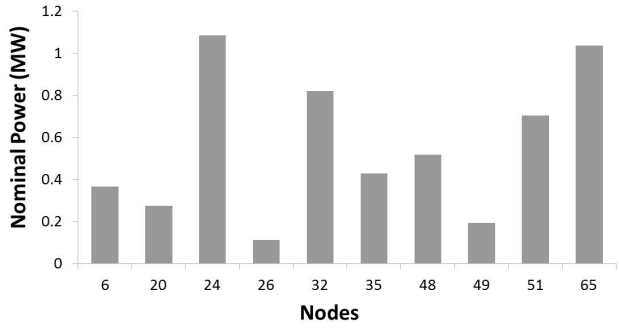

Figure 4: PV nominal power ratings for each PV node

cases, it can be desirable by the DSO to consider a limited number of battery systems or a battery system size minimum. If a minimum battery size was introduced into the problem, it would introduce a binary constraint making the problem NP Hard. Therefore, to deal with these small infeasible systems sizes, an iterative approach can be taken. At a first stage, nodes with the larger battery sizes are identified with the initial sizing and placement algorithm. Then, final sizing can be performed with added constraints eqs. (25) and (26) as a second iteration.

$$C^{nom}_{st,j,d} = 0 \quad for \quad J - J_{st} \tag{25}$$

$$P^{nom}_{st,j,d} = 0 \quad for \quad J - J_{st} \tag{26}$$

The criteria for choosing final node placement can be determined by choosing a maximum number of battery systems or an acceptable maximum and minimum size of battery systems. For sizing based on a maximum number of systems, J_{st} in eq. (26) represents the number of nodes n with the n largest values for the nominal capacity and power. For sizing based on an acceptable maximum and minimum size, J_{st} represents the nodes with feasible nominal power and capacity values.

3. Results

3.1. Case study

The example grid used for this study is a medium voltage distribution grid published here [29]. This grid is composed of 69 nodes with a nominal voltage of 12.66 kV and is assumed to be located in Nice, France. A map of the grid topology can be found in Fig 2.

3.2. Generation and load profiles

Electric load profiles were simulated using a load simulator as described in [30] for each low voltage substation load profile. Residential and commercial load profiles are simulated with statistically accurate representations of surface area, electric heating and number of individuals that align with the INSEE household inventory database of France. The location of each load node was chosen randomly due to the fact that no grid load data was available. The medium voltage feeder is assumed to be a 10 MVA transformer serving 21 low voltage substations. Load profiles aligning with meteorological data in Nice, France indicated a peak load of 4.7 MW during the summer and 5.9 MW during the winter with an average load of respectively 2.1 MW and 2.6 MW. Solar radiation data was simulated for Nice, France for the year 2012 by analyzing the global irradiation collected by HelioClim 3 [31]. The PV system production was calculated based on a statistical distribution of direct and diffuse irradiation [32]. This data is then integrated into a projection model to calculate the percentage of direct and diffuse irradiation exposed to the panels [33]. A system performance coefficient is then calculated based on the atmospheric conditions extrapolated from a performance data base of PV systems in the south of France.

An amount of 10 PV systems were randomly assigned to 10 nodes. The size of these systems was also chosen randomly to be between 125 - 1250 kW. Characteristics of the electric load profile nodes can be found in Fig. 3 and PV size information can be found in Figure 4.

3.3. Economic analysis

In order to analyze the economic viability of battery systems, market price variation and battery system costs

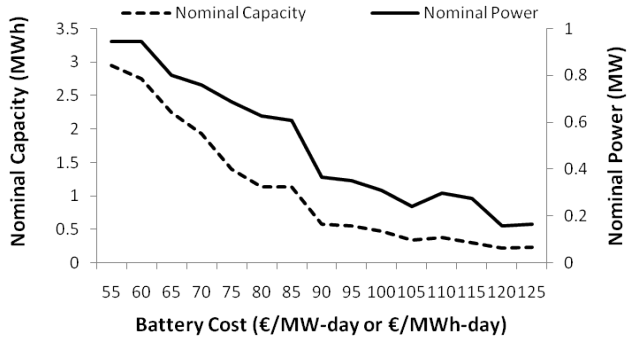

Figure 5: Total aggregated nominal capacity and power optimal system size as a function of battery costs

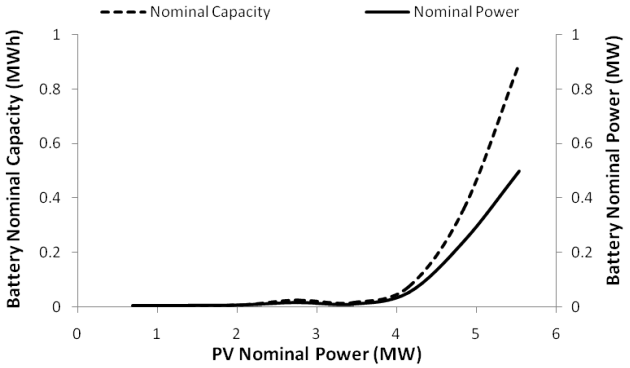

Figure 6: Sensitivity analysis of PV penetration in relation to optimal aggregated nominal power and capacity battery size for an investment cost of 85 €/MWh-day

were taken into account. Historical market data from France was used for 2012.

The capital cost of batteries for nominal capacity and power is determined by analyzing the study [34]. The nine case studies on high performance lead acid battery for transmission and distribution applications were analyzed to calculate the battery investment cost per MWh. Battery costs ranged from 500 k€/MWh to 2.5 M€/MWh. To integrate these costs into the daily analysis, the investment costs per MWh are divided by the lifetime of the system. For all economic analysis, the battery life is assumed to be 10 years as assumed also in [35]. Therefore, the "daily" investment costs ranged from 137.6 €/MWh-day to 678.6 €/MWh-day. Due to the large range of battery investment costs, a sensitivity analysis was completed to determine the price of batteries that is economically viable. In [35], operations and maintenance prices of the battery systems are given to be between 2-6 cents per kWh. For this study this cost is selected to be 2 cents/kWh.

3.4. Results

The two objective functions presented in eq. (18) and eq. (23) were analyzed to determine economically viable battery placement and sizing. In all considered scenarios, equation eq. (18) showed that battery investments were not economically viable for only loss minimization with the considered PV penetration and load profiles. A sensitivity analysis of the battery costs was performed with objective function eq. (23) to analyze the economic viability of storage systems used for loss minimization in addition to market participation. Results of the nominal power and capacity specifications calculated for each node using objective function eq. (23) can be found in Fig. 5.

This sensitivity analysis compares the sum of total nominal power and capacity for a feeder in relation to different investment costs. These total nominal capacity and power values are a sum of the individual nominal capacity and power values for each node. The price of batteries calculated by this study to be economically viable are lower than the battery costs found in [34]. For example, a battery with a capacity of 2 MWh and a nominal power rating of 1 MW cost on average 2.238 M€ according to the study [34]. In the sensitivity analysis, if the investment costs of the battery are 85 €/MWh-day, the total ideal nominal capacity and power for the feeder is 2 MWh and 1 MW. This per day investment cost can be translated into an initial investment cost by taking into account a life time of 10 years. The calculated initial investment cost of this system is therefore 310.25 k€. This implies that for this battery to be economically viable, capital costs must be 7.2 times cheaper than the battery costs published in [34].

For the specific example of a battery investment price of 85 €/MWh-day, a sensitivity analysis was performed comparing the PV penetration and associated battery size. This comparison is found in Fig. 6

This sensitivity analysis shows a high correlation between optimally sized battery systems and PV system size. Therefore grid connected battery systems become exponentially more economical with high penetration of DER. A comparison of centralized and decentralized optimally placed capacity is shown in Fig. 7. The centralized storage nodes are considered to be any node on the main branch of the grid topology tree. The list of centralized nodes for this network are therefore 0,1,2,3,4,5 and 6. All other nodes are considered to be decentralized placement nodes for storage devices.

As seen from this analysis, decentralized battery systems are prioritized for lower battery investment costs while centralized systems size is mostly stable over all investment costs. Decentralized battery systems are more prioritized when battery costs are low and overall total capacity and power installed is higher. When total capacity and power installed is smaller, the ratio of decentralized to centralized systems is also much smaller.

The partitioning of total nominal battery capacity and power as a function of battery investment cost is found in Fig. 8 to demonstrate the repartitioning of battery capacity and power.

As seen in 8, certain decentralized nodes including for example node 25, 34, 65 and 66 are prioritized for storage

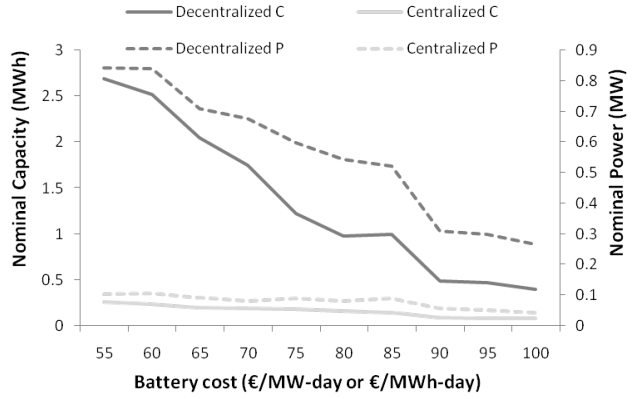

Figure 7: Comparison of centralized and decentralized nominal power (P) and capacity (C) optimal system size as a function of battery costs

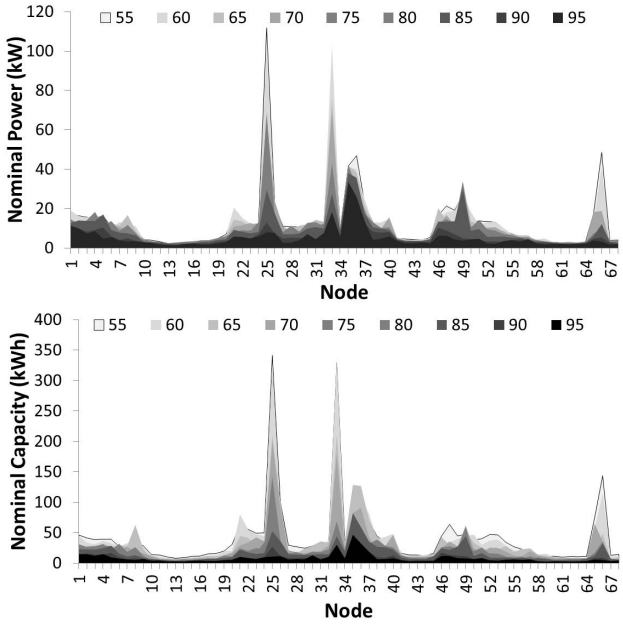

Figure 8: Calculated size of battery systems for each node including nominal power (upper) and nominal capacity (lower) with battery prices varying from 55 €/MWh-day to 95 €/MWh-day

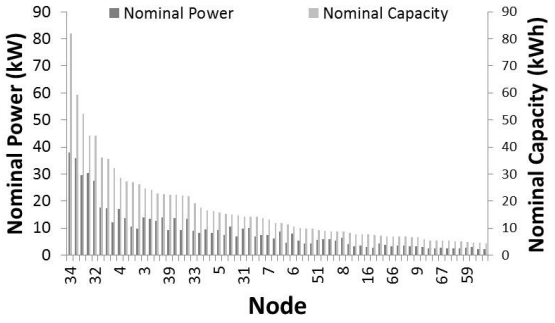

Figure 9: Calculated size of battery sizes for battery prices of 85 €/MWh-day

placement. These three nodes give three different examples of when storage is advantages. Node 25 is a priority due to the high nominal PV power installed at node 24 and also the fact that this system is at the end of an electric feeder. For the case of node 34, high nominal PV power at node 35 combined with high loading at node 34 makes this node a priority. Node 65 and 66 are two nodes relatively close to each other. Node 66 has a high load and node 65 has a large PV system. The algorithm assigned capacity to both nodes, however in all cases a larger capacity is assigned to node 65 than 66 prioritizing a placement closer to the PV system installation rather than the highly loaded node.

A closer look is taken into the case study with a battery cost of 85 €/MWh-day. The individual calculated sizes of battery systems for each node can be found in Fig. 9.

In Fig. 9 a nominal power and capacity value of storage devices is assigned to every node. This is due to the fact that many small systems allow to reduce losses and regulate the balanced of generation and consumption at each node. The size of the battery systems exponentially decreases when the nodes are ranked by size. This shows that certain nodes are high priority but having a storage at all nodes is ideal.

The objective function does not penalize small battery systems, therefore the infeasible small battery systems must be eliminated through an iterative qualitative analysis. The final optimal placement and sizing of battery systems can be calculated by limiting the possible nodes where battery systems can be placed. This selection is performed based on the initial sizing and placement analysis. For the case defined by 85 €/MWh-day, the total number of systems installed was fixed to be 10. Therefore, a final analysis is performed by using eq. (26) and setting fixed the set J_{st} as seen in eq. (27). The final resulting ideal sizing is found in Fig. 10.

$$J_{st} = 4, 34, 48, 35, 36, 32, 47, 25, 24, 65 \tag{27}$$

After fixing the maximum number of battery systems to be 10, a similar total nominal power and capacity is

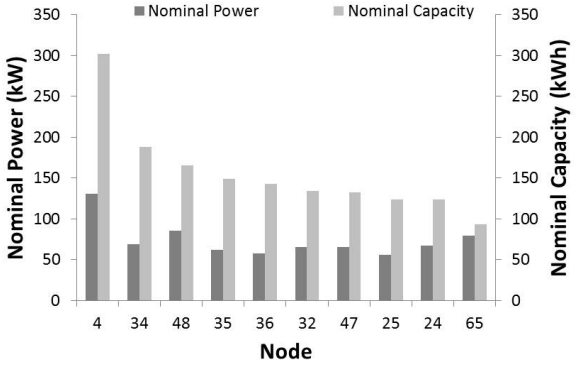

Figure 10: Final size of selected nodes with a battery cost of 85 €/MWh-day

Table 1: Operation of electrical feeder with and without battery integration. Annual analysis for the case of 85 €/MWh-day

Characteristic	With battery	Without battery
Total Cost of Energy Imports (thousand €)	467	489
Total Price of Energy Exports (thousand €)	1.64	2.13
PV Benefits (thousand €)	334	314
PV Curtailement (MWh)	1.05	1.39
Nominal PV Power Installed (MW)	5.53	5.53
Nominal Batt Power Installed (MW)	0.74	0.0
Nominal Batt Capacity Installed (MWh)	1.55	0.0

sized by the algorithm. Due to limited number of nodes for the repartition, the size of each system is therefore significantly larger than when all nodes are considered. Annual analysis results are then calculated by fixing the upper bounds of the nominal power and capacity of each battery system based on the values graphed in Fig. 10 and calculated by fig. 10. The feeder operation with and without battery systems is shown in Table 1.

The operation of the above feeder is affected by the presence of optimally placed and sized battery systems that allow for load shifting through pricing signals. The sum of imports and exports at the substation is therefore decreased. The first line in Table 1 shows that the optimized battery systems succeed to decrease the cost of imported energy. The level of exported energy shown in line two remains low due to the objective function that minimizes the absolute energy flow at the feeder. Line four shows a reduction in PV curtailment due to added battery systems therefore increasing PV benefits as shown in line three.

Table 2: Calculation time for daily and annual analysis

Algorithm	Simulated time steps	Calculation time (s)
multi-temporal SOCP OPF	24	2.7
multi-temporal SOCP OPF	24x365	2700

3.5. Algorithmic performance

The algorithmic performance of the simulation of a single time step and the full annual analysis has been observed as shown in Table 2.

The iterative approach to calculate $P^{nom}_{st,j,d}$ and $N^{nom}_{st,j,d}$ increases the daily analysis calculation time linearly depending on the number of iterations needed for convergence. The calculation time showed in 2 are therefore averages of all analysis performed.

4. Discussion

This algorithm is capable of calculating the placement and sizing of storage devices in a distribution grid. The size is sensitive to the investment cost of the batteries as shown by the sensitivity analysis. In the context of a project, the capital investment of the project may be lower than the ideal size of storage capacity and power. If an investment constraint exists, an investment constraint can be integrated into the optimization problem as seen in eq. (28).

$$c^{inv}_{st} \sum_{j=0}^{J} C^{nom}_{st,j,d} \leq I^{max} \tag{28}$$

This algorithm does not consider the planning of active demand as an alternative solution to electrochemical storage. While the algorithmic structure is very similar to modeling electrochemical storage elements, the calculation of the cost of demand side management is difficult. The costs are non-linear, client-dependent and data sets quantifying these costs are rare. Other possible solutions that were not explored include infrastructure upgrades.

A challenge identified in this paper was the capability to integrate non linear cost functions with respect to the nominal power and capacity of batteries. Another intersting improvement to the cost function could include the integration of variable battery technologies and the associated variable cost parameters. Future work can be done to integrate these non-linear characteristics into the SOCP convex relaxation algorithm.

5. Conclusion

This paper has successfully demonstrated an adaptation of a SOCP convex relaxation of the power flow equations for optimal sizing and placement of battery systems in a medium voltage distribution feeder. The proposed algorithm that simultaneously sizes and places battery systems can be effectively used to analyze the economic viability of operational case studies in comparison to investment and operational costs. The specific contributions of this paper include:

· A high performance algorithm for solving simultaneously the sizing and placement problem through decomposition into daily analysis and assessment of a typical year of operation of the system under study and taking into account the impact of the electrical network. This is a major contribution compared to the state of the art where these two problems of placement and sizing are often considered in a decoupled way

· A methodology to integrate operational case studies of battery management strategies into the planning phase of active distribution grids

· A qualitative study of battery investment costs and their operational benfits to make investment decisions about grid connected storage

· A demonstration of the increasing benefit of grid connected storage in the presence of high DER penetration

This type of innovative algorithm gives insights into the advantages of grid connected storage devices in distribution systems and the integration of operational strategies into the planning phase.

Acknowledgment

The authors would like to thank Mr. Thibaut Barbier for his support with the simulated load curves. Authors would like to thank Dr. Miguel Heleno from Lawrence Berkeley National Lab for useful discussions on possible comparative studies and existing sizing and placement tools. This work is performed in the frame of the Horizon 2020 project Sensible (Grant Agreement 645963) funded in part by the European Commission under the Horizon 2020 Framework Program as well as a PhD scholarship grant supported by the French Energy agency ADEME (Agence de l'Environnement et de la Matrise de l'Energie).

References

[1] M. L. Tuballa, M. L. Abundo, A review of the development of smart grid technologies, Renewable and Sustainable Energy Reviews 59 (2016) 710 – 725. doi:http://dx.doi.org/10.1016/j.rser.2016.01.011.
URL http://www.sciencedirect.com/science/article/pii/S1364032116000393

[2] M. H. Amini, M. P. Moghaddam, O. Karabasoglu, Simultaneous allocation of electric vehicles parking lots and distributed renewable resources in smart power distribution networks, Sustainable Cities and Society 28 (2017) 332 – 342. doi:https://doi.org/10.1016/j.scs.2016.10.006.
URL http://www.sciencedirect.com/science/article/pii/S2210670716304966

[3] A. Ogunjuyigbe, T. Ayodele, O. Akinola, User satisfaction-induced demand side load management in residential buildings with user budget constraint, Applied Energy 187 (2017) 352 – 366. doi:http://dx.doi.org/10.1016/j.apenergy.2016.11.071.
URL http://www.sciencedirect.com/science/article/pii/S0306261916317020

[4] F. Kamyab, M. Amini, S. Sheykhha, M. Hasanpour, M. M. Jalali, Demand response program in smart grid using supply function bidding mechanism, IEEE Transactions on Smart Grid 7 (3) (2016) 1277–1284. doi:10.1109/TSG.2015.2430364.

[5] H. Esen, M. Inalli, M. Esen, Technoeconomic appraisal of a ground source heat pump system for a heating season in eastern turkey, Energy Conversion and Management 47 (9) (2006) 1281 – 1297. doi:http://dx.doi.org/10.1016/j.enconman.2005.06.024.
URL http://www.sciencedirect.com/science/article/pii/S0196890405001755

[6] H. Esen, M. Inalli, M. Esen, A techno-economic comparison of ground-coupled and air-coupled heat pump system for space cooling, Building and Environment 42 (5) (2007) 1955 – 1965. doi:http://dx.doi.org/10.1016/j.buildenv.2006.04.007.
URL http://www.sciencedirect.com/science/article/pii/S0360132306000977

[7] M. Esen, T. Yuksel, Experimental evaluation of using various renewable energy sources for heating a greenhouse, Energy and Buildings 65 (2013) 340 – 351. doi:http://dx.doi.org/10.1016/j.enbuild.2013.06.018.
URL http://www.sciencedirect.com/science/article/pii/S0378778813003563

[8] X. Luo, J. Wang, M. Dooner, J. Clarke, Overview of current development in electrical energy storage technologies and the application potential in power system operation, Applied Energy 137 (2015) 511 – 536. doi:http://dx.doi.org/10.1016/j.apenergy.2014.09.081.

[9] P. Prakash, D. K. Khatod, Optimal sizing and siting techniques for distributed generation in distribution systems: A review, Renewable and Sustainable Energy Reviews 57 (2016) 111 – 130. doi:http://dx.doi.org/10.1016/j.rser.2015.12.099.
URL http://www.sciencedirect.com/science/article/pii/S1364032115014823

[10] M. Zidar, P. S. Georgilakis, N. D. Hatziargyriou, T. Capuder, D. krlec, Review of energy storage allocation in power distribution networks: applications, methods and future research, IET Generation, Transmission Distribution 10 (3) (2016) 645–652. doi:10.1049/iet-gtd.2015.0447.

[11] K. G. Boroojeni, M. H. Amini, A. Nejadpak, S. S. Iyengar, B. Hoseinzadeh, C. L. Bak, A theoretical bilevel control scheme for power networks with large-scale penetration of distributed renewable resources, in: 2016 IEEE International Conference on Electro Information Technology (EIT), 2016, pp. 0510–0515. doi:10.1109/EIT.2016.7535293.

[12] N. Etherden, M. Bollen, Increasing the hosting capacity of distribution networks by curtailment of renewable energy resources, in: Proceedings of 2011 IEEE PowerTech, Trondheim, Norway, 2011, pp. 1–7. doi:10.1109/PTC.2011.6019292.

[13] M. Nick, M. Hohmann, R. Cherkaoui, M. Paolone, Optimal location and sizing of distributed storage systems in active distribution networks, in: Proceedings of 2013 IEEE PowerTech Conference, Grenoble, France, 2013, pp. 1–6. doi:10.1109/PTC.2013.6652514.

[14] Z. Qing, Y. Nanhua, Z. Xiaoping, Y. You, D. Liu, Optimal siting amp; sizing of battery energy storage system in active distribution network, in: IEEE PES ISGT Europe 2013, 2013,

pp. 1–5. doi:10.1109/ISGTEurope.2013.6695235.

[15] A. El-Zonkoly, Optimal placement and schedule of multiple grid connected hybrid energy systems, International Journal of Electrical Power & Energy Systems 61 (2014) 239 – 247. doi:http://dx.doi.org/10.1016/j.ijepes.2014.03.040.

[16] M. Motalleb, E. Reihani, R. Ghorbani, Optimal placement and sizing of the storage supporting transmission and distribution networks, Renewable Energy 94 (2016) 651 – 659. doi:http://dx.doi.org/10.1016/j.renene.2016.03.101.
URL http://www.sciencedirect.com/science/article/pii/S0960148116302853

[17] S. Paudyal, C. Canizares, K. Bhattacharya, Three-phase distribution opf in smart grids: Optimality versus computational burden, in: Innovative Smart Grid Technologies (ISGT Europe), 2011 2nd IEEE PES International Conference and Exhibition on, 2011, pp. 1–7. doi:10.1109/ISGTEurope.2011.6162628.

[18] S. Mashayekh, M. Stadler, G. Cardoso, M. Heleno, A mixed integer linear programming approach for optimal der portfolio, sizing, and placement in multi-energy microgrids, Applied Energy 187 (2017) 154 – 168. doi:http://dx.doi.org/10.1016/j.apenergy.2016.11.020.
URL http://www.sciencedirect.com/science/article/pii/S0306261916316051

[19] L. Gan, S. H. Low, Convex relaxations and linear approximation for optimal power flow in multiphase radial networks, in: Power Systems Computation Conference (PSCC), 2014, 2014, pp. 1–9. doi:10.1109/PSCC.2014.7038399.

[20] H. Nazaripouya, Y. Wang, P. Chu, H. R. Pota, R. Gadh, Optimal sizing and placement of battery energy storage in distribution system based on solar size for voltage regulation, in: 2015 IEEE Power Energy Society General Meeting, 2015, pp. 1–5. doi:10.1109/PESGM.2015.7286059.

[21] C. Thrampoulidis, S. Bose, B. Hassibi, Optimal placement of distributed energy storage in power networks, IEEE Transactions on Automatic Control 61 (2) (2016) 416–429. doi:10.1109/TAC.2015.2437527.

[22] M. Ghofrani, A. Arabali, M. Etezadi-Amoli, M. S. Fadali, A framework for optimal placement of energy storage units within a power system with high wind penetration, IEEE Transactions on Sustainable Energy 4 (2) (2013) 434–442. doi:10.1109/TSTE.2012.2227343.

[23] I. Sharma, K. Bhattacharya, Optimal sizing of battery energy storage systems in unbalanced distribution feeders, in: Industrial Electronics Society, IECON 2013 - 39th Annual Conference of the IEEE, 2013, pp. 2133–2138. doi:10.1109/IECON.2013.6699461.

[24] Q. Li, R. Ayyanar, V. Vittal, Convex optimization for des planning and operation in radial distribution systems with high penetration of photovoltaic resources, IEEE Transactions on Sustainable Energy 7 (3) (2016) 985–995. doi:10.1109/TSTE.2015.2509648.

[25] A. El-Zonkoly, Optimal placement and schedule of multiple grid connected hybrid energy systems, International Journal of Electrical Power & Energy Systems 61 (2014) 239 – 247. doi:http://dx.doi.org/10.1016/j.ijepes.2014.03.040.

[26] J. F. Marley, D. K. Molzahn, I. A. Hiskens, Solving multiperiod opf problems using an ac-qp algorithm initialized with an socp relaxation, IEEE Transactions on Power Systems 32 (5) (2017) 3538–3548. doi:10.1109/TPWRS.2016.2636132.

[27] S. Abdelouadoud, R. Girard, F. Neirac, T. Guiot, Optimal power flow of a distribution system based on increasingly tight cutting planes added to a second order cone relaxation, International Journal of Electrical Power & Energy Systems 69 (2015) 9 – 17. doi:http://dx.doi.org/10.1016/j.ijepes.2014.12.084.

[28] E. Grover-Silva, R. Girard, G. Kariniotakis, Multi-temporal optimal power flow for assessing the renewable generation hosting capacity of an active distribution system, in: Proceedings of 2016 IEEE PES Transmission and Distribution Conference and Exposition (T D), Dallas, USA, 2016, pp. 1–5. doi:10.1109/TDC.2016.7520043.

[29] M. E. Baran, F. F. Wu, Optimal capacitor placement on radial distribution systems, IEEE Transactions on Power Delivery 4 (1) (1989) 725–734. doi:10.1109/61.19265.

[30] T. Barbier, R. Girard, F. P. Neirac, N. Kong, G. Kariniotakis, A novel approach for electric load curve holistic modelling and simulation, in: Proceedings of 2014 IEEE MedPower Conference, Athens, Greece, 2014, pp. 1–8. doi:10.1049/cp.2014.1704.

[31] P. Blanc, B. Gschwind, M. Lefevre, L. Wald, The HelioClim Project: Surface Solar Irradiance Data for Climate Applications, Remote Sensing 3 (2) (2011) 343–361, uRL : http://www.mdpi.com/2072-4292/3/2/343/. doi:10.3390/rs3020343.

[32] J. Ruiz-Arias, H. Alsamamra, J. Tovar-Pescador, D. Pozo-Vzquez, Proposal of a regressive model for the hourly diffuse solar radiation under all sky conditions, Energy Conversion and Management 51 (5) (2010) 881 – 893. doi:http://dx.doi.org/10.1016/j.enconman.2009.11.024.

[33] T. Muneer, Solar radiation and daylight models for the energy efficient design of buildings, Architectural Press, 1997.

[34] A. B. C. B. C. K. D. M. R. S. B. C. A. L. C. D. T. B. Abbas A. Akhil, Georgianne Huff, W. D. Gauntlett, Doe/epri electricity storage handbook in collaboration with nreca, Sandia Report (February 2015).

[35] G. C. Jim Eyer, Energy storage for the electricity grid: Benefits and market potential assessment guide, Sandia Report (February 2010).

A Stochastic Optimal Power Flow for Scheduling Flexible Resources in Microgrids Operation

Etta Grover-Silva[1,3], *Student Member, IEEE*, Miguel Heleno[2], *Member, IEEE*, Salman Mashayekh[2], *Member, IEEE*, Gonçalo Cardoso[2], Robin Girard[1], George Kariniotakis[1], *Senior Member, IEEE*

***Abstract*— Microgrid operations are challenging due to variability in loads and renewable energy generation. Advanced tools capable of taking uncertainty into account are essential to maximize microgrid benefits. This paper proposes a novel centralized algorithm for day-ahead microgrid economic dispatch considering uncertainty and detailed modeling of flexibility sources like storage and controllable loads. The proposed stochastic optimization is bound by end-user comfort constraints to more precisely quantify flexibility of controllable thermal loads, and constraint violations are considered in the deterministic and the stochastic approach. Other constraints consider uncertainty in outside air temperature, uncontrollable load profiles, electric water heating consumption and photovoltaic production. The IEEE 37 bus topology is used to represent a typical medium voltage microgrid with active demand, storage and photovoltaic production within a case study to validate the algorithm. An annual analysis shows that the stochastic day ahead planning strategy reduces energy consumption and feeder operational costs.**

***Index Terms*— demand response, microgrids, optimal power flow, photovoltaics, smart grid, stochastic optimization, storage**

NOMENCLATURE

Summary of notation:

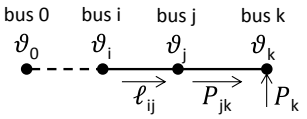

A. Indices:

t	period
ij	branch
j	node
pv	PV system association
ul	uncontrollable load
cl	controllable load
st	storage system association
hvac	heating, ventilation, and Air-Conditioning systems
ewh	electric water heater systems
ext	external air temperature
int	internal air temperature of each house
w	property of water
d	controllable device
s	scenario-dependent variables
+	positive domain
-	negative domain
0	substation node point of common coupling

B. Constants:

c_e	cost of wholesale electricity (€/MWh)
c_c	cost of wholesale electricity plus distribution and transmission costs(€/MWh)
c_{cf}	cost of comfort constraint violation (€/°C · h)
r_{ij}	resistance of a specific branch (Ω)
x_{ij}	reactance of a specific branch (Ω)
η	efficiency of a device
C_d	thermal capacity of a device (kWh/°C)
α	heat loss coefficient of building (kW/°C)
$\overline{P}$	maximum active power value allowable (MW)
$\overline{S}$	maximum apparent power value allowable (MVA)
$\underline{V}$	minimum voltage constraint of grid (V)
$\overline{V}$	maximum voltage constraint of grid (V)
$\overline{soc}$	maximum state of charge of battery (MWh)
$\underline{soc}$	minimum state of charge of battery (MWh)
$\underline{\theta}$	minimum temperature (°C)
$\overline{\theta}$	maximum temperature (°C)
c_w	water specific heat (J/g°C)
R_d	thermal resistance of device (°C/kW)
$\overline{\Delta\theta}_{low}$	maximum degrees of under-heating tolerated (°C)
$\overline{\Delta\theta}_{high}$	maximum degrees of overheating tolerated (°C)

C. Variables:

P	active power (MW)
ℓ	squared current magnitude (A)

This paper has been submitted for review on December 6, 2017. The work is performed in the frame of the project SENSIBLE (Grant No 645963) funded in part by the European Commission under the Horizon 2020 Framework Program as well as a PhD scholarship grant supported by the French Energy Agency ADEME. The international collaboration between MINES ParisTech PERSEE and LBNL was made possible by a mobility grant in the frame of the Electra IRP project (Grant No 609687) funded in part by the European Commission under the 7th Framework Program and of MINES ParisTech Foundation.

[1] MINES ParisTech, PSL Research University, PERSEE – Center for Processes, Renewable Energies and Energy Systems (e-mail: etta.grover-silva, robin.girard, georges.kariniotakis each @mines-paristech.fr)
[2]Ernest Orlando Lawrence Berkeley National Laboratory (Berkeley Lab) (email: miguelheleno, smashayekh, gfcardoso @lbl.gov)
[3] ADEME – French Environment and Energy Management Agency – France

Q	reactive power (MW)
ϑ	squared voltage magnitude (V^2)
soc	state of charge of a battery system (MWh)
θ	temperature (°C)
$v_{d,t}$	electric hot water consumption (l)
θ_{in}	inlet water temperature (^oC)
θ_{out}	desired outlet water temperature (^oC)
$\Delta\theta_{low}$	degrees of under-heating (^oC)
$\Delta\theta_{high}$	degrees of overheating (^oC)

I. Introduction

At the distribution grid level, uncertainties in renewable generation and load consumption represent a challenge to network operation, namely for day ahead planning of Distributed Energy Resources (DERs), such as grid connected storage, controllable loads or photovoltaic (PV) curtailment strategies, implemented in real time by a distribution management system (DMS). These challenges are magnified in microgrids, where uncertainties are higher due to minimal aggregation and smoothing effects. Since microgrids are more easily perturbed by DERs, an accurate control is needed to manage multiple electric storage systems, load devices and generation units, while ensuring a stable and reliable operation of the microgrid network and minimizing costs [1] [2].

Due to high uncertainties in load and renewable generation, microgrid control requires sophisticated forecasting tools and robust scheduling of controllable devices to guarantee power quality and security of supply. In particular, the control of individual loads, e.g. heating, ventilation and air-conditioning (HVAC) systems [3], brings new sources of uncertainty to the day ahead planning of DERs, such as ambient temperature, building occupancy and variations in consumption habits. This uncertainty has a modest impact on grid operations when aggregated at the distribution level but becomes relevant at the microgrid scale.

Optimization algorithms have been presented in the literature to solve the problem of day ahead scheduling of microgrid dispatchable resources. Numerous examples of deterministic [4] [5], stochastic [6] [7] and hybrid [8] [9] approaches to optimal scheduling used in the presence of DERs and controllable loads are presented in the literature. Optimization methods include quadratic programming (QP) [10], as well as heuristic and meta-heuristic techniques [4] [11]. In the optimal scheduling of DERs in multi-node microgrids, heuristics have the advantage of enabling exact network constraints [4], while QP requires a convex relaxation of power flow equations [9]. Due to the random aspect of search techniques in heuristic methods, calculation time can be high and the global optimal is not guaranteed. However, QP methods perform significantly better in terms of computational time. Thus, when combined with techniques that guarantee accuracy of the power flow calculations, e. g. linear cuts [12], they become a better solution.

Stochastic approaches have been used in optimal operation of microgrids to capture uncertainties of renewable sources [13]. Primarily, these strategies include either scenario trees [14] [7] or statistical parameters of the stochastic variables [15] [11] [16] that are integrated into the optimization problem. Monte Carlo simulation along with the distribution functions for generators and load are used to generate scenarios in [15]. Scenarios are constructed by analyzing the mean, standard deviation and probability density functions of load and generation in [11]. Upper and lower bounds on generation and load are considered in [16]. A scenario tree is developed to represent stochastic variables such as temperature, electricity prices and consumer occupancy through the calculation of quantiles and consideration of the probability density function (PDF) of historical data [7].

The day ahead operation of microgrids includes optimal scheduling of multiple DER technologies. Besides the generation and storage control solutions, demand response (DR) has been a valuable resource to compensate the variability of the renewable sources, especially through the control of thermal loads, such as HVAC and Electric Water Heaters (EWH). In fact, as shown in [8], load control can significantly reduce microgrid operation costs as well as CO_2 emissions. Two primary modeling strategies are presented in the literature for DR consideration: an aggregated model or individual modeling of devices. Aggregated models make acceptable assumptions about individual devices [14] and improve aggregated controllability of the microgrid, but the comfort of individual end users is not modeled in detail. Thus, individual load models become more appropriate for small scale applications (e.g. buildings) where a detailed comfort representation is required. In [9], individual load models are used in optimization of building operations with DR. A deterministic approach that considers end-user comfort constraints and PV for a 3 building micro-grid is detailed in [5]. An algorithm proposing an economic penalty for violations in thermal comfort constraints is presented in [7] however, this paper does not consider the electric network and instead performs only an energy balance.

A majority of the mentioned citations take into account the losses in the electrical lines in a two-step process and do not integrate a full AC optimal power flow (AC-OPF) into the optimization problem [13] [11] [15].

This paper advances the current state of the art by presenting a novel method for day ahead scheduling of DR and DERs that has a low calculation burden while considering network constraints. To the authors knowledge, it is the first time that a full AC-OPF algorithm is used while considering thermal comfort constraints of end users and uncertainties in multiple variables. The algorithm uses the second order cone program (SOCP) convex relaxation of the power flow equations proposed in [12] to guarantee an optimal solution and ensure a low calculation burden. However, during periods of high DER injection, this relaxation can be inexact, therefore, linear cuts are added to the problem to guarantee exactness. The only other study found implementing a SOCP and taking into account uncertainties is [17], where only uncertainty in wind generation and the corresponding effects on network losses is considered. Here, a more realistic case for distribution networks is considered where uncertainties in PV

generation, ambient temperature, EWH consumption and uncontrollable electric loads are taken into account.

In the method now introduced, the flexibilities considered include electrochemical storage and thermal loads, such as electric heating or cooling loads and EWH. Individual device models are considered in the scheduling task as proposed in [9]. The constraints on the DR devices are thermal comfort constraints of end users as described in [18]. The integration of comfort constraints into an optimization algorithm has been proposed in [7]. However, that paper does not consider constraints on the network which is critical in a microgrid context.

The proposed formulation merges contributions from three different areas of power systems optimization with primary contributions being:

- a multi-period SOCP adapted to consider uncertainties through scenarios of generation, load and also hot water consumption and ambient temperature to account for thermal loads;
- the optimal day-ahead scheduling of microgrid flexibilities, considering grid constraints, end-user comfort constraints, and the multi-temporal dispatch of different DER technologies;
- the behind-the-meter individual loads devices modeling and scheduling for optimal DR strategies, constrained by the comfort of end-users, and integrated with the microgrid stochastic dispatch.

By combining these contributions in a single stochastic AC-OPF, the authors aim at providing a valuable discussion on the implications of generation and load uncertainties for microgrids control and the resulting effects on end-user comfort while considering demand side management. Following this introductory section, section II describes the novel formulation introduced by this paper. Section III describes a case study to demonstrate the utility of the day-ahead scheduling strategies produced, and section IV discusses final conclusions.

II. Stochastic Optimal Power Flow Method

A. Methodology Overview

This section proposes a multi period stochastic algorithm for the day ahead scheduling of a microgrid. It is considered that the microgrid includes electric storage, controllable (CL) thermal loads, such as residential EWH and commercial HVAC units, at the building level, and uncontrollable loads (UL) that include other electronic appliances such as the television, computers, washing machines, cooking equipment, etc. This stochastic algorithm considers uncertainties in PV generation, uncontrollable loads, ambient temperature and hot water consumption. These uncertainties are considered in the form of forecast scenarios which are generated from probabilistic forecasts taking into account the spatial and temporal correlations in the processes. High and low scenarios for each variable are selected through a scenario reduction strategy and are assumed equally probable as described later in section II C.

The benefit introduced by the stochastic approach is measured by the value of the stochastic solution (VSS). This consists of comparing the expected value of perfect information (EVPI) given the stochastic solution and the deterministic average solution [19]. A schematic showing the methodology as a flow chart is shown in Fig. 1.

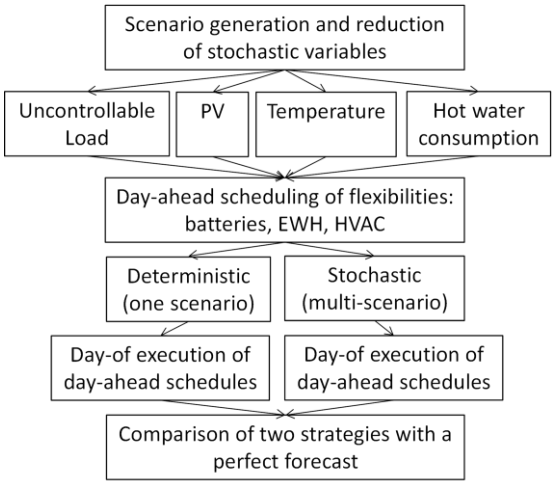

Fig. 1. Flow chart of proposed methodology

B. Formulation

The proposed formulation (1)-(22) is a multi-period (t) multi-scenario (s) optimal power flow that aims at reducing the day ahead microgrid operation costs through scheduling of batteries ($P_{\mathrm{st,j,t}}$) and controllable thermal loads, EWH ($P_{\mathrm{ewh,j,t}}$) and HVAC ($P_{\mathrm{hvac,j,t}}$), located at the nodes (j) of the microgrid.

1) Objective function

The operation cost function (1) considers differentiated rates for energy imports and exports, following the current regulatory mechanisms adopted by several European countries to promote self-consumption. Hence, the energy exports at the point of common coupling are remunerated at wholesale electricity market price, while the energy consumption costs are charged at the final electricity price, which corresponds to the hourly electricity market price with fixed rates, e. g. due to transmission and distribution cost. The comfort constraints of space heating systems are also considered in the objective function through a cost function associating a price penalty with under heating and overheating.

$$min. \sum_{\mathrm{s}} \sum_{\mathrm{t}} \left[\mathrm{c_{c,t}} tP_{0+,\mathrm{s,t}} + \mathrm{c_{e,t}} tP_{0-,\mathrm{s,t}} + \sum_{\mathrm{d}} \mathrm{c_{cf}} \left(\Delta\theta_{\mathrm{low,d,t}} + \Delta\theta_{\mathrm{high,d,t}} \right) \right] \quad (1)$$

2) Power flow constraints

The constraints of the problem include the nodal power balance considering different DER units (2)-(5). Equation (6) describes the convex relaxations of the line constraints. The result of each OPF calculation for each time step is compared to a forward backward sweep power flow calculation to verify that the convex relaxation of the line constraint equation (6) is exact. If the solution is not exact, linear cuts are added to the problem to guarantee exactness as explained in [12].

$$P_{\mathrm{ij,s,t}} = P_{\mathrm{ul,j,s,t}} + P_{\mathrm{cl,j,t}} + \sum_{\mathrm{k}} P_{\mathrm{jk,s,t}} + \mathrm{r_{ij}} \ell_{\mathrm{ij,s,t}} + P_{\mathrm{pv,j,s,t}} + P_{\mathrm{st,j,t}} \quad (2)$$

$$Q_{ij,s,t} = Q_{ul,j,s,t} + Q_{cl,j,s,t} + \sum_k Q_{jk,s,t} + x_{ij}\ell_{ij,s,t} + Q_{pv,j,s,t} \quad (3)$$

$$\vartheta_{j,s,t} = \vartheta_{i,s,t} - 2\left(r_{ij}P_{ij,s,t} + x_{ij}Q_{ij,s,t}\right) + \left(r_{ij}^2 + x_{ij}^2\right)\ell_{ij,s,t} \quad (4)$$

$$\underline{V}^2 \le \vartheta_{j,s,t} \le \overline{V}^2 \quad (5)$$

$$\ell_{ij,s,t} \ge \frac{P_{ij,s,t}^2 + Q_{ij,s,t}^2}{\vartheta_{i,s,t}} \quad (6)$$

3) Battery system constraints

Equations (7)-(10) represent the battery limits regarding power and state of charge.

$$-\overline{P}_{st,j} \le P_{st,j,t} \le \overline{P}_{st,j} \quad (7)$$

$$\underline{soc}_{st,j} \le soc_{st,j,t} \le \overline{soc}_{st,j} \quad (8)$$

$$P_{st,j,t} = P_{st+,j,t} + P_{st-,j,t} \quad (9)$$

$$soc_{st,j,t} = soc_{st,j,t-1} + t\eta_{st}P_{st+,j,t} + \frac{t}{\eta_{st}}P_{st-,j,t} \quad (10)$$

4) Thermal comfort constraints

The thermal comfort constraints associated with the individual HVAC and EWH controllable devices are shown in (12)-(19). The division of over and under heating in equation (20)-(22) allows for a piecewise linear penalty function of thermal constraint violations in the objective function.

$$P_{cl,j,t} = P_{hvac,j,t} + P_{ewh,j,t} \quad (12)$$

$$\sum_d P_{ewh,d,t} = P_{ewh,j,t} \quad (13)$$

$$0 \le P_{ewh,d,t} \le \overline{P}_{ewh,d} \quad (14)$$

$$\underline{\theta}_w < \theta_{ewh,d,t} < \overline{\theta}_w \quad (15)$$

$$\theta_{ewh,d,t} = \theta_{ewh,d,t-1} + \frac{t}{C_d}\left[-\alpha_d\left(\theta_{ewh,d,t-1} - \theta_{int,d,t}\right) - \nu_{d,t}c_w(\theta_{out} - \theta_{in}) + P_{ewh,d,t}\right] \quad (16)$$

$$\sum_d P_{hvac,d,t} = P_{hvac,j,t} \quad (17)$$

$$0 \le P_{hvac,d,t} \le \overline{P}_{hvac,d} \quad (18)$$

$$\theta_{hvac,d,t} = \theta_{hvac,d,t-1} - \frac{t}{C_d R_d}\left[\theta_{hvac,d,t-1} - \theta_{ext,t} + \eta_d R_d P_{hvac,d,t}\right] \quad (19)$$

$$\underline{\theta}_{hvac,d} - \overline{\Delta\theta}_{low,d} \le \theta_{hvac,d,t} \le \overline{\theta}_{hvac,d} + \overline{\Delta\theta}_{high,d} \quad (20)$$

$$\underline{\theta}_{hvac,d} - \theta_{hvac,d,t} = \Delta\theta_{low,d,t} \quad (21)$$

$$\theta_{hvac,d,t} - \overline{\theta}_{hvac,d} = \Delta\theta_{high,d,t} \quad (22)$$

These thermal equations are the first order physically-based load modes – considering the thermal capacity (C), resistance (R), and heat loss constant (α) - to describe the temperature behavior of thermal systems.

5) Stochastic variable and scenario generation

Controllable variables include the active power of EWH for residential clients and HVAC thermal loads for commercial clients ($P_{ewh,d,t}$ and $P_{hvac,d,t}$) and the active power of battery systems ($P_{st,j,t}$). A part of the load is considered to be uncontrollable ($P_{ul,j,t}$). A table summarizing the controllable variables, stochastic variables and scenario dependent variables is found in Table I.

The stochastic variables are represented in the linear constraint matrix of the optimization problem through parallel multi-period scenarios. This technique to integrate uncertainties into and OPF is classified as a probabilistic scenario-based technique for taking into account uncertainties in power systems as classified in [20] a.k.a. a deterministic equivalent formulation of the stochastic problem. Here we apply the approach proposed. Two main steps are necessary, the generation of scenarios and the reduction of scenarios. That paper uses a Monte Carlo scenario generation method applied to wind turbine generation and load profiles based on [22]. The scenario reduction technique that is used is based on probabilistic distance and fast-forward selection as described in [23].

TABLE I
VARIABLE TYPES

Type	Applicable Variables
Controllable Variables	P_{st} (P_{st+}, P_{st-}), P_{cl} (P_{hvac}, P_{ewh})
Scenario Dependent Variables	P_{ij}, ℓ_{ij}, Q_{ij}, ϑ_i
Stochastic Variables	P_{pv}, P_{ul}, $v_{d,t}$, θ_{ext}

Here we use the same scenario generation technique as [22] for the UL, ambient temperature and EWH scenarios. A three-month historical period is used to calculate the quantiles and the covariance matrix to generate normal Gaussian scenarios.

This technique is less effective when applied to PV production scenarios due to the fact that PV production profile has a very strong correlation associated with the irradiation which depends on the course of the sun during the day. This strong correlation with irradiation may dilute the other causes of variation in PV production such as cloud cover. The PV production profiles were therefore normalized by the clear sky index before applying the scenario generation method. This allows for a more precise analysis of inter-temporal variation due to cloud cover or other phenomena that are not correlated with irradiation. For further discussion on the necessity to stationnarise PV production time-series when modeling spatio-temporal correlations and also a more sophisticated stationnarisation techniques for that purpose, refer to [24].

It is noted that a limitation of the approach in [21] concerns the fact that the scenario generation techniques does not consider possible correlations between the stochastic variables considered. This could be part of the perspectives of the current work. The stochastic OPF optimization, through the use of multiple scenarios as input, aims at finding a solution that provides "hedging" to the considered physical system against uncertainties. This means that the system is prepared to face more situations than when optimized through the simpler deterministic approach. This strategy may consequently involve higher costs. To be able to evaluate this risk for higher costs we have adopted a simple but intuitive scenario reduction method that is based on choosing the "extreme" upper and lower scenarios resulting from the scenario generation step and then combine these opposite situations that these scenarios reflect. This can be considered as a pessimistic approach that could lead to amplified "hedging" costs compared to the deterministic case. Depending on the system this does not necessarily mean that there is no margin to reduce costs through the deterministic approach. It is a matter of tradeoff between the hedging cost

TABLE II
UL, CL AND DER CHARACTERISTICS PER NODE

Node	0	6	10	12	14	15	19	23	28	29	32
Average UL (kW)	28	-	95	62	95	64	76	66	-	21	8
Maximum UL (kW)	68	-	212	156	212	155	183	159	-	52	20
Nominal PV Power (kW)	-	313	-	819	428	-	518	-	542	-	-
Nominal Battery Power (kW)	-	250	-	250	250	-	250	-	250	-	-
Nominal Battery Capacity (kWh)	-	500	-	500	500	-	500	-	500	-	-
Number of EWH devices	4	-	7	5	4	4	6	6	-	10	3
Number of HVAC devices	0	-	0	2	1	2	2	1	-	3	0

mentioned above and the impact of the deviations from a deterministic schedule. The overall approach remains though generic as one can replace by scenarios resulting from more sophisticated reduction method (i.e. from in [23]) as done by the authors in [21] More precisely, here, three scenarios were selected based on the total cumulative values of the day. The three scenarios are chosen by selecting the maximum, minimum and closest to average value of the cumulative values in order to produce a high, low and average scenario for each variable. Performance Evaluation of Stochastic Method

C. Performance Evaluation of Stochastic Method

The stochastic approach is evaluated through VSS and EVPI. To calculate these performance indicators, the day-ahead schedules obtained in the deterministic approach and those obtained in the stochastic approach are benchmarked against a perfect forecast for real day-of conditions. VSS is the difference between the stochastic method and the deterministic one. The expected value of perfect information, EVPI, is the absolute difference between the expected value *with* perfect information, i.e., under a perfect forecast, and the expected value *without* perfect information – either the stochastic solution or the deterministic solution.

When evaluating each of these cases, the set points for EWH, HVAC and battery power are implemented with no intra-day adjustments for the real conditions. The thermal equations are used to simulate the evolution of temperatures in the buildings and in the hot water tanks. A forward backward sweep power flow calculation is performed to calculate the current and voltage of each node at each time step. Energy costs, grid constraint violations and thermal comfort profiles are then analyzed to assess the comfort of end-users in comparison with the economic performance of the optimization strategies.

III. CASE STUDY

In this section, the proposed methodology presented above is applied to a medium voltage IEEE 37 node network (4.8 kV). Even though this circuit is published as a medium voltage distribution grid in the US, the feeder topology is used here as a medium voltage microgrid for demonstrative purposes because it is a well-documented grid feeder. A map of the grid topology can be found in Fig. 2.

A. Generation and Load Data

The considered network is assumed to be located in the area of Grenoble city, France. Load profiles including EWH, HVAC and uncontrollable loads are generated using a bottom up load simulator detailed in [23]. This simulator produces a group of individual commercial and residential building load profiles. These profiles are generated to be statistically accurate representations of residential and commercial customer proportion, electric heating, building surface area and population using the INSEE building inventory database of France, and distributed randomly across the network. The medium voltage feeder is assumed to have a 5 MVA transformer serving 5 low voltage substations for a total of 312 clients, of which 300 are residential and 12 are commercial. Of the 300 residential clients, 49 residential hot water heaters are controllable. It was assumed that all 12 commercial clients have controllable HVAC systems. In addition, a total of 1.2 MW uncontrollable load, 155 kW of controllable EWH and 308 kW of controllable HVAC are considered.

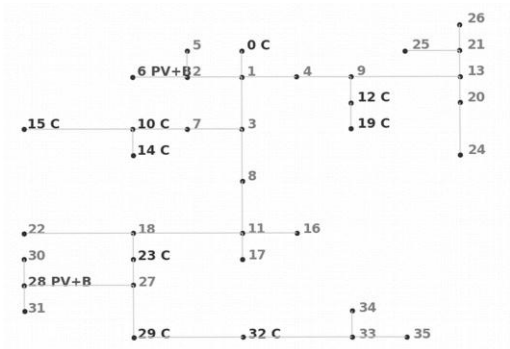

Fig. 2. Medium voltage microgrid case study feeder. C indicates a node with customer load, PV + B indicates nodes with PV and batteries

A total capacity of 2.62 MW of PV is distributed over 5 nodes, with production curves based on a real PV plant in Grenoble [24], normalized by the nominal power installed in each node. In addition, all 5 PV nodes are assumed to have a battery system with 250 kW nominal power and 500 kWh nominal capacity, totaling 1.25 MW and 2.5 MWh. The UL, CL and DER characteristics for each node can be found in Table II. The parameters used for the HVAC and EWH units are as follows: for EWH, the maximum power per device is between 2.0-6.0 kW, thermal capacities and heat loss coefficients are within 0.0877 – 0.2925 kWh/^{o}C and 0.0004-0.0012 kW/^{o}C, respectively. Cold water intake temperature (θ_{int}) and usage temperatures (θ_{out}) are 12^{o}C and 65 ^{o}C, while temperature limits are between 60 ^{o}C and 80 ^{o}C. For individual buildings HVAC systems, the maximum power is between 2.44 – 158.67, C and R values are within 0.2244 – 1318.4959 kWh/^{o}C and 0.0127-21.0012 ^{o}C/kW, respectively. The comfort temperatures are between 19 ^{o}C and 26 ^{o}C. The cost of discomfort for under heating and overheating was considered to be 10€/°Ch or 1€/°Ch for different case studies. The case study uses historical variable market prices for electricity cost in France for 2012.

TABLE III
CASE STUDY LABELS

Scenario	ST NO CL 2 S	ST NO CL 4 S	ST W T 10 €	ST W T 1 €	ST 2 S	ST C	ST PV	ST 4 S
1	$P_{pv}^{L} P_{ul}^{H} P_{ewh}^{M} \theta_{ext}^{M}$	$P_{pv}^{L} P_{ul}^{H} P_{ewh}^{M} \theta_{ext}^{M}$	$P_{pv}^{L} P_{ul}^{H} P_{ewh}^{H} \theta_{ext}^{L}$	$P_{pv}^{L} P_{ul}^{H} P_{ewh}^{H} \theta_{ext}^{L}$	$P_{pv}^{L} P_{ul}^{H} P_{ewh}^{M} \theta_{ext}^{M}$	$P_{pv}^{M} P_{ul}^{H} P_{ewh}^{M} \theta_{ext}^{M}$	$P_{pv}^{H} P_{ul}^{M} P_{ewh}^{M} \theta_{ext}^{M}$	$P_{pv}^{L} P_{ul}^{H} P_{ewh}^{M} \theta_{ext}^{M}$
2	$P_{pv}^{H} P_{ul}^{L} P_{ewh}^{M} \theta_{ext}^{M}$	$P_{pv}^{H} P_{ul}^{L} P_{ewh}^{M} \theta_{ext}^{M}$	$P_{pv}^{H} P_{ul}^{L} P_{ewh}^{H} \theta_{ext}^{H}$	$P_{pv}^{H} P_{ul}^{L} P_{ewh}^{L} \theta_{ext}^{H}$	$P_{pv}^{H} P_{ul}^{L} P_{ewh}^{M} \theta_{ext}^{M}$	$P_{pv}^{M} P_{ul}^{L} P_{ewh}^{M} \theta_{ext}^{M}$	$P_{pv}^{L} P_{ul}^{M} P_{ewh}^{M} \theta_{ext}^{M}$	$P_{pv}^{H} P_{ul}^{L} P_{ewh}^{M} \theta_{ext}^{M}$
3	-	$P_{pv}^{H} P_{ul}^{H} P_{ewh}^{M} \theta_{ext}^{M}$	$P_{pv}^{H} P_{ul}^{H} P_{ewh}^{H} \theta_{ext}^{M}$	$P_{pv}^{H} P_{ul}^{H} P_{ewh}^{H} \theta_{ext}^{M}$	-	-	-	$P_{pv}^{H} P_{ul}^{H} P_{ewh}^{M} \theta_{ext}^{M}$
4	-	$P_{pv}^{L} P_{ul}^{L} P_{ewh}^{M} \theta_{ext}^{M}$	$P_{pv}^{L} P_{ul}^{L} P_{ewh}^{L} \theta_{ext}^{L}$	$P_{pv}^{L} P_{ul}^{L} P_{ewh}^{L} \theta_{ext}^{L}$	-	-	-	$P_{pv}^{L} P_{ul}^{L} P_{ewh}^{M} \theta_{ext}^{M}$

B. Results

The results presented below focus on three primary topics: i) economic benefit of using a stochastic approach over a deterministic one, ii) economic benefits of combining stochastically managed storage devices with controllable loads and iii) thermal comfort improvements with stochastic techniques.

The annual operational costs with microgrid connected storage devices are calculated using both the stochastic and deterministic day-ahead management strategies. The deterministic case (denoted as "Det" for future Figures) uses the forecast that corresponds to the average daily cumulative value of the available forecasts for all stochastic variables. The stochastic case (denoted as "St" for future Figures) uses combinations of high and low generate forecasts for each stochastic variable of Table I. Multiple case studies are tested to quantify the effect of each stochastic variable on the total annual operational cost. The test cases consider high (H) and low (L) scenarios for between one and four of the four stochastic variables to analyze the effects of each stochastic variable independently as well as their compounded effects. If the high and low scenario is not used for a stochastic variable the average scenario is used (M). Table III details the labels for each case study used in the following figures.

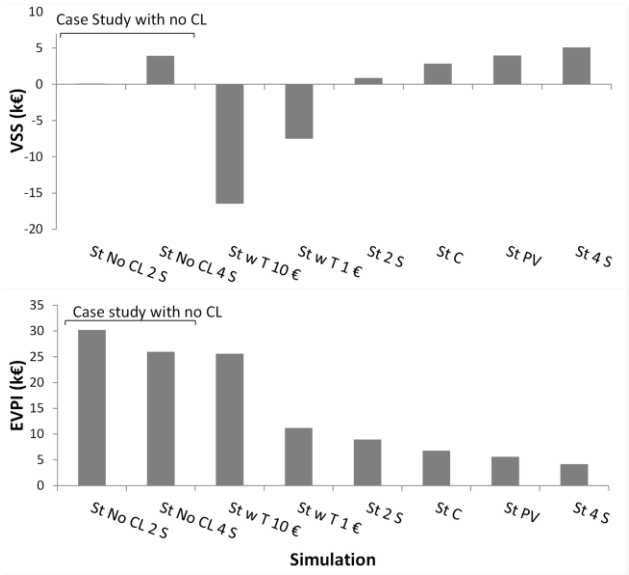

Fig. 3. Annual VSS (top) and EVPI (bottom) costs of case studies

Fig. 3 shows the stochastic performance measures of the annual operational cost. The case study with CL in Fig. 3 show that stochastic strategies result in lower annual costs. However, no major economic advantage is seen in using 4 scenarios instead of 2. In fact, the 2 initial scenarios already represent extreme the conditions of PV and UL and they have a dominant impact in the optimization. The added importance of the method presented in this paper is the integration of more flexibility in a microgrid operation though the active control of loads. Individual appliance schedules are calculated by the optimization algorithm for 49 EWH and 12 HVAC systems. The combination of microgrid connected storage and DR significantly increases the controllability of the microgrid loading characteristics.

As seen in Fig. 3, when integrating controllable load into the optimal scheduling problem, annual costs are reduced. This reduction is primarily due to shifting HVAC and EWH to less expensive periods.

The case study 'St w T 10 €' and 'St w T 1 €' do not only consider uncertainty in PV and UL but they also consider uncertainties in outside temperature (T) and EWH consumption. The difference between these two case studies is the cost penalty for violating comfort constraints, c_{cf} is 1 or 10 euros. With higher cost penalties for comfort constraints, annual costs increase due to the more conservative management of thermal loads by the stochastic algorithm. This results in the stochastic schedule having higher annual costs than the deterministic schedule. In general the stochastic scheduling results in lower annual costs except when uncertainties in temperature are considered.

An example day profile of the different battery and controllable load schedules for the deterministic and the stochastic strategies is shown in Fig. 4. The stochastic day ahead scheduling proved to reduce costs significantly when simulated with real day of conditions. This improvement can be explained by the transition periods between the hours 6 to 9 and 14 to 19. This improvement can be explained by the inability of the deterministic approach to respond to situations where PV production deviates from the predicted average. The deterministic strategy consisted in charging the battery between 6 and 9 AM, taking advantage of the early morning on-site PV generation. However, the actual generation is significantly lower, jeopardizing the deterministic economic solution in the subsequent periods.

In contrast, the stochastic approach took into account the possibility of low PV generation therefore scheduling a more conservative discharge during this period. The battery is therefore discharged during the hours 10-13, where low generation of PV is expected (in low scenario) and the electricity price is high. When the real conditions result in low PV production, the deterministic schedule incurs a high operational cost during the period 10-13.

From the analysis performed, a tradeoff was observed between annual operational costs and thermal comfort of the users. This tradeoff can be represented as a Pareto-optimality state with annual operational costs and end user comfort defining the Pareto-frontier.

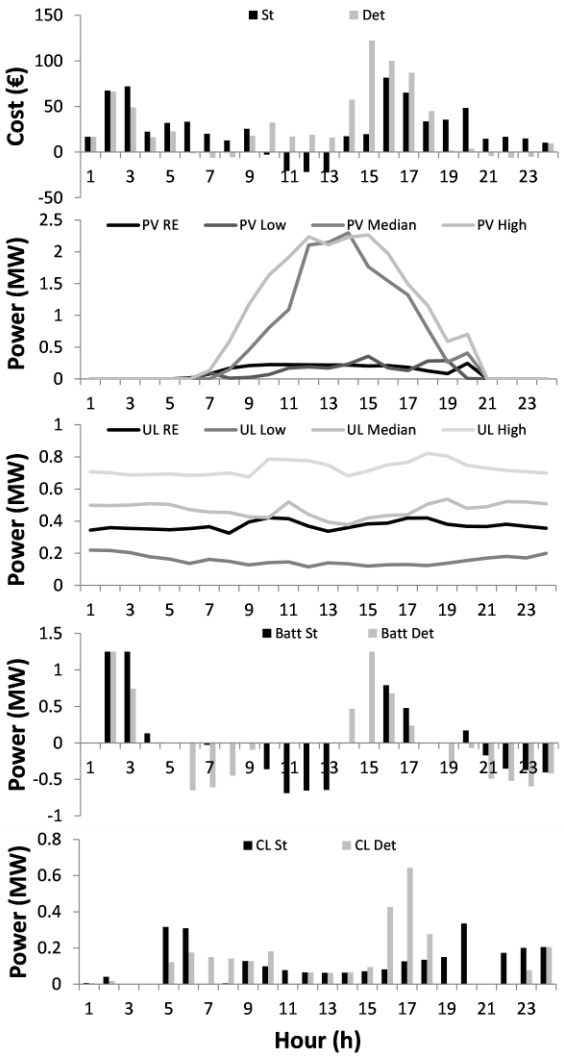

Fig. 4. Example day where stochastic scheduling results in lower operational costs than the deterministic one. From top to bottom: cost of electricity (1), PV scenarios and real PV production (2), uncontrollable load (UL) scenarios and real UL (3), stochastic and deterministic battery schedule (4), stochastic and deterministic controllable load schedule (5).

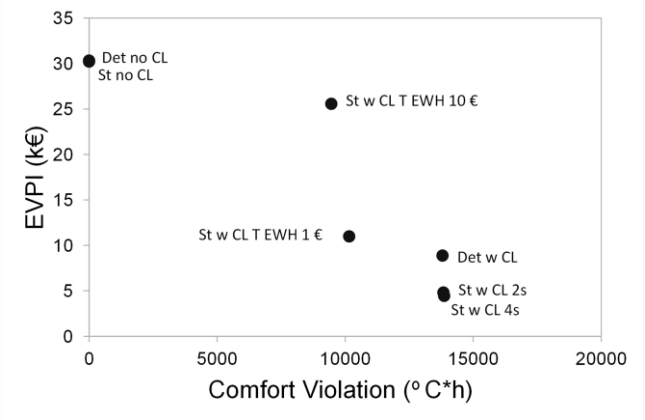

Fig. 5. EVPI vs comfort constraint violations of HVAC and EWH systems

As shown in Fig. 5, considering uncertainties in ambient temperature is a Pareto improvement for end user comfort in HVAC loads while not considering these uncertainties is a Pareto improvement for annual costs. Two different values for cost penalties were also tested, 1 €/°Ch and 10 €/°Ch. With higher cost penalties for temperature violations, annual costs were higher but fewer comfort violations resulted. In all cases the stochastic algorithm results in lower annual operational costs for the same number of comfort constraint violations when comparing stochastic and deterministic approaches.

C. Algorithm Performance

The algorithms presented in this paper have been implemented in Python and solved using the MOSEK SOCP solver on an 8-core, 3.4 GHz CPU. Due to the fact that the stochastic algorithm takes into account multiple scenarios the calculation time of this algorithm is higher. A performance analysis was completed to compare the time of calculation for the deterministic algorithm and varying amounts of scenarios in the stochastic algorithm. The average calculation time of stochastic and deterministic methods for 24 coupled time steps is shown in Table IV. Therefore the stochastic algorithm is about 3 times slower with the consideration of 2 scenarios and 6 times slower with the consideration of 4 scenarios.

TABLE IV
ALGORITHMIC PERFORMANCE

Analysis	Number of Scenarios	Coupled Timesteps	CL present	Time (s)
Deterministic	1	24	No	3
Stochastic	2	24	No	8
Stochastic	4	24	No	14
Deterministic	1	24	Yes	7
Stochastic	2	24	Yes	15
Stochastic	4	24	Yes	45

IV. CONCLUSION

This paper presents a multi-temporal stochastic algorithm that performs a centralized day-ahead scheduling of a microgrid including controllable loads and microgrid connected storage. The algorithm permits the scheduling of the behind-the-meter individual loads. It considers grid constraints and end-user comfort constraints through an OPF. It integrates a multi-period SOCP adapted to consider uncertainties through a scenarios approach. Scenarios of the different stochastic variables are generated based on a Monte Carlo technique that takes into account spatio-temporal correlations in the variables. The stochastic optimization approach is compared to a deterministic one to quantify the benefit of taking into account uncertainty for the day-ahead scheduling of controllable loads and battery systems. The use of the stochastic algorithm resulted in a reduction in the cost of operating the grid for the case study presented in comparison with the deterministic strategy. However, given that the stochastic approach permits hedging over a higher number of scenarios for the input variables to anticipate risks, the cost reduction is moderate. Significant savings can be achieved by harnessing DR in day-ahead scheduling of microgrids as shown in this paper. However individual devices and end user comfort constraints must be considered. The primary conclusions of this paper are: i) considering uncertainties in UL and PV during day ahead scheduling can decrease annual operational costs; ii) considering DR in microgrids decreases annual costs; iii) considering detailed

DR models and end user comfort constraints is important to effectively implement DR without affecting end user comfort.

REFERENCES

[1] Aris L. Dimeas, Antonis G. Tsikalakis, Georges Kariniotakis, and George Korres, *Microgrids Control Issues in Microgrids: Architectures and Control (ed N. Hatziargyriou)*. Chichester, United Kingdom: John Wiley and Sons Ltd, 2014.

[2] Salman Mashayekh, Michael Stadler, Gonçalo Cardoso, and Miguel Heleno, "A mixed integer linear programming approach for optimal DER portfolio, sizing, and placement in multi-energy microgrids," *Applied Energy*, vol. 187, pp. 154-168, February 2017.

[3] A. Alqurashi, A. H. Etemadi, and A. Khodaci, "Treatment of uncertainty for next generation power systems: State-of-the-art in stochastic optimization," *Electric Power Systems Research*, vol. 141, pp. 233 -245, 2016.

[4] Avirup Maulik and Debapriya Das, "Optimal operation of microgrid using four different optimization techniques," *Sustainable Energy Technologies and Assessments*, vol. 21, pp. 100-120, 2017.

[5] Simone Baldi, Athanasios Karagevrekis, Iakovos T. Michailidis, and Elias B. Kosmatopoulos, "Joint energy demand and thermal comfort optimization in photovoltaic-equipped interconnected microgrids," *Energy Conversion and Management*, vol. 101, pp. 352-363, September 2015.

[6] Z. Wang, B. Chen, J. Wang, M. M. Begovic, and C. Chen, "Coordinated Energy Management of Networked Microgrids in Distribution Systems," *in IEEE Transactions on Smart Grid*, vol. 6, no. 1, pp. 45-53, January 2015.

[7] N. Good, E. Karangelos, A. Navarro-Espinosa, and P. Mancarella, "Optimization Under Uncertainty of Thermal Storage-Based Flexible Demand Response With Quantification of Residential Users' Discomfort," *IEEE Transactions on Smart Grid*, vol. 6, no. 5, pp. 2333-2342, February 2015.

[8] Luhao Wang, Qiqiang Li, Ran Ding, Mingshun Sun, and Guirong Wang, "Integrated scheduling of energy supply and demand in microgrids under uncertainty: A robust multi-objective optimization approach," *Applied Energy*, vol. 130, pp. 1-14, July 2017.

[9] K. R. Krishnanand, D. C. Hoang, S. K. Panda, and R. Zhang, "Optimal appliance scheduling in building operating systems for cost-effective energy management," in *IEEE Industrial Electronics Society*, Dallas, TX, 2014.

[10] E. Grover-Silva, R. Girard, and G Kariniotakis, "Stochastic Multi-temporal Optimal Power Flow Approach for the Management of Grid Connected Storage," in *CIRED International Conference on Electricity Distribution*, Glasgow, Scotland, 2017.

[11] F. S. Gazijahani, H. Hosseinzadeh, A. A. Abadi, and J. Salehi, "Optimal day ahead power scheduling of microgrids considering demand and generation uncertainties," in *Iranian Conference on Electrical Engineering (ICEE)*, Tehran, Iran, 2017, pp. 943-94.

[12] S. Y. Abdelouadoud, R. Girard, F. P. Neirac, and T. Guiot, "Optimal power flow of a distribution system based on increasingly tight cutting planes added to a second order cone relaxation," *International Journal of Electrical Power & Energy Systems*, pp. 9-17, 2015.

[13] Wencong Su, Jianhui Wang, and Jaehyung Roh, "Stochastic Energy Scheduling in Microgrids With Intermittent Renewable Energy Resources," *IEEE Transactions on Smart Grid*, vol. 5, no. 4, pp. 1876-1883, July 2014.

[14] V. Trovato, F. Teng, and G. Strbac, "Role and Benefits of Flexible Thermostatically Controlled Loads in Future Low-Carbon Systems," *IEEE Transactions on Smart Grid*, vol. PP, no. 99, pp. 1-1, 2017.

[15] Nima Nikmehr, Aajad Najafi-Ravadanegh, and Amin Khodaei, "Probabilistic optimal scheduling of networked microgrids considering time-based demand response programs under uncertainty," *Applied Energy*, vol. 198, pp. 267-279, July 2017.

[16] Y. Zhang, N. Gatis, and G. B. Giannakis, "Robust Energy Management for Microgrids With High-Penetration Renewables," *IEEE Transactions on Sustainable Energy*, vol. 4, no. 4, pp. 944-953, September 2013.

[17] Mohamadreza Baradar and Mohammad R. Hesamzaheh, "A stochastic SOCP optimal power flow with wind power uncertainty," in *PES General Meeting Conference & Exposition*, National Harbor, MD, USA, 2014.

[18] M. Heleno, M. A. Matos, and J. A. P. Lopes, "Availability and flexibility of loads for the provision of reserve," *IEEE Transactions on Smart Grid*, vol. 6, no. 2, pp. 667-674, March 2015.

[19] A. A. Eajal, Mostafa F. Shaaban, Kumaraswamy Ponnambalam, and E.F. El-Saadany, "Stochastic Centralized Dispatch Scheme for AC/DC Hybrid Smart Distribution Systems," *IEEE Transactions on Sustainable Energy*, vol. 7, no. 3, pp. 1046-1059, July 2016.

[20] Morteza Aien, Ali Hajebrahimi, and Mahmud Fotuhi-Firuzabad, "A somprehensive review on uncertainty modeling techniques in power system studies," *Renewable and Sustainable Energy Reviews*, vol. 57, no. Summlement C, pp. 1077-1089, January 2016.

[21] E. A. Bakirtzis and P.N. Biskas, "Multiple time resolution stochastic scheduling for systems with high renewable penetration," *IEEE Transactions on Power Systems*, vol. 4, pp. 1030-1040, March 2017.

[22] Pierre Pinson, Henrik Madsen, Henrik Aa. Nielsen, George Papaefthymiou, and Bernd Klockl, "From probabilistic forecasts to statistical scenarios of short-term wind power production," *Wind Energy*, pp. 51-62, 2009.

[23] T. Barbier, R. Girard, F. P. Neirac, N. Kong, and G. Kariniotakis, "A novel approach for electric load curve holistic modeling and simulation," in *IEEE MedPower*, Athens, Greece, 2014, pp. 1-8.

[24] Solaire lgm. (2016, November) Solaire lgm. [Online]. http://solaire.lgm.ac-grenoble.fr/

Etta Grover-Silva was born in Eureka, Ca., USA and completed her B.S. at Smith College in Engineering with a focus in Alternative Energy R&D. She received a Master's degree (2012) in Renewable Energy specializing in Hybrid Systems from the European Union Renewable Energy Center (EUREC) Agency in collaboration with Loughborough University and University of Kassel. She is currently pursuing her PhD in Optimal Renewable Energy Grid Integration at MINES ParisTech in Sophia Antipolis, France.

Miguel Heleno received the MSc degree in Electrical and Computers Engineering from the University of Porto, Portugal and a PhD in sustainable Energy Systems from the same institution within the MIT-Portugal Program. Currently he is Sr. Scientific Engineering Associate at Lawrence Berkeley National Laboratory (LBNL), CA United States. His work is focused on optimization methods applied to planning, operation and control of microgrids.

Salman Mashayekh received his BSc and MSc in Electrical Engineering - Power Systems from University of Tehran, Iran, in 2006 and 2008, respectively and a PhD from in Texas A&M University, College Station, TX. He is currently a Principal Scientific Engineering Associate at LBNL, working with operation and investment/planning of DER-CAM (Distributed Energy Resources Customer Adoption Model) development teams.

Gonçalo Cardoso received a M.Sc. in Civil Engineering from University of Lisbon, Portugal and later Ph.D. in Sustainable Energy Systems from the same institution within the MIT-Portugal Program. He is currently a Principal Scientific Engineering Associate at LBNL, working for the Grid Integration Group of the Energy Storage and Distributed Resources Department.

Robin Girard received a Master's degree (2004) in Computer Science and Applied Mathematics from INPG in Grenoble, France and a PhD degree (2008) in applied Mathematics from Joseph Fourier University in Grenoble. He is currently a Research Engineer at the Centre of Energy and Processes of the Ecole des Mines de Paris.

George Kariniotakis (S95-M02-SM11) was born in Athens, Greece. He received his Eng. and M.Sc. degrees from Greece in 1990 and 1992 respectively, and his Ph.D. degree from Ecole des Mines de Paris in 1996. He is currently with the Centre PERSEE of MINES ParisTech as a senior scientist and head of the Renewable Energies and Smartgrids Group. He has authored more than 220 scientific publications in journals and conferences. He has been involved as participant or coordinator in more than 40 R&D projects in the fields of renewable energies and distributed generation.

A STOCHASTIC MULTI-TEMPORAL OPTIMAL POWER FLOW APPROACH FOR THE MANAGEMENT OF GRID CONNECTED STORAGE

Etta GROVER-SILVA[1,2] Xwégnon Ghislain AGOUA[1] Robin GIRARD[1] Georges KARINOTAKIS[1]
[1]MINES ParisTech, PSL – Research University, PERSEE – Centre for Process Energies and Energy Systems France
[2]ADEME - French Environment and Energy Management Agency - France
E-mail addresses: {etta.grover-silva, xwegnon.agoua, robin.girard, georges.kariniotakis}@mines-paristech.fr

ABSTRACT

Renewable energy (RE) integration into distribution grids is becoming more common in the context of the energy transition. The management of wind or solar generation due to their variability and low predictability are challenging for distribution system operators (DSO). To that may be added uncertainties related to electric load profiles. The role of flexibility, coming from decentralized storage devices, will be important for DSOs trying to manage uncertain loads as well as high levels of RE penetration. The introduction of automation and smart metering in distribution grids allows for the optimized management of storage devices to maximize the capability of current infrastructure to integrate RE generators. These optimized management strategies can be calculated with optimal power flow (OPF) algorithms. This paper uses a convex relaxation of the power flow equations to expand the multi-temporal deterministic approach presented in [1] to a stochastic one. The stochastic algorithm implies the integration of a scenario tree to plan the charging and discharging schedule of batteries one day in advance. When comparing deterministic and stochastic operation planning strategies, the stochastic method annually increases total economic benefit by 3.1% while requiring lower annual cycling of the battery therefore increasing battery life.

INTRODUCTION

Renewable energy generators are becoming more common in the distribution system as a result of the transition from traditional electric generation to more sustainable technologies. These decentralized generators, such as photovoltaic (PV) systems, introduce new technical difficulties for distribution system operators (DSO) including bi-directional power flow, over current and voltage profile shifting. Smart meters are gaining popularity as a solution to improved visibility and controllability in distribution grids. The automation of distribution grids can allow for the optimization of existing grid architecture to avoid unnecessary infrastructure upgrades.

The new possibility to control decentralized generators and loads in the distribution system requires new and innovative management strategies. Optimal power flow algorithms are effective at calculating optimal set points for decentralized controllable devices while guaranteeing that no power quality requirements are violated. These types of algorithms can take into account the voltage and current constraints of an electrical distribution grid while minimizing an overall cost function.

At the distribution grid level, the uncertainties of renewable energy production and electric loads are high due to minimal aggregation effects. These uncertainties introduce a challenge for DSOs to optimize their controllable devices. Management strategies have been employed by DSOs to optimize decentralized controllable devices under uncertainty. These management strategies include real time flexibility of the system through grid connected storage or PV curtailment strategies managed by a real time distribution management system (DMS). However, real time control of a distribution system can imply sophisticated communication networks. This flexibility can also be scheduled on a day-ahead basis to reduce the need for real time power flow control.

Stochastic optimization has been presented in the literature as effective for planning operational strategies of controllable grid connected devices under uncertainty. For example reactive power compensation under uncertainty was explored by using statistical probability distribution curves and a Monte Carlo sampling technique to represent prediction errors in an OPF algorithm [2]. A similar probability distribution using multi-stage stochastic programming with a chance-constrained optimization problem uses probabilistic penalty constraints associated with prediction errors [3]. However, these techniques imply a precise estimation of the distribution profile of errors associated with each forecast.

The use of scenarios to take uncertainties into account requires less detailed forecast data. Accounting for uncertainties through scenarios is present in the literature. For example, a simulation of a deterministic scenario and associated forecast limits of load and PV for a three-phase distribution grid is presented in [4]. This analysis is a single time step analysis performed for each hour of the day. This daily analysis does not take into account variables that have temporal dependencies. A multi-temporal algorithm is necessary to consider time

dependent variables such as storage devices and controllable loads.

Multi-temporal stochastic OPF can be applied to distribution grids to analyze the benefits of grid connected storage devices under uncertainty. However, the integration of multi-temporal and multi-scenario aspects into an OPF algorithm can increase exponentially the size of the problem. Therefore, intelligent scenario selection and a certain decoupling are necessary to effectively resolve this type of problem for annual analysis. There exist few algorithms that take into account temporal dependencies and uncertainties at the same time for the distribution grid.

This paper presents a stochastic OPF algorithm whose structure allows the integration of scenarios and multi-temporal aspects for day ahead planning of storage devices. It utilizes convex relaxations of the power flow equations in the form of a second order cone program (SOCP) and iterative cuts to guarantee exactness as described in [5]. Just as the convex relaxations exploit the radial geometry of distribution grids, a radial geometry is also used for the scenario tree. This innovative approach proposes a simple scenario generation strategy based on historical data that shows a higher performance in comparison to a deterministic day ahead planning strategy.

The paper organization includes the definition of the algorithm in section 2, the algorithmic performance in section 3, the demonstration of such an algorithm for a French case study in section 4 followed by the case study results in section 5 and final conclusions in section 6.

STOCHASTIC OPTIMAL POWER FLOW ALGORITHM

SOCP Optimization Problem Formulation

The SOCP optimization objective function is defined in eq. (1).

$$\boldsymbol{min.} \sum_{t=0}^{T} \boldsymbol{C_{e,t}} |\boldsymbol{P_{0,t}}| + \sum_{t=0}^{T} \sum_{n=0}^{N} \boldsymbol{C_{e,t}} \left[\boldsymbol{r_{ij}} \boldsymbol{\ell_{ij,t}} + \left(\bar{\boldsymbol{P}}_{\boldsymbol{pv,j,t}} - \boldsymbol{P_{pv,j,t}} \right) \right] \quad \textbf{(1)}$$

Where the definition of node specific variables will use the convention below:

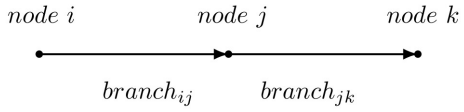

$C_{e,t}$ is the price of electricity for the time step t, $P_{0,t}$ is the active power at the substation at time step t, r_{ij} is the resistance of branch ij, $\ell_{ij,t}$ is the square of the magnitude of the current on branch ij at time t, $\bar{P}_{pv,j,t}$ is the maximum PV injection at node j at time step t, $P_{loss,j,t}$ is the actual injection at node j at time step t, and $P_{loss,j,t}$ is the losses of the battery system at node j at time step t.

The optimization constraints include the PV power limits eq. (2), PV apparent power limits eq. (3) – eq. (4), the power flow equations eq. (5) – eq. (7), the relaxation of the current equation eq. (8) – eq. (9), the voltage limits eq. (10), battery power constraints eq. (11) and the constraints associated with the battery capacity eq. (12) – eq. (13).

$$\boldsymbol{P_{pv,j,t}} \leq \bar{\boldsymbol{P}}_{\boldsymbol{pv,j,t}} \quad \textbf{(2)}$$

$$\boldsymbol{S_{pv,j,t}} \leq \bar{\boldsymbol{S}}_{\boldsymbol{pv,j}} \quad \textbf{(3)}$$

$$\boldsymbol{S_{pv,j,t}} = \sqrt{\boldsymbol{P_{pv,j,t}^2} + \boldsymbol{Q_{pv,j,t}^2}} \quad \textbf{(4)}$$

$$\boldsymbol{P_{ij,t}} = \boldsymbol{P_{l,j,t}} + \sum_{k=0}^{K} \boldsymbol{P_{jk,t}} + \boldsymbol{r_{ij}} \boldsymbol{\ell_{ij,t}} + \boldsymbol{P_{pv,j,t}} + \boldsymbol{P_{st,j,t}} \quad \textbf{(5)}$$

$$\boldsymbol{Q_{ij,t}} = \boldsymbol{Q_{l,j,t}} + \sum_{k=0}^{K} \boldsymbol{Q_{jk,t}} + \boldsymbol{x_{ij}} \boldsymbol{\ell_{ij,t}} + \boldsymbol{Q_{pv,j,t}} \quad \textbf{(6)}$$

$$\boldsymbol{v_{j,t}} = \boldsymbol{v_{i,t}} - 2\left(\boldsymbol{r_{ij}} \boldsymbol{P_{ij,t}} + \boldsymbol{x_{ij}} \boldsymbol{Q_{ij,t}} \right) + \left(\boldsymbol{r_{ij}^2} + \boldsymbol{x_{ij}^2} \right) \boldsymbol{\ell_{ij,t}} \quad \textbf{(7)}$$

$$\boldsymbol{S_{ij,t}} \geq \sqrt{\boldsymbol{P_{ij,t}^2} + \boldsymbol{Q_{ij,t}^2}} \quad \textbf{(8)}$$

$$\boldsymbol{S_{ij,t}} \geq \boldsymbol{\ell_{ij,t}} \boldsymbol{v_{i,t}} \quad \textbf{(9)}$$

$$\underline{\boldsymbol{V}}^{\boldsymbol{2}} \leq \boldsymbol{v_{j,t}} \leq \bar{\boldsymbol{V}}^{\boldsymbol{2}} \quad \textbf{(10)}$$

$$\boldsymbol{0} \leq \boldsymbol{P_{st,j}} \leq \bar{\boldsymbol{P}}_{\boldsymbol{st,j}} \quad \textbf{(11)}$$

$$\boldsymbol{soc_{st,j,t-1,s}} = \boldsymbol{soc_{st,j,t,s}} + \boldsymbol{t} \boldsymbol{P_{st,j,t,s}} + \boldsymbol{t} \boldsymbol{P_{loss,j,t,s}} \quad \textbf{(12)}$$

$$\boldsymbol{P_{loss,j,t}} = \boldsymbol{\eta} \left| \boldsymbol{P_{st,j,t}} \right| \quad \textbf{(13)}$$

where $S_{pv,j,t}$ is the apparent power injection of the PV system at time step t, $\bar{S}_{pv,j}$ is the maximum apparent power rating of the PV inverter, $Q_{pv,j,t}$ is the apparent power of the PV system at time step t, $P_{ij,t}$ is the active power of branch ij at time step t, $P_{l,j,t}$ is the active load at node j at time step t, $P_{st,j,t}$ is the active power injection of the battery system at node j at time step t, $Q_{ij,t}$ is the reactive power of branch ij at time step t, $Q_{l,j,t}$ is the reactive load at node j at time step t, x_{ij} is the reactance of branch ij, $Q_{pv,j,t}$ is the reactive power injection of the PV system at node j at time step t, $v_{j,t}$ is the square of the voltage magnitude at node j at time step t, $\overline{V}$ is the maximum voltage, $\underline{V}$ is the minimum voltage, $soc_{st,j,t,s}$ is the state of charge of the battery system at node j at time step t for scenario s. The temporal and scenario dependencies are a result of eq. (12).

Scenario Generation and Structure

Scenarios are generated for the PV production and load profiles for each node. The scenarios are generated by using historical PV production and load data. A quantile regression is completed using a historical learning set period of 60 days to then predict the 25th, 50th and 75th quantile of PV production and load profile for the next two day period. The deterministic approach analyzes a daily period consisting of 24 coupled time steps and using the 50th percentile for the PV production and load profiles for the predicted profiles. The stochastic approach combines the 25th and 75th quantile scenarios of PV and load profiles to create 4 combination scenarios. These combination scenarios are then used in conjunction with the 50th quantile scenario to generate four stochastic OPF problems, here after called calculation blocks. Within each of these four calculation blocks there is a target period and a scenario period as shown by the time steps in black in Figure 2. The target period is defined as a period where there is only one variable representing the power of each battery system or controllable load which also corresponds to the 50th PV quantile and 50th load quantile in all scenarios. The scenario period is characterized by multiple optimal values of the battery power injection or controllable load power for each time step. The physical meaning of multiple optimal values of the controllable power injection is the optimal power injection for each unique scenario. The target is coupled with each independent scenario therefore finding the optimal injection of the target period for all following injection possibilities. These blocks include using the 50th quantile for the target period and the 4 combination scenarios for the scenario period. The target period for the first three blocks is 6 hours while the target period for the last block is 12 hours. The deterministic problem scenario tree is found in Figure 1 while the stochastic OPF scenario tree can be found in Figure 2.

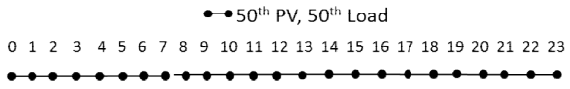

Figure 1: Deterministic analysis with a single scenario using the 50th quantile of PV and load profiles

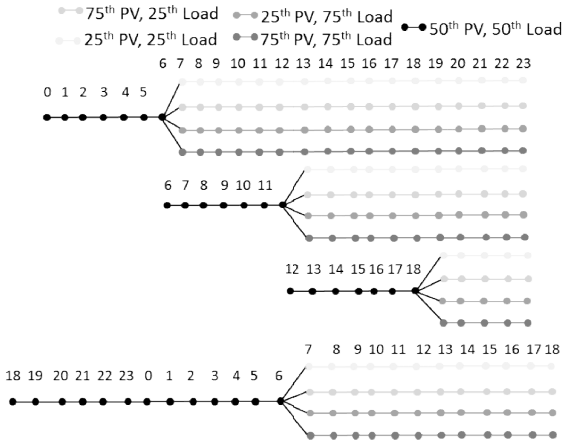

Figure 2: Stochastic analysis with a four dimensional scenario tree using 25th, 50th and 75th quantiles of PV and load profiles

After a scenario tree splits, the four combination scenarios are considered to be independent. Therefore the final optimal charging schedule of the battery is composed of the solution calculated during the target period for each block. For the deterministic problem, the target period is the same length as the total simulation period. Therefore only one problem is solved during the deterministic algorithm. The stochastic algorithm solves four different stochastic problems taking into account critical periods where scenarios could be significantly different. The coupling between the four blocks is done by setting the state of charge and power of the battery systems at the end of one target period equal to the first time step of the next block's target period. The final daily optimal charging schedule is composed of the target periods of each block.

ALGORITHMIC PERFORMANCE

An annual analysis is performed to calculate the annual benefit possible from using a stochastic day ahead scheduling in comparison to the deterministic day ahead scheduling. The algorithmic performance of the deterministic approach and the stochastic approach are shown in

Approach	Coupled time steps	Time (s)
Deterministic	24	3.4
Stochastic	24	31.1

The deterministic algorithm has a lower calculation time in comparison to the stochastic algorithm.

CASE STUDY

Grid Feeder

An example urban electric grid in France was studied to demonstrate the use of the algorithm. The medium voltage distribution grid feeder is composed of 137 nodes with a nominal voltage of 30 kV and is assumed to be located in Nice, France. A map of the grid topology can be found in Figure 3.

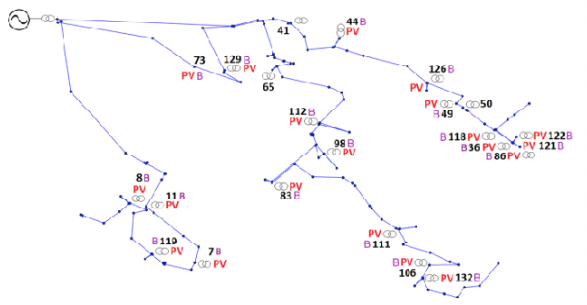

Figure 3: Grid topology with low voltage substation connections of medium voltage urban feeder in France.

Generation and Load Profiles

Electric load profile data was simulated with a bottom up load simulator detailed in [6] for each low voltage substation. A statistically accurate representation of residential and commercial customer proportion, electric heating, living surface area and population was simulated using the INSEE building inventory database of France. The location of each load profile was determined randomly due to the fact that no grid load data was available. The transformer connecting the medium voltage feeder and the high voltage grid is an 8 MVA transformer serving 21 low voltage substations. Load profiles aligning with meteorological data in Grenoble, France indicated a peak load of 3.0 MW during the summer and 7.7 MW during the winter with an average load of respectively 2.8 MW and 4.2 MW. Solar system production data was based on the normalized real production of a PV plant in Grenoble France [7].

An amount of 20 PV systems and 20 battery systems were assigned to 20 nodes, a majority were chosen to be the same nodes as the nodes hosting low voltage substations. The size of these systems was chosen randomly to be between 35-250 kW. Characteristics of the final load profile nodes can be found in Figure 4 and PV size information can be found in Figure 5.

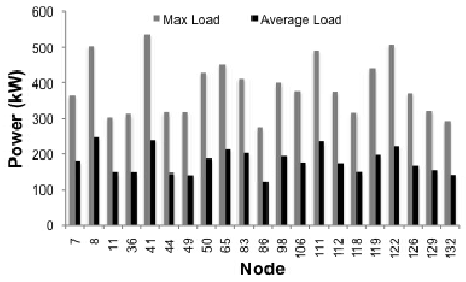

Figure 4: Maximum and average load for indicated nodes

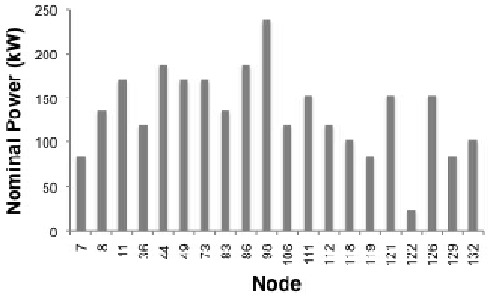

Figure 5: Nominal power of PV systems installed at indicated nodes

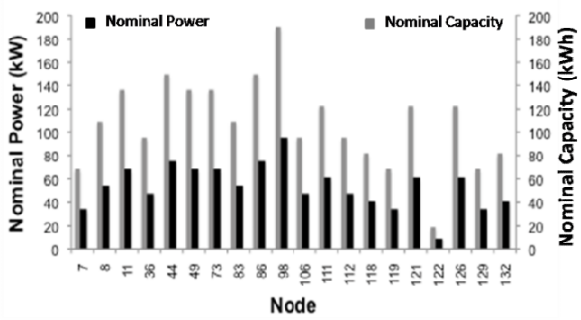

Figure 6: Nominal power and capacity of battery systems installed at indicated nodes

RESULTS

An annual analysis was performed to compare the effectiveness of day ahead planning for storage devices with stochastic and deterministic techniques. An example detailed profiles of the charging and discharging schedule for node 86 can be found in Figure 7. These profiles show the different charging profiles solved by the stochastic and deterministic algorithms.

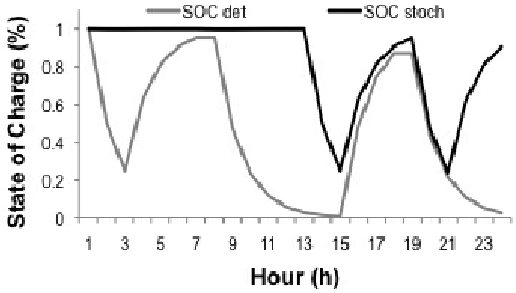

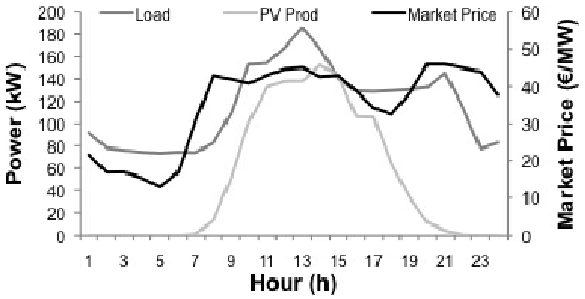

Figure 7: Charging schedule for July 11, 2012 of stochastic and deterministic planning methods (top) and associated load profile, PV production and market price (bottom)

As seen by the figure above, the stochastic battery charging schedule is more conservative using the battery less during the day. While the number of full cycles of the battery systems are lower in the stochastic case study the economic annual benefit is higher as seen in Table 1.

This table shows that stochastic day ahead planning not only increases the battery life by decreasing the annual battery cycles but also increases annual economic benefit by 3.1 %.

Table 1: Comparison of stochastic and deterministic charging schedule annual performance

Algorithm	Energy (MWh)	Cost (M€)	Battery Cycles
Deterministic	30.02	1441	908
Stochastic	30.65	1396	589

CONCLUSION

This paper has presented two day-ahead battery operations scheduling for a distribution grid: one deterministic method and one stochastic method. These two methods are then compared quantifying the benefits of using stochastic analysis in distribution grid for storage operations management. The primary difference between the stochastic and deterministic analysis is that the stochastic algorithm calculated a more conservative use of the battery systems. This conservative usage decreases the number of cycles per year of the battery while increasing economic benefit by 3.1%. Another advantage of this type of algorithm is that the quantile regression method used to calculate the scenarios has a low calculation burden and requires a short historical data set of only three months. Future work could be done on improving the scenario generation method to be more precise and integrating parallel programming to decrease the calculation time.

ACKNOWLEDGEMENTS

The authors would like to thank ENEDIS for the provision of some of the data used in this study. Mr. Thibaut Barbier is thanked for his support with the simulated load curves. This work is being carried out as a part of the research and innovation project SENSIBLE (Storage ENabled SustaInable energy for BuiLdings and communitiEs - www.h2020-projectsensible.eu) that has received funding from the European Union's under the Horizon 2020 Framework Programme (Grant No 645963). It is also supported from a PhD grant by ADEME (Agence de l'Environnement et de la Matrise de l'Energie) and ARMINES.

REFERENCES

[1] Florin Capitanescu, 2016, "Critical review of recent advances and further developments needed in AC optimal power flow", *Electric Power Systems Research*, vol. 136, 57-68.

[2] Vassilis Kekatos, Gang Wang, and Georgios B. Giannakis, 2014, "Stochastic Loss Minimization for Power Distribution Networks", *Proceedings of North American Power Symposium,* pp. 1-6

[3] T. Summers, J. Warrington, M. Morari and J. Lygeros, 2014, "Stochastic optimal power flow based on convex approximations of chance constraints", *Proceedings of Power Systems Computation Conference*, pp. 1-7

[4] M. Chehreghani Bozchalui, Chenrui Jin and R. Sharma, 2014, "Rolling Stochastic Optimization based operation of distribution systems with Pvs and Energy Storages", *Proceedings of Innovative Smart Grid Technologies Conference (ISGT)*, IEEE PES, pp. 1-5

[5] S. Abdelouadoud, R. Girard, F. Neirac, and T. Guiot, 2015, "Optimal power flow of a distribution system based on increasingly tight cutting planes added to a second order cone relaxation", International Journal of Electrical Power & Energy Systems, vol. 69, 9 – 17

[6] T. Barbier, R. Girard, F. P. Neirac, and G. Kariniotakis, 2014, "A novel approach for electric load curve holistic modeling and simulation", *Proceedings of MedPower Conference*, IET, pp 1 – 8

[7] "Dix ans de production d'énergie solaire au Lycée du Grésivaudan de Meylan." *Académie de Grenoble*. November 28, 2011. http://www.ac-grenoble.fr/admin/spip/spip.php?article3505

Multi-temporal Optimal Power Flow for Assessing the Renewable Generation Hosting Capacity of an Active Distribution System

Etta Grover-Silva*, Robin Girard*, George Kariniotakis*, *SMIEEE*
*MINES ParisTech, PSL - Research University, PERSEE - Center for Processes, Renewable Energies and Energy Systems
06904 Sophia Antipolis, France
Email: etta.grover-silva@mines-paristech.fr

***Abstract*—The detailed modeling of distribution grids is expected to be critical to understand the current functionality limits and necessary retrofits to satisfy integration of massive amounts of distributed generation, energy storage devices and the electric consumption demand of the future. Due to the highly dimensional non-convex characteristics of the power flow equations, convex relaxations have been used to ensure an efficient calculation time. However, these relaxations have been proven to be inexact during periods of high RES injection. In this paper additional linear constraints were introduced in the power flow formulation to guaranty an exact relaxation. This convex relaxation is then applied within a multi-temporal algorithm in order to evaluate the benefits of storage grid integration. The case study of a French medium voltage feeder is studied to evaluate the maximum capacity of the grid to host RES sources and the advantages of storage systems in reducing curtailment of RES.**

I. Introduction

The electric distribution system is critical for energy security and economic stability. With the exploration of new energy production solutions including renewable energy sources (RES) and associated storage devices, the architecture and functionality of the current distribution grid has been a subject of high interest. For example, a renewable energy source could include wind turbines, hydro turbines or photovoltaic panels. The simulation of current functionality limits with new decentralized renewable energy generation can in turn indicate the advantages of the automation and control of components in the distribution grid. This automation and control is typically labeled as an active distribution system. The added control possibilities of an active distribution grid can allow for a high capacity of decentralized generators to be installed without major infrastructure upgrades. The capacity of a grid to integrate decentralized generators without violating operational limits can be called a distribution grid hosting capacity. In order to quantify the hosting capacity of a distribution grid, detailed AC power flow models are necessary. However, for AC power flow algorithms to be useful and applicable, computation time must be optimized.

There exists many different techniques of AC power flow modeling. However, power flow calculations are non-linear, non-convex and highly dimensional, which can be extremely computationally intensive. Existing power flow algorithms include the forward/backward sweep, Newton Raphson method [1], [2], fast-decoupled load-flow method [3], [4], z-bus matrix construction method [5], and loop impedance method [6], [7]. The quantification of the current hosting capacity of the electric grid is evaluated in [8]. As noted within this study, possible strategies to increase this current hosting capacity include curtailment and dynamic line rating. Other strategies well explored in the literature include the use of storage elements [9].

The development of smart grid solutions and grid automation has increased the passive hosting capacity by controlling certain components during critical times. However, management algorithms for optimal control must resolve this highly dimensional non-convex power flow problem. Convex optimum power flow relaxation algorithms have been developed to optimize the controllable components while ensuring algorithmic efficiency as seen in [10], [11]. Heuristic methods have also been explored to solve the non-convex power flow equations as seen in [12]. However, heuristic algorithms often require a larger calculation burden as noted in [13] when compared to convex relaxation algorithms. The family of convex relaxation algorithms that is most commonly used for distribution grids is called a Quadratically Constrained Quadratic Program (QCQP). In multiple studies, the non-convex power flow equations have been cast as a QCQP as shown in [14], [15]. Within the QCQP family, two convex relaxation algorithms exist including the Second-Order Cone Program (SOCP) or the Semi-Definite Program (SDP). An SDP convex relaxation has been proved to be exact under certain conditions by [16]. While an SOCP relaxation has also proved to be exact under certain conditions as stated in [17], [10], [18]. However, these relaxations have been proven to be inexact during periods of high renewable energy production feeding into the grid due to elevated line losses [19]. In order to determine the hosting capacity of a distribution grid, it is critical to have a precise and accurate calculation methodology when RE production is high. An example of this difficulty could be high photovoltaic (PV) production during the summer season. In order to overcome the challenge of inaccurate results at periods of high PV injection, [19] presents an AC optimum power flow algorithm that integrates linear cuts implemented in a iterative fashion to ensure an exact and feasible relaxation of the power flow equations. This single

phase AC optimum power flow algorithm minimizes losses in the system, while also minimizing the distance between the curtailed production and the real PV production capacity. This methodology allows for the instantaneous assessment of grid operational limits with a certain PV injection and a certain consumption. However, this algorithm does not allow for the assessment of time dependent components such as storage devices. In contrast to the literature, the consideration of multiple time steps permits to properly assess the impact of storage since decisions for charging/discharging involve temporal dependencies. Here, the second order cone program (SOCP) convex relaxation algorithm will be implemented using the same linear cuts in a multi-temporal application. The advantage of a multi-temporal problem formulation is the optimization of the charging and discharging schedule of a given time period, here between 12-96 consecutive time-steps.

The importance of multi-temporal coupling in an optimum power flow algorithm is directly related to the evaluation of the role of storage within an active distribution network. An alternative solution to curtailment on the RES generation is the storage of this energy in order to mitigate grid constraint violations. This stored energy can then be later used to minimize the high consumption peak periods. This multi-temporal coupling is critical in order to evaluate the technical constraints of the storage elements and the possible benefits. In this paper, an example active medium voltage distribution grid will be modeled in order to understand the existing RES hosting capacity with curtailment in comparison with centralized and decentralized storage options. This multi-temporal algorithm will allow the quantification of storage element advantages and their optimum placement.

II. Problem Formulation

A. Power Flow Model

Two different sets of equations can be used within a power flow model, the bus injection model (BIM) or the branch flow model (BFM). While both models can be effective for various applications, the BFM system of equations will be used due to better convergence characteristics as explained in [10] specifically in relation to a radial network topology. Let the labeled nodes i, j and k be oriented as described in the figure below.

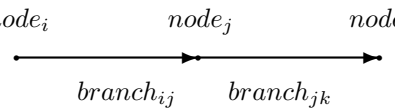

When considering a radial distribution system with decentralized PV generation and decentralized storage elements, the power flow equations can be written as shown below.

$$P_{ij} = P_{load,j} + \sum_{k=1}^{n} P_{jk} + r_{ij} I_{ij}^2 + P_{pv,j} + P_{st,j} \quad (1)$$

$$Q_{ij} = Q_{load,j} + \sum_{k=1}^{n} Q_{jk} + x_{ij} I_{ij}^2 + Q_{pv,j} + Q_{st,j} \quad (2)$$

Equation (1) and (2) describe the balance of power from the upstream and downstream branches where P_{load}, P_{pv}, and P_{st} are respectively the instantaneous consumption, PV production and battery storage charge or discharge at a given timestep. P_{jk}, r_{jk}, Q_{jk},x_{jk} and I_{ij}^2 are respectively the power, the resistance, the reactive power, the reactance and the current associated with the branch *jk*. Q_{load}, Q_{pv}, and Q_{st} are respectively the instantaneous reactive consumption, PV reactive production, and battery reactive power values. The voltage at each node can be calculated by equation (3).

$$|V_j|^2 = |V_i|^2 - 2(r_{ij} P_{ij} + x_{ij} Q_{ij}) + (r_{ij}^2 + x_{ij}^2) I_{ij}^2 \quad (3)$$

where $|V_j|$ is the voltage magnitude at node *j*. The current of each branch is calculated as shown in equation (4).

$$I_{ij}^2 = \frac{P_{ij}^2 + Q_{ij}^2}{|V_i|^2} \quad (4)$$

B. System Constraints

The system constraints of an electrical distribution network include maximum and minimum voltage limits, maximum and minimum current limits, and operational limits imposed by individual components. The network voltage and current limits can be described as shown below:

$$\underline{V}_i \leq |V_i| \leq \overline{V}_i \quad (5)$$

where $\underline{V}_i$ and $\overline{V}_i$ are respectively the lower and upper limits of the voltage on a line. Individual components such as the PV and battery systems were modeled through their inverter behavior as described in the following sections.

1) PV Inverter Model: The PV inverter behavior was modeled as active and reactive generation source with upper and lower limits, $\overline{P}^{pv}$ and $\underline{P}^{pv}$ respectively on active power and $\overline{s}^{pv}$, $\underline{s}^{pv}$ on total apparent power injection for a given timestep.

$$\begin{aligned} \underline{P}_{pv} \leq |P_{pv}| \leq \overline{P}_{pv} \\ \underline{s}_{pv} \leq |s_{pv}| \leq \overline{s}_{pv} \end{aligned} \quad (6)$$

where s_{pv} is the total apparent power of the power injection as defined below.

$$\begin{aligned} s_{pv}^2 &= P_{pv}^2 + Q_{pv}^2 \\ s_{pv} &= \sqrt{P_{pv}^2 + Q_{pv}^2} \end{aligned} \quad (7)$$

2) Battery Inverter Model: The battery inverter was modeled as either a power injection or power consumption for a given node at a given timestep. The time coupling variable indicating the state of charge (SOC) was calculated based on a charging and discharging efficiency associated with the inverter.

$$\begin{aligned} E_{batt,t1} &= E_{batt,t0} - \eta_{ch} P_{ch,t1} - \eta_{dch} P_{dch,t1} \\ P_{st} &= P_{ch} + P_{dch} \\ \underline{s}_{st} &\leq |s_{st}| \leq \overline{s}_{st} \end{aligned} \quad (8)$$

where η^{ch}, $P_{ch,t1}$, η_{dch}, $P_{dch,t1}$, $\overline{s}_{st}$ and $\underline{s}_{st}$ is the charging efficiency, power absorbed during charging, discharging efficiency, power injected into the grid, upper limit and lower

limit of total apparent power exchange with the grid. P_{st} is the power injection or absorbed by the battery as defined below:

$$\begin{aligned} s_{st}^2 &= P_{st}^2 + Q_{st}^2 \\ s_{st} &= \sqrt{P_{st}^2 + Q_{st}^2} \end{aligned} \tag{9}$$

The power flow equations are non-linear and non-convex. Therefore, when solving a highly dimensional power flow problem, convex relaxation have been used to ensure high performance algorithms.

III. Optimum Power Flow Formulation

The same SOCP convex relaxation used in [19] and [17] is implemented in a multi-temporal model in order to analyze the hosting capacity of a distribution grid. This relaxation entails the relaxation of certain equality constraints and the substitution of certain quadratic terms for linear terms. The equality constraints in question, (4), (5) and (6), are relaxed ultimately relaxing the magnitude of currents within each branch and using a conic formation on the limitation of active power exchange with the grid. Two new variables are introduced to replace quadratic terms, $\upsilon_i = |V_i|^2$ and $\ell = |I_{ij}|^2$ in order to successfully formulate an SOCP problem as explained in [17].

A. Objective Function

In order to optimize the total system functionality, the objective function is composed of two parts. The first part is the minimization of the total losses of the system. The second part minimizes the curtailment of the PV systems in order to maximize renewable energy consumption within the grid. Therefore the objective function is formulated as seen below:

$$min \sum_{i=1}^{n} r_{ij}\ell_{ij} + (P_{ideal,i}^{pv} - P_i^{pv}) \tag{10}$$

B. SOCP Problem Formulation

The complete SOCP formulation is then found below:

$$min \sum_{i=1}^{n} r_{ij}\ell_{ij} + (P_{ideal,i}^{pv} - P_i^{pv}) \tag{11}$$

$$\begin{aligned} & s.t. \\ & (6), (7), (8), (9) \\ P_{ij} &= P_j^{load} + \sum_{k=1}^{n} P_{jk} + r_{ij}\ell + P_j^{pv} + P_j^{st} \\ Q_{ij} &= Q_j^{load} + \sum_{k=1}^{n} Q_{jk} + x_{ij}\ell + Q_j^{pv} + Q_j^{st} \\ \upsilon_j &= \upsilon_i - 2(r_{ij}P_{ij} + x_{ij}Q_{ij}) + (r_{ij}^2 + x_{ij}^2)\ell_{ij} \\ \ell_{ij} &\geq \frac{P_{ij}^2 + Q_{ij}^2}{\upsilon_i} \\ \underline{V}_i^2 &\leq \upsilon \leq \overline{V}_i^2 \end{aligned} \tag{12}$$

TABLE I
For a given timestep, the inexact instances present and calculation time in seconds

Timesteps coupled	Inexact instances	Calculation time (s)
12	0	33
12	2	38
48	0	121
48	18	158
96	0	289
96	36	339

IV. Algorithmic Performance

The optimization of storage elements and PV curtailment was analyzed for a time scale of 0.5 to 4 days. An example urban electric grid in France was studied in order to evaluate the performance of this algorithm. The network studied is a 30 kV 137 nodes typical urban grid topology. Network data was acquired through a partnership with ErDF. Twenty PV systems with equivalent power ratings were placed randomly throughout the grid topology with an associated battery system installed at the same node. The time of execution of the algorithm was recorded for varying time coupling scenarios as shown below.

This multi-temporal coupling allows the optimization of PV curtailment and battery storage utilization for up to a four day period with a satisfactory calculation burden. It also ensures that the relaxation is exact and applies linear cuts to timesteps that are not exact in order to guaranty the exactness of the relaxation.

V. Case Study

An example urban electric grid in France was studied to demonstrate possible algorithm utilization. The grid is composed of 137 nodes at 30 kV and serves as a medium voltage distribution grid feeder. A map of the grid topology can be found below.

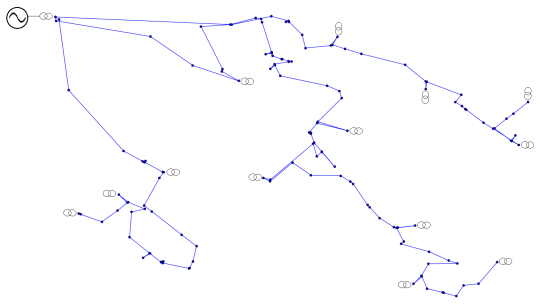

Fig. 1. Case study of typical medium voltage electric grid topology

Consumption load profiles were simulated using an aggregation load simulator as described in [20] for each low voltage substation and medium voltage consumer. This load

simulator takes into account a mix of residential and commercial customers. Residential consumption is simulated with statistically accurate representations of surface area, electric heating and number of individuals that align with the INSEE building inventory database of France. Industrial load profiles are simulated by assuming a typical industrial activity mix in France from a medium voltage substation. The two medium voltage customers were modeled as office building complexes with typical business hours operation. A peak of 5 MW during the winter and 2.9 MW during the summer was simulated for the medium voltage substation transformer with a maximum apparent power limit of 10 MW. Solar radiation data from a site in the south of France was used to calculate expected PV production as a function of system nominal power.

Four different seasonal scenarios were studied in order to understand a typical annual operation. Within each season, three renewable energy solutions were studied: the hosting capacity of a typical grid topology without storage, the hosting capacity with decentralized storage elements installed at the same nodes as the PV systems and the hosting capacity with centralized storage elements close to the high voltage transformer. The hosting capacity of a feeder was defined as the maximum capacity of PV that does not violate grid constraints without using curtailment. Twenty sites were chosen for PV decentralized installations and nominal power of each system was increased until either current or voltage limits were reached.

VI. Results

A three day simulation period was chosen in order to allow for at least one full cycle of charging and discharging of the storage elements. Three day typical profiles were chosen for four different seasons in order to understand the annual performance of the system. Considering only PV installations without storage elements, the maximum current limit of the lines was reached during low loading periods and high peak PV injection in summer. Multiple capacities for 20 decentralized PV systems were tested until curtailment was necessary to not exceed voltage or apparent power limits of the network. The maximum installed capacity where curtailment was unnecessary was achieved with a PV penetration of 10 MW nominal power installed. A a total of 701 kWh of the 156 MWh produced during a three-day simulation was necessary to ensure maximum apparent power limits were not exceeded. During typical daily profiles for fall, winter and spring, no curtailment was necessary for a 10 MW systems. In all simulations, the summer period was the most critical to monitor for grid stability verification, therefore the rest of the results section will focus on summer production and consumption profiles. A comparison of the net consumption of the high voltage transformer and the total power injected into the high voltage grid from the medium voltage substation during summer periods can be found in figure 2.

The curtailment necessary and the losses on the lines were then compared as seen in figure 3.

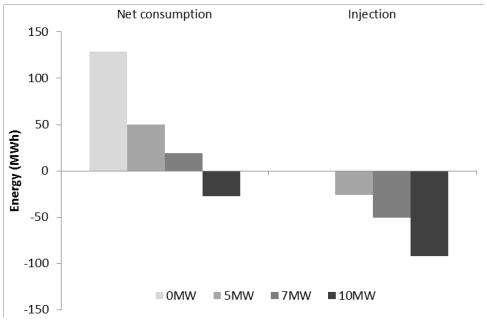

Fig. 2. Comparison of net consumption of feeder and total PV injection during a three day period using typical summer profiles

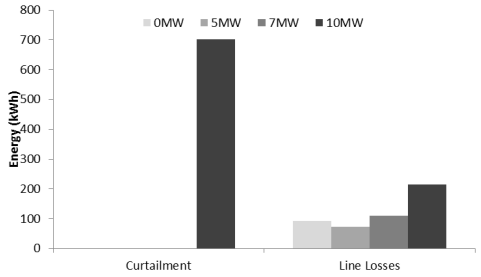

Fig. 3. Comparison of line losses of feeder and total PV curtailment necessary during a three day period using typical summer profiles

Added storage capacity was then integrated into the grid in order to quantify the additional hosting capacity possible. Initially storage elements were placed at the same nodes as all PV installations to represent a decentralized storage configuration. Therefore 20 systems of 116 kWh energy storage capacity were modeled through their inverter behavior as described in equation 8. For 10 MW of PV capacity installed, no curtailment was needed within all seasons. The improvement in system performance can be seen in figure 4 as a percentage increase or decrease for each parameter.

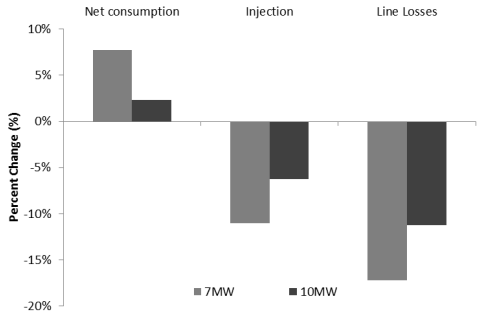

Fig. 4. Percentage increase or decrease due to added storage elemnts at each PV production node. Calculations for a 7 MW and 10 MW systems during a three days period using typical summer profiles

The same amount of storage capacity was then used in a centralized configuration. This centralized storage was placed very close to the high voltage transformer offering the same services. The necessary curtailement was also reduced

to zero for the 10 MW system. However, the centralized battery system also resulted in higher overall line losses. The percentage change due to the presence of a centralized battery system is shown in figure 5.

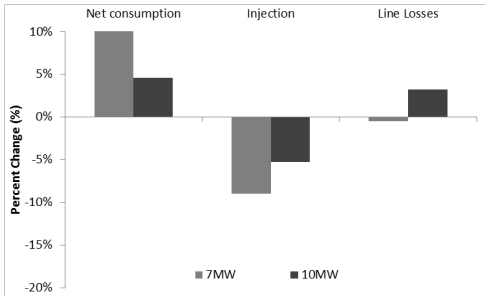

Fig. 5. Percentage increase or decrease due to an added centralized storage elemnt when comparing 7 MW and 10 MW systems during a three days period using typical summer profiles

VII. Conclusion

The optimization algorithm proposed in this paper successfully applied a convex relaxation algorithm with linear cuts to a multi-temporal application for battery storage analysis. This algorithm was shown to be effective when studying a distribution system for a 3-4 day time span. The multi-temporal algorithm allows for the assessment of battery storage functionality while taking into account the technology limitations such as charging and discharging efficiency, and maximum injection and absorption. The algorithm also calculates an optimal charging and discharging schedule based on the objective function. A French medium voltage distribution feeder was successfully analyzed to determine the hosting capacity, decentralized and centralized battery systems effects on curtailment. This algorithm could be used for comparison studies between different grid stability control strategies such as real time curtailment, centralized and decentralized battery installations. The use of this algorithm for real time management could also be effective if real time predicted PV production profiles and expected load profiles are used as inputs. The optimization of charging and discharging schedules of batteries can effectively increase hosting capacity of a distribution network by reducing the necessity to curtail PV systems.

Acknowledgment

The authors would like to thank ERDF for the provision of some of the data used in this study. Mr. Thibaut Barbier is thanked for his support with the simulated load curves. This work is performed in the frame of the European project Sensible (Grant Agreement 645963) funded in part by the European Commission under the Horizon 2020 Framework Program.

References

[1] A. Vinkovic, M. Suhadolc, and R. Mihalic, "Current-based models of {FACTS} devices for three-phase load-flow calculations using the newtonraphson method," *International Journal of Electrical Power & Energy Systems*, vol. 45, no. 1, pp. 117 – 128, 2013.

[2] D. R. R. Penido, L. R. de Araujo, S. C. Jnior, and J. L. R. Pereira, "A new tool for multiphase electrical systems analysis based on current injection method," *International Journal of Electrical Power & Energy Systems*, vol. 44, no. 1, pp. 410 – 420, 2013.

[3] M. Abdel-Akher, K. Nor, and A. Rashid, "Improved three-phase power-flow methods using sequence components," *Power Systems, IEEE Transactions on*, vol. 20, pp. 1389–1397, Aug 2005.

[4] X. Yang, Z. Wei, G. Sun, Y. Sun, Y. Yuan, Z. Lu, X. Xu, and L. Huang, "Power flow calculation for unbalanced three-phase distribution network with dgs based on phase-sequence hybrid modeling," in *Smart Energy Grid Engineering (SEGE), 2013 IEEE International Conference on*, pp. 1–6, Aug 2013.

[5] H. E. Farag, E. El-Saadany, R. E. Shatshat, and A. Zidan, "A generalized power flow analysis for distribution systems with high penetration of distributed generation," *Electric Power Systems Research*, vol. 81, no. 7, pp. 1499 – 1506, 2011.

[6] W. Wu and B. Zhang, "A three-phase power flow algorithm for distribution system power flow based on loop-analysis method," *International Journal of Electrical Power & Energy Systems*, vol. 30, no. 1, pp. 8 – 15, 2008.

[7] T.-H. Chen and N.-C. Yang, "Loop frame of reference based three-phase power flow for unbalanced radial distribution systems," *Electric Power Systems Research*, vol. 80, no. 7, pp. 799 – 806, 2010.

[8] N. Etherden and M. Bollen, "Increasing the hosting capacity of distribution networks by curtailment of renewable energy resources," in *PowerTech, 2011 IEEE Trondheim*, pp. 1–7, June 2011.

[9] S. Abdelouadoud, R. Girard, and T. Guiot, "Planning-oriented yearly simulation of energy storage operation in distribution system for profit maximization, voltage regulation and reserve provisionning," in *Electricity Distribution (CIRED 2013), 22nd International Conference and Exhibition on*, pp. 1–4, June 2013.

[10] L. Gan and S. H. Low, "Convex relaxations and linear approximation for optimal power flow in multiphase radial networks," in *Power Systems Computation Conference (PSCC), 2014*, pp. 1–9, Aug 2014.

[11] R. Madani, S. Sojoudi, and J. Lavaei, "Convex relaxation for optimal power flow problem: Mesh networks," in *Signals, Systems and Computers, 2013 Asilomar Conference on*, pp. 1375–1382, Nov 2013.

[12] M. Ghasemi, S. Ghavidel, M. Gitizadeh, and E. Akbari, "An improved teachinglearning-based optimization algorithm using lvy mutation strategy for non-smooth optimal power flow," *International Journal of Electrical Power & Energy Systems*, vol. 65, no. 0, pp. 375 – 384, 2015.

[13] S. Paudyal, C. Canizares, and K. Bhattacharya, "Three-phase distribution opf in smart grids: Optimality versus computational burden," in *Innovative Smart Grid Technologies (ISGT Europe), 2011 2nd IEEE PES International Conference and Exhibition on*, pp. 1–7, Dec 2011.

[14] X. Bai and H. Wei, "Semi-definite programming-based method for security-constrained unit commitment with operational and optimal power flow constraints," *Generation, Transmission Distribution, IET*, vol. 3, pp. 182–197, February 2009.

[15] J. Lavaei and S. Low, "Zero duality gap in optimal power flow problem," *Power Systems, IEEE Transactions on*, vol. 27, pp. 92–107, Feb 2012.

[16] S. Bose, S. Low, T. Teeraratkul, and B. Hassibi, "Equivalent relaxations of optimal power flow," *Automatic Control, IEEE Transactions on*, vol. 60, pp. 729–742, March 2015.

[17] M. Farivar, R. Neal, C. Clarke, and S. Low, "Optimal inverter var control in distribution systems with high pv penetration," in *Power and Energy Society General Meeting, 2012 IEEE*, pp. 1–7, July 2012.

[18] N. Li, L. Chen, and S. Low, "Exact convex relaxation of opf for radial networks using branch flow model," in *Smart Grid Communications (SmartGridComm), 2012 IEEE Third International Conference on*, pp. 7–12, Nov 2012.

[19] S. Y. Abdelouadoud, R. Girard, F.-P. Neirac, and T. Guiot, "Iterative linear cuts strenghtening the second-order cone relaxation of the distribution system optimal power flow problem," in *T D Conference and Exposition, 2014 IEEE PES*, pp. 1–4, April 2014.

[20] T. Barbier, R. Girard, F.-P. Neirac, N. Kong, and G. Kariniotakis, "A novel approach for electric load curve holistic modelling and simulation," in *MedPower 2014 - The 9th Mediterranean Conference on Power Generation, Transmission Distribution and Energy Conversion*, (Athènes, Greece), Nov. 2014.

Bibliography

[1] A. N. Espinosa, "Low voltage networks models and low carbon technology profiles," May 2015.

[2] I. E. A. (IEA), "Statistics for 2008, 2010," 2016.

[3] P. CARRIVE, "Réseaux de distribution structure et planification," *Techniques de l'ingénieur Réseaux électriques de distribution publique*, vol. base documentaire : TIB264DUO., no. ref. article : d4210, 2015. fre.

[4] H. Dutrieux, *Methodes pour la planification pluriannuelle des reseaux de distribution. Application a l'analyse technico-economique des solutions d'integrations des energies renouvelables intermittentes*. PhD thesis, l'Ecole Centrale de Lille, 2015.

[5] G. J. Ikenberry, "The irony of state strength: comparative responses to the oil shocks in the 1970s," *International Organization*, vol. 40, no. 1, pp. 105–137, 1986.

[6] B. D. Solomon and K. Krishna, "The coming sustainable energy transition: History, strategies, and outlook," *Energy Policy*, vol. 39, no. 11, pp. 7422 – 7431, 2011. Asian Energy Security.

[7] E. S. O. the European Committee for Standardization (CEN), E. C. for Electrotechnical Standardization (CENELEC), and E. T. S. I. (ETSI), "Smart grids," 2017.

[8] C. Defeuilley, "Histoire de courbe: 50 ans d'extension du réseau électrique en france," *Flux*, vol. 46, pp. 85 – 87, 2001.

[9] L. commission de reglementation de l'energie, "Bilan de l'ouverture des marches de detail de l'energie," 2015.

[10] E. R. D. France, "Description physique du reseau public," 2008.

[11] B. Puluhen, A. Pelletier, L. Joseph-Auguste, and T. Pelinski, "Concept grid: A new test platform for smart grid systems general presentation and experiments," in *Electricity Distribution (CIRED 2015), 23rd International Conference and Exhibition on*, pp. 1–4, June 2015.

[12] R. G. Verdier, "Grid4eu-nice grid project: How to facilitate the integration of distributed energy resources into the local grid," in *2014 Saudi Arabia Smart Grid Conference (SASG)*, pp. 1–3, Dec 2014.

[13] C. Chardonnet and B. de Boissezon, "Gdf suez 2014; greenlys wp2: Estimating the benefits and costs of a smart electrical system in french urban areas in 2020 2013;2030," in *2013 IEEE Grenoble Conference*, pp. 1–6, June 2013.

[14] M.-C. Alvarez-Herault, *Architectures des Reseaux de Distribution du Futur en Presence de Production Decentralisee*. PhD thesis, Institut National Polytechnique de Grenoble - INPG, 2010.

[15] R. d. t. d. RTE, "Generation adequacy report on the electricity supply-demand balance in france," tech. rep., 2016.

[16] A. Vinkovic, M. Suhadolc, and R. Mihalic, "Current-based models of {FACTS} devices for three-phase load-flow calculations using the newton raphson method," *International Journal of Electrical Power & Energy Systems*, vol. 45, no. 1, pp. 117 – 128, 2013.

[17] D. R. R. Penido, L. R. de Araujo, S. C. Jenior, and J. L. R. Pereira, "A new tool for multiphase electrical systems analysis based on current injection method," *International Journal of Electrical Power & Energy Systems*, vol. 44, no. 1, pp. 410 – 420, 2013.

[18] M. Abdel-Akher, K. Nor, and A. Rashid, "Improved three-phase power-flow methods using sequence components," *Power Systems, IEEE Transactions on*, vol. 20, pp. 1389–1397, Aug 2005.

[19] X. Yang, Z. Wei, G. Sun, Y. Sun, Y. Yuan, Z. Lu, X. Xu, and L. Huang, "Power flow calculation for unbalanced three-phase distribution network with dgs based on phase-sequence hybrid modeling," in *Smart Energy Grid Engineering (SEGE), 2013 IEEE International Conference on*, pp. 1–6, Aug 2013.

[20] H. E. Farag, E. El-Saadany, R. E. Shatshat, and A. Zidan, "A generalized power flow analysis for distribution systems with high penetration of distributed generation," *Electric Power Systems Research*, vol. 81, no. 7, pp. 1499 – 1506, 2011.

[21] W. Wu and B. Zhang, "A three-phase power flow algorithm for distribution system power flow based on loop-analysis method," *International Journal of Electrical Power & Energy Systems*, vol. 30, no. 1, pp. 8 – 15, 2008.

[22] T.-H. Chen and N.-C. Yang, "Loop frame of reference based three-phase power flow for unbalanced radial distribution systems," *Electric Power Systems Research*, vol. 80, no. 7, pp. 799 – 806, 2010.

[23] D. K. Molzahn, F. Dörfler, H. Sandberg, S. H. Low, S. Chakrabarti, R. Baldick, and J. Lavaei, "A survey of distributed optimization and control algorithms for electric power systems," *IEEE Transactions on Smart Grid*, vol. PP, no. 99, pp. 1–1, 2017.

[24] J. D. Watson, N. R. Watson, and I. Lestas, "Optimized dispatch of energy storage systems in unbalanced distribution networks," *IEEE Transactions on Sustainable Energy*, vol. PP, no. 99, pp. 1–1, 2017.

[25] A. Castillo and D. Gayme, "Evaluating the effects of real power losses in optimal power flow based storage integration," *IEEE Transactions on Control of Network Systems*, vol. PP, no. 99, pp. 1–1, 2017.

[26] A. Maulik and D. Das, "Optimal operation of microgrid using four different optimization techniques," *Sustainable Energy Technologies and Assessments*, vol. 21, pp. 100 – 120, 2017.

[27] S. Baldi, A. Karagevrekis, I. T. Michailidis, and E. B. Kosmatopoulos, "Joint energy demand and thermal comfort optimization in photovoltaic-equipped interconnected microgrids," *Energy Conversion and Management*, vol. 101, pp. 352 – 363, 2015.

[28] L. Wang, Q. Li, R. Ding, M. Sun, and G. Wang, "Integrated scheduling of energy supply and demand in microgrids under uncertainty: A robust multi-objective optimization approach," *Energy*, vol. 130, pp. 1 – 14, 2017.

[29] N. Good, E. Karangelos, A. Navarro-Espinosa, and P. Mancarella, "Optimization under uncertainty of thermal storage-based flexible demand response with quantification of residential users discomfort," *IEEE Transactions on Smart Grid*, vol. 6, pp. 2333–2342, Sept 2015.

[30] K. R. Krishnanand, D. C. Hoang, S. K. Panda, and R. Zhang, "Optimal appliance scheduling in building operating systems for cost-effective energy management," in *IECON 2014 - 40th Annual Conference of the IEEE Industrial Electronics Society*, pp. 5394–5399, Oct 2014.

[31] Q. Li, R. Ayyanar, and V. Vittal, "Convex optimization for des planning and operation in radial distribution systems with high penetration of photovoltaic resources," *IEEE Transactions on Sustainable Energy*, vol. 7, pp. 985–995, July 2016.

[32] M. Nick, R. Cherkaoui, and M. Paolone, "Optimal planning of distributed energy storage systems in active distribution networks embedding grid reconfiguration," *IEEE Transactions on Power Systems*, vol. PP, no. 99, pp. 1–1, 2017.

[33] M. Zidar, P. S. Georgilakis, N. D. Hatziargyriou, T. Capuder, and D. Škrlec, "Review of energy storage allocation in power distribution networks: applications, methods and future research," *IET Generation, Transmission Distribution*, vol. 10, no. 3, pp. 645–652, 2016.

[34] J. Driesen and R. Belmans, "Distributed generation: challenges and possible solutions," in *2006 IEEE Power Engineering Society General Meeting*, pp. 8 pp.–, 2006.

[35] R. A. Walling, R. Saint, R. C. Dugan, J. Burke, and L. A. Kojovic, "Summary of distributed resources impact on power delivery systems," *IEEE Transactions on Power Delivery*, vol. 23, pp. 1636–1644, July 2008.

[36] K. Karoui, H. Crisciu, and L. Platbrood, "An optimum power flow tool for optimising the expansion plan of reactive power compensation," in *GCC Conference and Exhibition (GCC), 2011 IEEE*, pp. 275–278, Feb 2011.

[37] K. Turitsyn, P. Sulc, S. Backhaus, and M. Chertkov, "Distributed control of reactive power flow in a radial distribution circuit with high photovoltaic penetration," in *Power and Energy Society General Meeting, 2010 IEEE*, pp. 1–6, July 2010.

[38] 110th US Congress, "Energy independence and security act of 2007," 2007.

[39] R. Hidalgo, C. Abbey, and G. Joos, "A review of active distribution networks enabling technologies," in *Power and Energy Society General Meeting, 2010 IEEE*, pp. 1–9, July 2010.

[40] G. C. Jim Eyer, "Energy storage for the electricity grid: Benefits and market potential assessment guide." Sandia Report, February 2010.

[41] A. A. Akhil, G. Huff, A. B. Currier, and al., "Doe/epri electricity storage handbook in collaboration with nreca." Sandia Report, February 2015.

[42] T. Kishore and S. Singal, "Optimal economic planning of power transmission lines: A review," *Renewable and Sustainable Energy Reviews*, vol. 39, no. 0, pp. 949 – 974, 2014.

[43] S. Boyd and L. Vandenberghe, *Convex Optimization*. New York: Cambridge University Press, 2004.

[44] P. Phonrattanasak, "Optimal placement of dg using multiobjective particle swarm optimization," in *Mechanical and Electrical Technology (ICMET), 2010 2nd International Conference on*, pp. 342–346, Sept 2010.

[45] J. Jamian, M. Mustafa, H. Mokhlis, and M. Baharudin, "Simulation study on optimal placement and sizing of battery switching station units using artificial bee colony algorithm," *International Journal of Electrical Power & Energy Systems*, vol. 55, pp. 592 – 601, 2014.

[46] A. El-Zonkoly, "Optimal placement and schedule of multiple grid connected hybrid energy systems," *International Journal of Electrical Power & Energy Systems*, vol. 61, pp. 239 – 247, 2014.

[47] M. H. Moradi, M. Abedini, S. R. Tousi, and S. M. Hosseinian, "Optimal siting and sizing of renewable energy sources and charging stations simultaneously based on differential evolution algorithm," *International Journal of Electrical Power & Energy Systems*, vol. 73, pp. 1015 – 1024, 2015.

[48] M. Sedghi, A. Ahmadian, and M. Aliakbar-Golkar, "Optimal storage planning in active distribution network considering uncertainty of wind power distributed generation," *IEEE Transactions on Power Systems*, vol. 31, pp. 304–316, Jan 2016.

[49] S. Paudyal, C. Canizares, and K. Bhattacharya, "Three-phase distribution opf in smart grids: Optimality versus computational burden," in *Innovative Smart Grid Technologies (ISGT Europe), 2011 2nd IEEE PES International Conference and Exhibition on*, pp. 1–7, Dec 2011.

[50] L. Gan and S. H. Low, "Convex relaxations and linear approximation for optimal power flow in multiphase radial networks," in *Power Systems Computation Conference (PSCC), 2014*, pp. 1–9, Aug 2014.

[51] R. Madani, S. Sojoudi, and J. Lavaei, "Convex relaxation for optimal power flow problem: Mesh networks," in *Signals, Systems and Computers, 2013 Asilomar Conference on*, pp. 1375–1382, Nov 2013.

[52] X. Bai and H. Wei, "Semi-definite programming-based method for security-constrained unit commitment with operational and optimal power flow constraints," *Generation, Transmission Distribution, IET*, vol. 3, pp. 182–197, February 2009.

[53] J. Lavaei and S. Low, "Zero duality gap in optimal power flow problem," *Power Systems, IEEE Transactions on*, vol. 27, pp. 92–107, Feb 2012.

[54] S. Bose, S. Low, T. Teeraratkul, and B. Hassibi, "Equivalent relaxations of optimal power flow," *Automatic Control, IEEE Transactions on*, vol. 60, pp. 729–742, March 2015.

[55] M. Farivar, R. Neal, C. Clarke, and S. Low, "Optimal inverter var control in distribution systems with high pv penetration," in *Power and Energy Society General Meeting, 2012 IEEE*, pp. 1–7, July 2012.

[56] N. Li, L. Chen, and S. Low, "Exact convex relaxation of opf for radial networks using branch flow model," in *Smart Grid Communications (SmartGridComm), 2012 IEEE Third International Conference on*, pp. 7–12, Nov 2012.

[57] S. Abdelouadoud, R. Girard, F. Neirac, and T. Guiot, "Optimal power flow of a distribution system based on increasingly tight cutting planes added to a second order cone relaxation," *International Journal of Electrical Power & Energy Systems*, vol. 69, pp. 9 – 17, 2015.

[58] E. Grover-Silva, R. Girard, and G. Kariniotakis, "Multi-temporal optimal power flow for assessing the renewable generation hosting capacity of an active distribution system," in *Proceedings of 2016 IEEE PES Transmission and Distribution Conference and Exposition, Dallas, USA*, pp. 1–5, May 2-5 2016.

[59] E. Dall'Anese, G. Giannakis, and B. Wollenberg, "Optimization of unbalanced power distribution networks via semidefinite relaxation," in *North American Power Symposium (NAPS), 2012*, pp. 1–6, Sept 2012.

[60] C. de regulation de l'energie, "Description generale."

[61] A. Pasdar and S. Mirzakuchaki, "Three phase power line balancing based on smart energy meters," in *EUROCON 2009, EUROCON '09. IEEE*, pp. 1876–1878, May 2009.

[62] S. Choi and M. Jang, "Analysis and control of a single-phase-inverter-zigzag-transformer hybrid neutral-current suppressor in three-phase four-wire systems," *Industrial Electronics, IEEE Transactions on*, vol. 54, pp. 2201–2208, Aug 2007.

[63] "Simulation tool - opendss."

[64] W. Kersting, *Distribution System Modeling and Analysis*. The electric power engineering series, CRC Press, 2001.

[65] Z. Hu and F. Li, "Cost-benefit analyses of active distribution network management, part i: Annual benefit analysis," *Smart Grid, IEEE Transactions on*, vol. 3, pp. 1067–1074, Sept 2012.

[66] E. Dall'Anese, G. B. Giannakis, and B. F. Wollenberg, "Optimization of unbalanced power distribution networks via semidefinite relaxation," in *North American Power Symposium (NAPS), 2012*, pp. 1–6, Sept 2012.

[67] L. Gan and S. Low, "Convex relaxations and linear approximation for optimal power flow in multiphase radial networks," in *Power Systems Computation Conference (PSCC), 2014*, pp. 1–9, Aug 2014.

[68] A. S. Zamzam, N. D. Sidiropoulos, and E. Dall'Anese, "Beyond relaxation and newton-raphson: Solving ac opf for multi-phase systems with renewables," *IEEE Transactions on Smart Grid*, vol. PP, no. 99, pp. 1–1, 2017.

[69] A. O'Connell and A. Keane, "Multi-period three-phase unbalanced optimal power flow," in *IEEE PES Innovative Smart Grid Technologies, Europe*, pp. 1–6, Oct 2014.

[70] Y. Cao, Y. Tan, C. Li, and C. Rehtanz, "Chance-constrained optimization-based unbalanced optimal power flow for radial distribution networks," *IEEE Transactions on Power Delivery*, vol. 28, pp. 1855–1864, July 2013.

[71] Q. Peng and S. H. Low, "Distributed algorithm for optimal power flow on an unbalanced radial network," in *2015 54th IEEE Conference on Decision and Control (CDC)*, pp. 6915–6920, Dec 2015.

[72] Y. Han, L. Chen, Z. Wang, S. Mei, L. Chen, S. Mei, and W. Liu, "Fully distributed optimal power flow for unbalanced distribution networks based on admm," in *2016 IEEE International Conference on Power System Technology (POWERCON)*, pp. 1–6, Sept 2016.

[73] A. Anwar and H. R. Pota, "Optimum capacity allocation of dg units based on unbalanced three-phase optimal power flow," in *2012 IEEE Power and Energy Society General Meeting*, pp. 1–8, July 2012.

[74] S. Bruno, S. Lamonaca, G. Rotondo, U. Stecchi, and M. La Scala, "Unbalanced three-phase optimal power flow for smart grids," *Industrial Electronics, IEEE Transactions on*, vol. 58, pp. 4504–4513, Oct 2011.

[75] B. Zhang, A. Y. S. Lam, A. D. Dominguez-Garcia, and D. Tse, "An optimal and distributed method for voltage regulation in power distribution systems," *IEEE Transactions on Power Systems*, vol. 30, pp. 1714–1726, July 2015.

[76] M. L. Tuballa and M. L. Abundo, "A review of the development of smart grid technologies," *Renewable and Sustainable Energy Reviews*, vol. 59, pp. 710 – 725, 2016.

[77] X. Luo, J. Wang, M. Dooner, and J. Clarke, "Overview of current development in electrical energy storage technologies and the application potential in power system operation," *Applied Energy*, vol. 137, pp. 511 – 536, 2015.

[78] P. Prakash and D. K. Khatod, "Optimal sizing and siting techniques for distributed generation in distribution systems: A review," *Renewable and Sustainable Energy Reviews*, vol. 57, pp. 111 – 130, 2016.

[79] N. Etherden and M. Bollen, "Increasing the hosting capacity of distribution networks by curtailment of renewable energy resources," in *Proceedings of 2011 IEEE PowerTech, Trondheim, Norway*, pp. 1–7, June 19-23 2011.

[80] M. Nick, M. Hohmann, R. Cherkaoui, and M. Paolone, "Optimal location and sizing of distributed storage systems in active distribution networks," in *Proceedings of 2013 IEEE PowerTech Conference, Grenoble, France*, pp. 1–6, June 16-20 2013.

[81] Z. Qing, Y. Nanhua, Z. Xiaoping, Y. You, and D. Liu, "Optimal siting amp; sizing of battery energy storage system in active distribution network," in *IEEE PES ISGT Europe 2013*, pp. 1–5, Oct 2013.

[82] A. El-Zonkoly, "Optimal placement and schedule of multiple grid connected hybrid energy systems," *International Journal of Electrical Power & Energy Systems*, vol. 61, pp. 239 – 247, 2014.

[83] M. Motalleb, E. Reihani, and R. Ghorbani, "Optimal placement and sizing of the storage supporting transmission and distribution networks," *Renewable Energy*, vol. 94, pp. 651 – 659, 2016.

[84] S. Mashayekh, M. Stadler, G. Cardoso, and M. Heleno, "A mixed integer linear programming approach for optimal der portfolio, sizing, and placement in multi-energy microgrids," *Applied Energy*, vol. 187, pp. 154 – 168, 2017.

[85] H. Nazaripouya, Y. Wang, P. Chu, H. R. Pota, and R. Gadh, "Optimal sizing and placement of battery energy storage in distribution system based on solar size for voltage regulation," in *2015 IEEE Power Energy Society General Meeting*, pp. 1–5, July 2015.

[86] C. Thrampoulidis, S. Bose, and B. Hassibi, "Optimal placement of distributed energy storage in power networks," *IEEE Transactions on Automatic Control*, vol. 61, pp. 416–429, Feb 2016.

[87] M. Ghofrani, A. Arabali, M. Etezadi-Amoli, and M. S. Fadali, "A framework for optimal placement of energy storage units within a power system with high wind penetration," *IEEE Transactions on Sustainable Energy*, vol. 4, pp. 434–442, April 2013.

[88] I. Sharma and K. Bhattacharya, "Optimal sizing of battery energy storage systems in unbalanced distribution feeders," in *Industrial Electronics Society, IECON 2013 - 39th Annual Conference of the IEEE*, pp. 2133–2138, Nov 2013.

[89] S. Y. Abdelouadoud, R. Girard, F.-P. Neirac, and T. Guiot, "Iterative linear cuts strenghtening the second-order cone relaxation of the distribution system optimal power flow problem," in *T D Conference and Exposition, 2014 IEEE PES*, pp. 1–4, April 2014.

[90] M. E. Baran and F. F. Wu, "Optimal capacitor placement on radial distribution systems," *IEEE Transactions on Power Delivery*, vol. 4, pp. 725–734, Jan 1989.

[91] T. Barbier, R. Girard, F. P. Neirac, N. Kong, and G. Kariniotakis, "A novel approach for electric load curve holistic modelling and simulation," in *Proceedings of 2014 IEEE MedPower Conference, Athens, Greece*, pp. 1–8, Nov 2-5 2014.

[92] P. Blanc, B. Gschwind, M. Lefevre, and L. Wald, "The HelioClim Project: Surface Solar Irradiance Data for Climate Applications," *Remote Sensing*, vol. 3, pp. 343–361, Feb. 2011. URL : http://www.mdpi.com/2072-4292/3/2/343/.

[93] J. Ruiz-Arias, H. Alsamamra, J. Tovar-Pescador, and D. Pozo-Vázquez, "Proposal of a regressive model for the hourly diffuse solar radiation under all sky conditions," *Energy Conversion and Management*, vol. 51, no. 5, pp. 881 – 893, 2010.

[94] T. Muneer, *Solar radiation and daylight models for the energy efficient design of buildings*. Architectural Press, 1997.

[95] A. L. Dimeas, G. K. Antonis G. Tsikalakis, and G. Korres, *Microgrids: Architectures and Control*, ch. Microgrids Control Issues. Chichester, United Kingdom: John Wiley and Sons Ltd, 2014.

[96] A. Alqurashi, A. H. Etemadi, and A. Khodaei, "Treatment of uncertainty for next generation power systems: State-of-the-art in stochastic optimization," *Electric Power Systems Research*, vol. 141, pp. 233 – 245, 2016.

[97] R. Bessa, C. Möhrlen, V. Fundel, M. Siefert, J. Browell, S. H. E. Gaidi, B.-M. Hodge, U. Cali, and G. Kariniotakis, *Towards Improved Uncerstanding of the Applicability of Uncertainty Forecasts in the Electric Power Industry*. Switzerland: Energies, 2017.

[98] Z. Wang, B. Chen, J. Wang, M. M. Begovic, and C. Chen, "Coordinated energy management of networked microgrids in distribution systems," *IEEE Transactions on Smart Grid*, vol. 6, pp. 45–53, Jan 2015.

[99] F. S. Gazijahani, H. Hosseinzadeh, A. A. Abadi, and J. Salehi, "Optimal day ahead power scheduling of microgrids considering demand and generation uncertainties," in *2017 Iranian Conference on Electrical Engineering (ICEE)*, pp. 943–948, May 2017.

[100] V. Trovato, F. Teng, and G. Strbac, "Role and benefits of flexible thermostatically controlled loads in future low-carbon systems.," *IEEE Transactions on Smart Grid*, vol. PP, no. 99, pp. 1–1, 2017.

[101] N. Nikmehr, S. Najafi-Ravadanegh, and A. Khodaei, "Probabilistic optimal scheduling of networked microgrids considering time-based demand response programs under uncertainty," *Applied Energy*, vol. 198, pp. 267 – 279, 2017.

[102] F. S. Gazijahani, H. Hosseinzadeh, A. A. Abadi, and J. Salehi, "Optimal day ahead power scheduling of microgrids considering demand and generation uncertainties," in *2017 Iranian Conference on Electrical Engineering (ICEE)*, pp. 943–948, May 2017.

[103] Y. Zhang, N. Gatsis, and G. B. Giannakis, "Robust energy management for microgrids with high-penetration renewables," *IEEE Transactions on Sustainable Energy*, vol. 4, pp. 944–953, Oct 2013.

[104] E. A. Bakirtzis and P. N. Biskas, "Multiple time resolution stochastic scheduling for systems with high renewable penetration," *IEEE Transactions on Power Systems*, vol. 32, pp. 1030–1040, March 2017.

[105] P. Pinson, H. Madsen, H. A. Nielsen, and G. Papaefthymiou, "From probabilistic forecasts to statistical scenarios of short-term wind power production," *Wind Energy*, vol. 12, pp. 51–62, January 2009.

[106] M. Aien, A. Hajebrahimi, and M. Fotuhi-Firuzabad, "A comprehensive review on uncertainty modeling techniques in power system studies," *Renewable and Sustainable Energy Reviews*, vol. 57, no. Supplement C, pp. 1077 – 1089, 2016.

[107] M. Heleno, M. A. Matos, and J. A. P. Lopes, "Availability and flexibility of loads for the provision of reserve," *IEEE Transactions on Smart Grid*, vol. 6, pp. 667–674, March 2015.

[108] A. A. Eajal, M. F. Shaaban, K. Ponnambalam, and E. F. El-Saadany, "Stochastic centralized dispatch scheme for ac/dc hybrid smart distribution systems," *IEEE Transactions on Sustainable Energy*, vol. 7, pp. 1046–1059, July 2016.

[109] L. du Grésivaudan, "Solaire lgm," 2016.

Résumé

Dans le contexte de la transition énergétique, il existe des inconnues liées à la fonctionnalité du réseau électrique futur avec l'augmentation de la consommation et l'introduction de nouvelles formes de production. L'adaptation du système actuel est inévitable, néanmoins, les solutions efficaces sont difficiles à définir. Les stratégies actuelles de la planification du réseau de distribution ne répondent pas précisément aux problématiques des nouvelles productions décentralisées, le changement du profil de la consommation, l'automation du réseau de distribution avec de nouvelles stratégies de gestion du réseau ainsi que la déréglementation du marché de l'électricité. De plus, la visibilité et la contrôlabilité du réseau de distribution est limité, l'implémentation d'une gestion active optimale n'est pas à présent une réalité. L'évaluation du réseau intelligent est critique pour comparer aux solutions traditionnelles.
L'objectif principal de cette thèse est d'éxplorer les barrières technico-économiques pour l'intégration massive des énergies renouvelables sur le réseau de distribution. Cette thèse explore plusieurs solutions au travers d'algorithmes d'optimisation de type flux de puissance qui utilisent des relaxations convexes. Pour le cas du réseau électrique basse tension, des systèmes triphasés déséquilibrés sont considérés. Pour analyser les incertitudes associées avec la génération et la demande, des algorithmes stochastiques sont abordés. Ces outils sont utilisés pour i) l'optimisation de l'emplacement et le dimensionnement des batteries, ii) l'optimisation des stratégies de gestion de la demande, iii) l'évaluation des stratégies d'opération de flexibilité du réseau centralisé et aussi décentralisé et iv) étudier l'impact de différents scénarios de pénétration des énergies renouvelables sur les réseaux existants.

Mots Clés

Système Electrique intelligent, réseau de distribution, énergies renouvelables, planification, optimisation

Abstract

In the context of the energy transition, there are many unknowns related to the required capabilities of future electric distribution systems to meet the growing electric load and new forms of electric production. The transformation of current electric distribution systems is inevitable, however, the most cost-effective investments are difficult to evaluate. Current electric distribution grid planning strategies are inadequate to take into account the accommodation of massive decentralized production, increased electric load with higher volatility, automation of distribution grids and unbundling of electricity markets. Due to a lack of observability and controllability in the distribution grid, the feasibility of optimal power flow management is not currently a reality. The quantification of smart distribution grids is critical to evaluate the added benefit of this solution in comparison to infrastructure upgrades.
The primary objective of my PhD is to explore the techno-economical barriers of massive renewable energy integration into the distribution grid. This thesis will explore different solutions through convex relaxations of optimal power flow analysis. For the low voltage distribution grid case, three-phase unbalanced power flow analysis is considered. In order to consider realistically the uncertainties related to renewable generation and demand, stochastic optimal power flow (OPF) algorithms are proposed. These tools are used among others to i) optimize placement and sizing of grid connected storage, ii) optimize demand response strategies, iii) study different operation strategies for storage devices including centralized and decentralized ones and iv) study the impact of different renewable energy integration scenarios into real-world distribution grids.

Keywords

Smart Grid, electric distribution grid, renewable energy, planning, optimization